Rep. Prog. Phys. 53 (1990) 837–915. Printed in the UK

Physics of white dwarf stars

Detlev Koester and Ganesar Chanmugam

Department of Physics and Astronomy, Louisiana State University, Baton Rouge, LA 70803, USA

Abstract

White dwarf stars, compact objects with extremely high interior densities, are the most common end product in the evolution of stars. In this paper we review the history of their discovery, and of the realisation that their structure is determined by the physics of the degenerate electron gas. Spectral types and surface chemical composition show a complicated pattern dominated by diffusion processes and their interaction with accretion, convection and mass loss. While this interaction is not completely understood in all its detail at present, the study may ultimately lead to important constraints on the theory of stellar evolution in general. Variability, caused by non-radial oscillations of the star, is a common phenomenon and is shown to be a powerful probe of the structure of deeper layers that are not directly accessible to observation. Very strong magnetic fields detected in a small fraction of white dwarfs offer a unique opportunity to study the behaviour of atoms under conditions that cannot be simulated in terrestrial laboratories.

This review was received in its present form in December 1989.

0034-4885/90/070837+79$14.00

Contents

1. Introduction

The theory of stellar structure knows three final states for a star: black holes, neutron stars and white dwarfs (for a recent review see e.g. Shapiro and Teukolsky 1983). Candidates for black holes have been proposed in certain binary star systems, at the centres of galaxies (possibly even our own Milky Way), and as the energy sources in quasi-stellar objects, but to date their actual existence has not been proven. The existence of neutron stars, extremely compact objects with masses similar to the sun but radii of about 10 km, was proven with the discovery of pulsars and their interpretation, and we may at the present time witness the birth of a new object of this class as the remnant of the supernova explosion in the Large Magellanic Cloud in 1987. Neutron stars and black holes are exotic objects with spectacular properties and certainly deserve the great attention they get in the current astrophysical research.

The vast majority (of the order of 90%, see Koester and Weidemann 1980) of all stars, however, including our sun, will finally evolve towards the third final state, that of white dwarfs. White dwarfs have about the same masses as neutron stars, but sizes of the order of the earth; typical interior densities are therefore $\sim 10^6$ g cm^{-3}. The evolution towards white dwarfs is the dominant channel in galaxies, which determines the evolution and final fate of most of their mass. For the same reasons the population of white dwarfs contains a wealth of information on the evolution of individual stars from birth to death, on the previous history of the galaxy and on the rate of star formation (Koester and Weidemann 1980).

According to our current understanding, the primary parameter that determines the final fate of a star is its mass at birth. All stars below a critical value, estimated to be in the range of 6 to 8 solar masses ($M_\odot$), will finally become white dwarfs, while the more massive stars will become neutron stars or black holes or even possibly be totally disrupted. Because the maximum mass of a white dwarf ($\simeq 1.4\ M_\odot$) is much smaller than this value a large fraction of the original stellar mass must be lost to the surrounding interstellar medium. This mass loss is indeed confirmed by observations of stars in the progenitor stages, although a theoretical derivation is still missing and an estimate of total mass loss during the life of a star is difficult.

Observations of white dwarfs can at least partly fill this gap. By determining the masses of white dwarfs and tracing their evolution back to their progenitors, it is possible at least in a statistical sense to estimate the total mass loss. This provides valuable constraints for theoretical attempts to understand this phenomenon as well as for calculations of stellar evolution.

On the other hand, the difference between initial and final mass must have been given back, almost unchanged, to the interstellar medium and is available for the formation of new stars. The study of white dwarfs therefore provides important insights into the mass budget of the galaxy: how much is locked up forever in the interior of white dwarfs and how much is given back to be used again in a new cycle?

Although the white dwarf state is a final state in the sense that no nuclear energy generation occurs, the observable white dwarfs still evolve. They are 'born' with

high luminosities (L = total radiative energy loss per second), and gradually, over 5 to 10 billion years fade away into invisibility. The faintest observed white dwarfs are therefore very old and contain information about the early phases of our galaxy. Recently, it was even proposed that these observations indicate that star formation in the galactic disk began about 9 billion years ago (Winget *et al* 1987a).

Besides these implications for the galaxy, however, white dwarfs are also extremely interesting objects in their own right. At their extremely high densities the electrons become degenerate and their quantum mechanical nature, through the Pauli principle, determines the equation of state, the structure of white dwarfs and the existence of a limiting mass.

These extreme densities cannot be simulated in terrestrial laboratories. The properties of matter under these conditions must therefore be calculated theoretically, and to the degree that the predictions can be confirmed by observations white dwarfs can be considered to be a 'physics laboratory' for matter at extreme densities and pressures.

The case for white dwarfs as physical laboratories can be made even more convincing. At the present time 26 white dwarfs are known to have magnetic fields in the range 10^6 to 10^9 G (Schmidt 1989). By comparison, the largest steady field that can be produced in the laboratory is only 10^5 G because for higher fields the magnetic pressure exceeds that of steel. Transient fields up to 10 MG may be produced in implosions. Thus white dwarfs provide a unique opportunity to study the effect of strong magnetic fields in great detail from the ultraviolet to the infrared. These observations have provided the main motivation in recent years to extend theoretical calculations of energy eigenvalues and oscillator strengths in hydrogen atoms into this very difficult intermediate range, where the Coulomb forces are of the same order of magnitude as the magnetic interaction (Henry and O'Connell 1985, Wunner *et al* 1987).

Pulsating stars in general have provided extremely important tests for theoretical calculations of stellar structure and evolution. This is also true for white dwarfs: several classes of pulsating white dwarfs are now known (Winget 1986, Cox 1986). In white dwarfs, the oscillations are non-radial, complicating the analysis considerably as compared to radial oscillations, but nevertheless providing important information about the structure of the deeper layers below the visible surface. These observations and their subsequent analysis with theoretical models have, for example, confirmed that the outer, non-degenerate envelopes of white dwarfs show a layered structure: in most cases a very thin almost pure hydrogen layer floating on top of a helium layer. It has even been possible to estimate the thickness of these layers, although at present there exists some controversy regarding the interpretation of the data.

The locations of the 'instability strips' in the Hertzsprung–Russell diagram (HRD) have also been used to constrain the free parameter (mixing-length/pressure scale height) in the mixing-length approximation that is used in stellar evolution calculations to model the convective energy transport (Bradley *et al* 1989).

Oscillation periods depend on the structure of the pulsating star. In principle, periods and their rates of change can be measured with very high accuracy, although in practice the observations are often complicated for white dwarfs because many periods are present simultaneously and the necessary frequency resolution may require long observing runs. Nevertheless, it may become possible in the near future to compare the structural changes in a pulsating white dwarf, derived from observed period changes, with theoretical calculations for the evolution and thus for the first time directly observe stellar evolution in white dwarfs (Kawaler and Hansen 1989).

The spectra emitted by white dwarf atmospheres show a quite varied pattern, unlike any other stellar group. The majority have lines of hydrogen only, extremely broadened by the high gravitational fields and correspondingly high pressures in the atmospheres; others show only the spectral lines of neutral helium, or only the Swan bands of the C_2 molecule. Yet, others show only indications of calcium, magnesium and iron, especially in the ultraviolet spectra. Detailed analysis, however, reveals an underlying simplicity: with very few exceptions the main constituent of the atmosphere is either hydrogen or helium, the two most abundant elements in the universe. Only traces of other elements are present (Koester 1987a).

The basic mechanism responsible for the unusual composition was proposed by Schatzman (1958). Under the combined influence of gravitational and electric fields in the outer layers, elements with different atomic weights separate by diffusion: heavy elements move downwards, while the lightest one present (either hydrogen or helium) floats to the top of the atmosphere. The time scales for this diffusion process are always short compared to the evolutionary time scales of white dwarfs (Paquette *et al* 1986a), we can therefore in most cases assume that the equilibrium state has been reached in observed objects. This simple picture is, however, complicated by the action of competing processes such as convection, stellar winds and accretion. The study of the very complicated interaction between these processes and its implication for the observed white dwarf population is currently at the forefront of active research. A basic understanding has already emerged, but many problems remain to be solved (Koester 1987a).

Progress in this and other fields of white dwarf research is of course intimately connected to progress in observational methods and instrumentation. The last decade has seen tremendous technical advances due to the construction of large telescopes (white dwarfs are very faint objects), the availability of new electronic detectors (CCD), and especially satellite projects that made accessible the ultraviolet and soft X-ray range of the electromagnetic spectrum (International Ultraviolet Explorer (IUE), Einstein, Exosat). In this paper, however, we will concentrate on the physics that govern the interior structure and outer layers of white dwarfs. The coverage of the wealth of observational data will be very incomplete; the reader interested in this aspect is referred to the excellent reviews by, for example, Liebert (1980), Sion (1986), the recent conference proceedings of IAU Colloquium No 114 (Wegner 1989a), Weidemann (1990) and D'Antona and Mazzittelli (1990).

A good introduction to the basic physics of white dwarfs can be found in chapters 2 to 4 of the textbook by Shapiro and Teukolsky (1983), which places the white dwarfs in the more general context of 'compact objects'. A very useful source will certainly be the monograph on white dwarfs currently being prepared by Van Horn and Liebert (1989).

We have also restricted the scope of this paper to the discussion of single white dwarfs. The first two white dwarfs to be discovered (see below) were members of binary systems, and today many more are known. But in these cases the binaries are wide systems, meaning that the structure and evolution of the white dwarf is not significantly influenced by the presence of a companion. We wish to exclude, however, cataclysmic variables which include novae, where the interaction between the two stars, normally by the transfer of matter and the formation of an accretion disk surrounding the white dwarf, dominates the evolution and the observational features. Recent reviews of this large and interesting field can be found in Patterson (1984), Bath (1985) and Mauche (1990).

2. History: Early observations and theoretical interpretation

2.1. Discovery

The first realisation that a new class of stars quite different from 'ordinary' stars exists can be traced back to 1910. Schatzman (1958) gives a lively description of that event in the words of Henry Norris Russell. What Russell had detected is shown in figure 1, one of the first examples of the HRD, which was to become one of the most important tools in astrophysics. This particular version of the diagram is of the 'observational' form, it uses the observed astronomical parameters of spectral type and absolute magnitude. This diagram is topologically equivalent to a more physical diagram, although the transformations are sophisticated and non-linear, where the vertical axis corresponds to the total luminosity of the star (increasing upwards) and the horizontal axis to a surface temperature (increasing to the left).

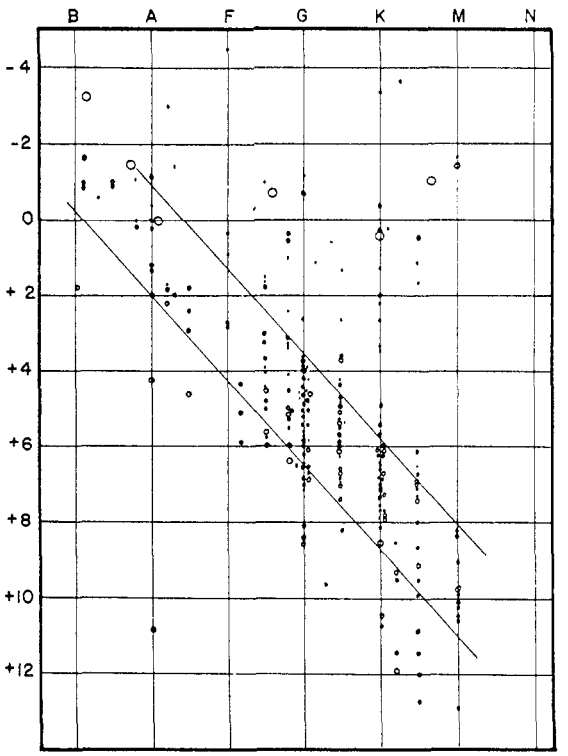

Figure 1. Absolute magnitude versus spectral type for stars of known distance. After Russell (1914), reproduced from Lang and Gingerich (1979).

This surface temperature is defined in astronomy as the effective temperature $T_{\rm eff}$ by means of Stefan's law, so that

$$L = 4\pi R^2 \sigma T_{\rm eff}^4 \tag{2.1}$$

where L is the luminosity, R the radius of the star and σ the radiation constant from Stefan's law. Thus $T_{\rm eff}$ is a measure of the energy flux at the surface and not a

real temperature, but it nevertheless constitutes a useful measure of the atmospheric temperature of the star. From the definition it is obvious that stars in the lower left part of this diagram are hot (white) and have small radii, while stars in the upper right corner are large and red ('red giants'). The position of our sun in this diagram would be near (G,4.8), close to the centre of the figure. By studying this diagram, Russell noticed, that all white stars of classes B and A are bright, far exceeding the luminosity of the sun; all very faint stars are red — the single exception being the star now known under the name 40 Eridani B, a member of the triple stellar system 40 Eridani. The position implies, as noted above, a very small radius, hence the name 'white dwarf' for the new class.

A similar puzzle was provided by the star Van Maanen 2, for which Van Maanen (1913) had determined a spectral type that made the star appear too hot for its faint luminosity. Though it was clear that these new objects had the size of a planet, their masses were not known at that time. Further physical insight into the problem was obtained from the third of the so-called 'classical white dwarfs' to be discovered, Sirius B, the binary companion of the bright star Sirius.

Between 1834 and 1844 the mathematician and astronomer Bessel had observed oscillations in the apparent path of Sirius across the sky, which had finally enabled him to show that Sirius was a double star. The companion, Sirius B, was detected visually by the American telescope maker Alvan Clark in 1861, and the first orbit determination published shortly thereafter. In 1910 the mass of the companion was determined as 0.94 $M_\odot$ (Boss 1910; a more recent value is 1.053 $M_\odot$ (Gatewood and Gatewood 1978). From the spectral type (Adams 1915) an effective temperature of 8000 K was assigned, which together with the known luminosity provided the first estimate of the radius according to equation (2.1) and a density of 5×10^4 g cm^{-3}, to which it was considered proper, as Eddington (1926) puts it in his famous book, to append the statement 'this is absurd'. The derived effective temperature was a severe underestimate, due to the observational problems posed by the close proximity of the much brighter Sirius A. A more modern value is 27 000 K (Thejll and Shipman 1986), implying a mean density of 3×10^6 g cm^{-3}.

An independent test of the high density became feasible around 1920, when Sirius A and B reached the greatest apparent separation in their orbit. Einstein (1907) had predicted the redshift of light originating in a strong gravitational field, depending on the stellar parameters as $\Delta\lambda/\lambda = GM/Rc^2$. With the values of mass and radius for Sirius B assumed at that time, the expected redshift of Hα was $\sim$ 0.4 Å, corresponding to a velocity of recession via the Doppler effect of $\sim$ 25 km s^{-1}. When Adams (1925) reported the detection of a shift equivalent to $\sim$ 19 km s^{-1} this was considered as a triumphant confirmation of general relativity as well as of the high densities in white dwarfs.

Somewhat embarrassingly, the modern values for M and R require a much larger shift, equivalent to $\simeq$ 85 km s^{-1}, which was confirmed by later observations (Greenstein *et al* 1971). Greenstein *et al* (1985) have recently given an excellent historical account of the circumstances surrounding Adam's measurement and their own subsequent attempts to determine the shift.

Thus in 1920 only three white dwarfs were known, but it was already evident to Eddington (1926) that they must be among the most common objects in our galaxy. All three were very close to the sun that is within 5 pc (1 pc = 3.26 light years), and only their intrinsic faintness limited further observations. By 1939, a total of 18 was known, and by 1950 the number had increased to 111 (Schatzman 1958).

Systematic searches for white dwarfs have capitalised on two properties of the class. Because white dwarfs are intrinsically faint, they are discovered only relatively close to the sun and should therefore show large tangential motions with respect to the sun ('proper motion' in astronomical nomenclature). Searches for this motion were initiated in 1929 by Luyten (Bruce Proper Motion Survey) and the results published in a series of papers (e.g. Luyten 1970, 1977 and references therein). A similar search was conducted at the Lowell Observatory (e.g. Giclas *et al* 1980, and references to earlier papers). White dwarfs are also 'too blue' for their luminosities, when compared with ordinary main sequence stars. This property was first exploited by Humason and Zwicky (1947) and more recently with the Palomar–Green Survey of faint blue objects (Green *et al* 1986). Major advances in the understanding of white dwarfs have been made by the extensive spectroscopic and photometric observational work of Greenstein and Eggen (cf Greenstein 1984a, Eggen 1985 and references therein).

An up-to-date list of 1279 spectroscopically identified white dwarfs is the catalogue by McCook and Sion (1987). The study of white dwarfs has thus come a long way from three exotic objects to an important part of stellar astrophysics, as documented very recently at the IAU Colloquium No 114 on 'White Dwarfs' (Wegner 1989a).

2.2. The degenerate electron gas

Taking the current best estimates for the mass and radius of Sirius B, its average density is $\sim 3 \times 10^6$ g cm^{-3}. Assuming for simplicity an interior composition of pure carbon we can estimate a typical distance r_c between carbon nuclei from $(4\pi/3)n_c r_c^3 = 1$, where n_c is the number density of heavy particles. The value is $r_c = 1.2 \times 10^{-10}$ cm, much less than the Bohr radius even for a carbon ion with only one remaining electron. There is thus no room for bound orbits, and the matter in white dwarfs must be completely 'pressure ionised'. Similarly a typical distance between the electrons is $r_e \simeq 6.4 \times 10^{-11}$ cm, which is smaller than the thermal de Broglie wavelength of the electrons for all but extremely high temperatures ($> 10^9$ K), so that the correct thermodynamic description of matter under these conditions requires quantum mechanics.

In 1926, it was shown that the electrons obey what is now called Fermi–Dirac statistics (Fermi 1926, Dirac 1926). This rule was immediately applied to solve the white dwarf puzzle by Fowler (1926), who realised that the pressure supporting these stars against gravity is supplied by the (almost) completely degenerate electrons. This pressure remains even at zero temperature, due to zero-point motion, thus establishing that white dwarfs are really stable final configurations and opening up the field of study of zero-temperature configurations.

Anderson (1929) and Stoner (1930) noticed that at the extreme densities in the most massive white dwarfs the velocities must become relativistic and calculated relativistic corrections to Fowler's equation of state. Chandrasekhar (1931) discovered that the relativistic 'softening' of the equation of state leads to the existence of a limiting mass, now called the 'Chandrasekhar limit', where gravitational forces overwhelm the pressure support, and no stable white dwarf can exist, a conclusion independently arrived at by Landau (1932). This provided the first clue to a fundamental difference in the evolution and final stages of low and high mass stars.

During the next eight years Chandrasekhar worked out the complete theory of the equation of state (EOS) at all densities, including the effects of finite temperatures and special relativity, and the resulting structure of zero-temperature models and their mass–radius relation (Chandrasekhar 1939).

3. Equation of state, interior structure and mass–radius relation

3.1. Equation of state for the ideal electron gas

Derivations of the EOS for ideal, non-interacting electrons are given in many sources. In this section we loosely follow the approach of Cox and Giuli (1968) where, in a thorough discussion, many tables of useful functions and further references can be found.

In statistical physics a complete description of a system in equilibrium is provided by the dimensionless distribution function in phase space, $f(\boldsymbol{x},\boldsymbol{p})$, defined by

$$\frac{\mathrm{d}n(\boldsymbol{x},\boldsymbol{p})}{g\mathrm{d}^3x\mathrm{d}^3p/h^3} = f(\boldsymbol{x},\boldsymbol{p}). \tag{3.1}$$

Here $\mathrm{d}n$ denotes the number of electrons in the volume element of phase space $\mathrm{d}^3x\mathrm{d}^3p$, g the number of internal degrees of freedom (two for electrons), and the denominator on the left is the number of 'cells' corresponding to the phase space volume. The function f thus gives the average occupation number of a cell in phase space. From this distribution function all interesting quantities (number density n, pressure p, energy density u) can be derived using the relativistic relation between momentum and kinetic energy

$$\varepsilon(p) = mc^2\left[\sqrt{1+(p/mc)^2}-1\right] \tag{3.2}$$

and the distribution function for an ideal Fermi gas in equilibrium

$$f(\varepsilon) = \frac{1}{\exp\left[(\varepsilon-\mu)/kT\right]+1}. \tag{3.3}$$

Here k is Boltzmann's constant and μ the chemical potential. For sufficiently low particle densities and high temperatures, $f(\varepsilon)$ reduces to the Maxwell–Boltzmann distribution. For completely degenerate fermions ($T \to 0$), μ is called the Fermi energy ε_{F}, and

$$f(\varepsilon) = \begin{cases} 1 & \varepsilon \le \varepsilon_{\mathrm{F}} \\ 0 & \varepsilon > \varepsilon_{\mathrm{F}} \end{cases}. \tag{3.4}$$

The momentum corresponding to ε_{F} according to (3.2) is called the Fermi momentum p_{F}. The EOS can be derived from the distribution function in parametrised form through functions of two dimensionless variables, the 'degeneracy parameter' $\eta = \mu/kT$ and the 'relativity parameter' $\beta = kT/mc^2$. In terms of these variables

$$P = \frac{16\pi\sqrt{2}}{3}\frac{m^4c^5}{h^3}\beta^{5/2}\left[F_{3/2}(\eta,\beta)+(\beta/2)F_{5/2}(\eta,\beta)\right] \tag{3.5}$$

$$n = 8\pi\sqrt{2}\frac{m^3c^3}{h^3}\beta^{3/2}\left[F_{1/2}(\eta,\beta)+\beta F_{3/2}(\eta,\beta)\right] \tag{3.6}$$

$$u = 8\pi\sqrt{2}\frac{m^4c^5}{h^3}\beta^{5/2}\left[F_{3/2}(\eta,\beta)+\beta F_{5/2}(\eta,\beta)\right] \tag{3.7}$$

where P, n and u are the pressure, number density and energy density. The functions F_k appearing here are defined by the integrals

$$F_k(\eta,\beta) = \int_0^\infty \frac{x^k(1+(\beta/2)x)^{1/2}\,\mathrm{d}x}{\exp(\eta+x)+1} \tag{3.8}$$

and can in general only be evaluated numerically. Cox and Giuli (1968) give tables for some of the functions as well as very useful expansions for the different physical regimes (high versus low degeneracy, relativistic versus non-relativistic, etc).

Fortunately, it is almost always possible to work with these much simpler expansions, because in real white dwarfs low degeneracy always implies the non-relativistic regime, whereas relativistic effects are only important at very high degeneracy. The most significant simplification results from the assumption of complete degeneracy ($T \to 0$), the realm of 'zero-temperature stars'. In this case β is no longer useful as a measure of the effects of relativity, and could be replaced by $\eta\beta = \mu/mc^2$ with the limit ε_F/mc^2 for complete degeneracy. It is customary, however, to use $x = p_F/mc$ instead, related to $\eta\beta$ through (3.2)

$$1 + x^2 = (1 + \eta\beta)^2. \tag{3.9}$$

Asymptotic expansions for $\eta \to \infty$ can be obtained for the F_k (Cox and Giuli 1968), it is, however, simpler to use directly the simple form of $f(\varepsilon)$ for complete degeneracy (3.4). The number density is

$$n = \frac{2}{h^3}\int_0^{p_F} 4\pi p^2\,\mathrm{d}p = \frac{8\pi}{3h^3}p_F^3 = \frac{8\pi m^3c^3}{3h^3}x^3 = n_0x^3 \qquad \text{with } x = p_F/mc \tag{3.10}$$

and the pressure

$$P = \frac{8\pi}{3h^3}\int_0^{p_F} \frac{(p^4/m)\,\mathrm{d}p}{\sqrt{1+(p/mc)^2}} = \frac{\pi m^4c^5}{3h^3}f(x) = P_0f(x) \tag{3.11}$$

where $f(x)$ stands for

$$f(x) = x(x^2+1)^{1/2}(2x^2-3) + 3\ln(x + \sqrt{1+x^2}) \tag{3.12}$$

and should not be confused with f in (3.4). It is interesting to note that the constants P_0 and n_0 in the above expressions involve only fundamental physical constants, and especially h, emphasising the role of quantum mechanics in the structure of white dwarfs.

For the construction of stellar models we need the matter density ρ instead of the electron number density n. These two are related through the requirement of electrical neutrality. In completely ionised matter of atomic mass number A and charge Z the number of heavy ions is n/Z and the mass density $\rho = nAH/Z$, where H is the atomic mass unit. Equation (3.10) can therefore be replaced by

$$\rho = \rho_0\mu_e x^3 \qquad \text{with } \rho_0 = n_0H \qquad \text{and} \qquad \mu_e = A/Z. \tag{3.13}$$

Here μ_e is called the 'molecular weight per electron' and should not be confused with the symbol μ for the chemical potential. It has the value 2 for realistic compositions. For hydrogen it would be 1, for completely ionised iron 2.15. If the composition is a mixture of several elements, appropriate averages must be taken.

Finally we consider the limiting cases $x \to 0$ (non-relativistic) and $x \to \infty$ (extremely relativistic). In both cases expansions of $f(x)$ allow elimination of the variable x, resulting in very simple equations:

$$P = \begin{cases} \dfrac{8P_0}{5\rho_0^{5/3}}\left(\dfrac{\rho}{\mu_e}\right)^{5/3} = \dfrac{3^{2/3}h^2}{8^{2/3}5\pi^{2/3}mH^{5/3}}\left(\dfrac{\rho}{\mu_e}\right)^{5/3} & x \ll 1 \\ \dfrac{2P_0}{\rho_0^{4/3}}\left(\dfrac{\rho}{\mu_e}\right)^{4/3} = \dfrac{2\,3^{1/3}hc}{8^{4/3}\pi^{1/3}H^{4/3}}\left(\dfrac{\rho}{\mu_e}\right)^{4/3} & x \gg 1\,. \end{cases} \tag{3.14}$$

3.2. Simple models, the mass–radius relation and the Chandrasekhar limit

The structure of a spherically symmetric star is completely determined by four basic equations, derived from the conservation laws of energy, mass and momentum, and the law describing the transport of energy in the presence of a temperature gradient (e.g. Clayton 1968, Cox and Giuli 1968). For zero-temperature stars only two of these are needed, the equation of hydrostatic equilibrium

$$\frac{\mathrm{d}P}{\mathrm{d}r} = -\frac{Gm\rho}{r^2} \tag{3.15}$$

and of mass conservation

$$\frac{\mathrm{d}m}{\mathrm{d}r} = 4\pi r^2 \rho. \tag{3.16}$$

Here r is the radial variable (= 0 at the centre), and m the mass inside a sphere of radius r. The system of equations is completed with the EOS $P = P(\rho, \mu_e)$, and the boundary conditions:

$$m(0) = 0 \quad \text{at the centre} \qquad \text{and} \qquad P(R) = 0 \quad \text{at the surface.} \tag{3.17}$$

Chandrasekhar (1939) has shown how the system can be reformulated into a second-order differential equation for a dimensionless function, with two parameters: μ_e and ρ_c, the central density. This function must be determined numerically and is tabulated in Chandrasekhar (1939) and Cox and Giuli (1968). It is, however, easy to see how the solution can be obtained in principle from equations (3.15) to (3.17). For a fixed value of μ_e (chemical composition) a value of ρ_c is chosen. The integration of (3.15) and (3.16) then proceeds from the centre until $P(r) = 0$ is reached. This determines the radius R and the mass $M = M(R)$ of the model. For a given value of μ_e a one-parameter family of models is thus obtained, defining implicitly a relation between mass and radius, the famous mass–radius relation (Chandrasekhar 1935). In the limit $\rho_c \to \infty$, R becomes zero, while the mass approaches a limiting value $M_{Ch} = 5.826/\mu_e^2\ M_\odot$, the 'Chandrasekhar limiting mass'.

It is possible to understand these basic features of the mass–radius relation without actually solving the above equations from a simple dimensional analysis. From (3.15) and (3.16) we can derive the general relations

$$P_c \propto \frac{GM^2}{R^4} \qquad \text{and} \qquad \rho_c \propto \frac{M}{R^3} \tag{3.18}$$

for the physical quantities at the centre. For low density models ($x \ll 1, \rho \ll \rho_0 \mu_e$ the non-relativistic form of the EOS (3.14) together with (3.18) leads to

$$P_c \propto \frac{P_0}{(\rho_0 \mu_e)^{5/3}} \frac{M^{5/3}}{R^5}. \tag{3.19}$$

In equilibrium the 'gravitational pressure' (3.18) must be balanced by the electron pressure (3.19). This can always be achieved by adjusting the radius, leading to a mass–radius relation

$$R \propto \frac{P_0}{G(\rho_0 \mu_e)^{5/3}}\ M^{-1/3}. \tag{3.20}$$

The neglected constants in the above expressions are dimensionless numbers of order unity. Equation (3.20) shows that for low-density white dwarfs the radius decreases with increasing mass as $M^{-1/3}$.

For the highly relativistic case (high central densities) on the other hand, one gets

$$P_c \propto \frac{P_0}{(\rho_0 \mu_e)^{4/3}} \frac{M^{4/3}}{R^4}. \tag{3.21}$$

In this case both pressures depend on the radius in the same way and hydrostatic equilibrium is possible only for a uniquely determined mass

$$M_{Ch} \propto \frac{(P_0/G)^{3/2}}{(\rho_0 \mu_e)^2} \propto \frac{(hc)^{3/2}}{G^{3/2} H^2} \mu_e^{-2}. \tag{3.22}$$

The radius has dropped from the result; equilibrium is therefore possible at arbitrary radius. This, however, is not realistic, because the assumption of the extremely relativistic EOS requires infinite density and $R = 0$. The physical interpretation is as follows:

Only for $M \equiv M_{Ch}$ can gravitational and electron pressure be in balance. For a slightly larger mass, the gravitational pressure wins and the star collapses dynamically to a singularity. For a slightly smaller mass, the electron pressure dominates. The star starts to expand, lowering the density and approaching the non-relativistic EOS in parts of the interior, until equilibrium can be obtained at a finite radius. It is interesting to note that the electron mass m has also dropped from (3.22). Similar arguments for the degenerate neutrons in neutron stars therefore lead to the prediction of a limiting mass for neutron stars of the same order of magnitude. In figure 2 the Chandrasekhar mass–radius relation for white dwarfs with $\mu_e = 2$ and $\mu_e = 2.15$ is displayed, together with results for more realistic EOSs discussed below.

3.3. Refinements to the equation of state — Hamada and Salpeter

Although the ideal, non-interacting electron gas accounts for the dominant contribution to the EOS at high densities, a real stellar plasma consists of electrons together with heavy, positively charged ions of one or more species. Kothari (1931, 1936, 1938) studied the effects of Coulomb interactions on the EOS and the structure of non-relativistic white dwarfs. Auluck and Mathur (1959) extended this work by including exchange and correlation effects. Kirzhnits (1960) argued that the matter in white dwarfs should be in a 'condensed state', and Abrikosov (1961, 1962) computed the properties of this crystal lattice phase. A comprehensive discussion of the EOS, and the results for energy and pressure of a zero-temperature plasma were provided by Salpeter (1961). In the following sections we follow closely the approach by Van Horn and Liebert (1989), based on Salpeter's work.

The thermodynamic properties of matter are completely determined if the Helmholtz free energy $F(T, V, N)$ is known for the system. The pressure, for example, can be obtained from

$$P = \left(\frac{\partial F}{\partial V}\right)_{T,N}. \tag{3.23}$$

Because $F = E - TS$, at zero temperature all that is needed is the energy $E(V, N)$, where N stands collectively for the particle numbers. In the following we will discuss

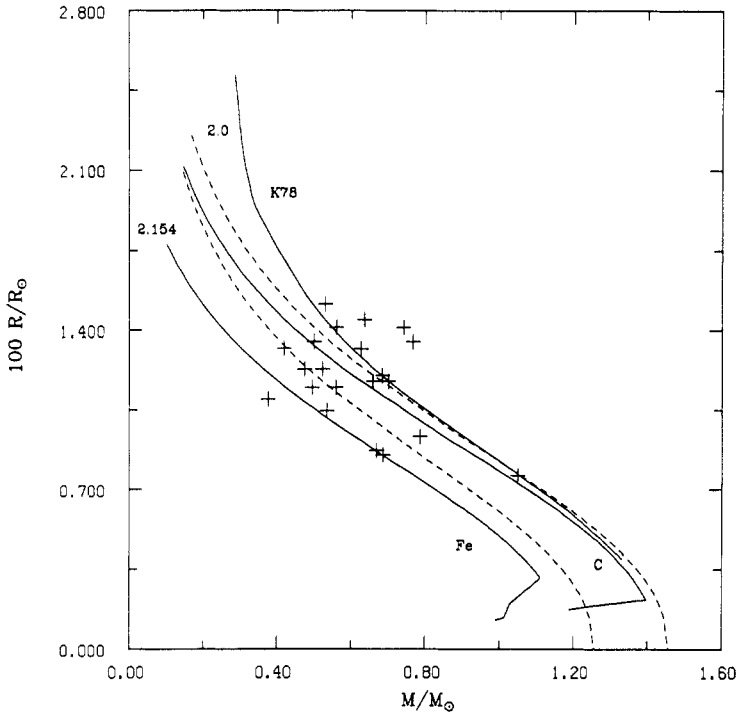

Figure 2. Mass–radius relations for white dwarfs. The two broken curves are the Chandrasekhar relations for $\mu_e = 2$ and $\mu_e = 2.15$. Continuous relations (C,Fe) are from Hamada and Salpeter (1961), and (K78) from Koester (1978) for a central temperature of 10^8 K. The best observational data available are shown as crosses.

the various contributions to the energy, normalised to the total number of heavy ions. Some useful relations are:

$$n_e = N_e/V = ZN_i/V = Zn_i = \rho Z/AH \tag{3.24}$$

where the index i stands for positive ions, and e for electrons. We will consider only a single ionic species of charge Z and atomic mass number A. Generalisations to a mixture of different ions by taking appropriate averages are straightforward but cumbersome. Instead of n_i we will sometimes use a related variable r_i, defined through

$$\tfrac{4}{3}\pi r_i^3 n_i = 1 \tag{3.25}$$

which defines the radius of sphere containing on average one ion and Z electrons.

3.3.1. The kinetic energy of the electrons. The average kinetic energy of the electrons is related to the Fermi energy, which in turn is completely determined by the matter density. In the non-relativistic limit, $\varepsilon_F = p_F^2/2m$, and (3.10) gives:

$$N_e/V = ZN_i/V = Z\rho/AH = \frac{8\pi}{3h^3}(2m\varepsilon_F)^{3/2}. \tag{3.26}$$

The kinetic energy in this case is:

$$E_e/V = \frac{4\pi}{5mh^3}\, p_F^5 = \frac{4\pi\ 2^{5/2}m^{3/2}}{5h^3}\, \varepsilon_F^{5/2}. \tag{3.27}$$

From the ratio the average electronic energy *per ion* can be derived:

$$E_e/N_i = \tfrac{3}{5} Z\varepsilon_F. \tag{3.28}$$

Similarly, in the extreme relativistic limit, $\varepsilon_F = p_F c$, and

$$N_e/V = \frac{8\pi}{3h^3c^3}\,\varepsilon_F^3 \qquad E_e/V = \frac{2\pi c}{h^3}\,p_F^4 = \frac{2\pi}{h^3c^3}\,\varepsilon_F^4 \qquad \text{and} \qquad E_e/N_i = \tfrac{3}{4} Z\varepsilon_F. \tag{3.29}$$

3.3.2. The Coulomb interaction energy. As discussed by Salpeter (1961) the electronic screening radius for an ion is of order $Z^{-1/3}a_0$, the Thomas–Fermi 'mean radius' of a free neutral atom; a_0 is the Bohr radius. If the typical separation between ions, r_i, is much less than this, as in typical white dwarfs, the electronic charge density is almost uniform and unaffected by the distribution and motion of the ions. The effective Coulomb repulsion between ions is essentially less than that for unshielded charges. The average repulsion energy between ions is a minimum for a regular lattice and, after including the attraction energy of the electrons, leads to a negative Coulomb energy E_C per ion. Keeping the ions fixed near lattice sites leads necessarily to a positive kinetic energy, the zero-temperature vibrations of the lattice. This contribution is shown to be small compared to the Coulomb energy, and neglected by Salpeter (1961).

Under these conditions the Coulomb energy for regularly distributed ions in a homogenous negative charge distribution is given by

$$E_C/N_i = -S_M \frac{(Ze)^2}{r_i} \tag{3.30}$$

where the S_M are the 'Madelung sums' and depend on the lattice geometry. Since the completely ionised ions have no preferred direction, the lowest energy lattice is a cubic lattice. The numerical values of S_M for the three cubic lattice types are 0.880059442 (SC), 0.895929256 (FCC), and 0.895873615 (BCC). The most stable form at zero-temperature is the BCC lattice, although the differences are small. The numerical values are also very close to 9/10, the Coulomb energy of a 'Wigner–Seitz sphere' (Wigner and Seitz 1934), where each lattice site is replaced by a sphere consisting of a central positive ion of charge $+Ze$ embedded in a uniform density of neutralising electrons, and the interaction *between cells* is neglected. This is the model adopted by Salpeter (1961); it is an adequate approximation for zero-temperature models.

In order to estimate the importance of Coulomb effects we may compare E_C with the electronic energy E_e. In the non-relativistic limit we have

$$E_C/E_e = -\frac{(9/10)Z^2e^2/r_i}{(3/5)Z\varepsilon_F}. \tag{3.31}$$

From (3.26), replacing the variable n_i in ε_F with r_i, we obtain

$$\varepsilon_F = \frac{9^{2/3}h^2}{2\ 32^{2/3}\pi^{4/3}m}\,Z^{2/3}/r_i^2 \tag{3.32}$$

and

$$E_C/E_e = -\frac{32^{2/3}\,9^{1/3}}{12\pi^{2/3}}\,Z^{1/3}\,(r_i/a_0) \simeq -0.8145\,Z^{1/3}\,(r_i/a_0). \tag{3.33}$$

For realistic values of Z (6 to 8) this is indeed much smaller than 1, although not negligible and by far the largest correction to the ideal Fermi gas EOS. In the relativistic limit

$$\varepsilon_F = \left(\frac{9}{32\pi^2}\right)^{1/3} hc\,Z^{1/3}/r_i \tag{3.34}$$

and

$$E_C/E_e = -\frac{(9/10)\,Z^2e^2/r_i}{(3/4)\,Z\varepsilon_F} = -\frac{6}{5}\left(\frac{4}{9\pi}\right)^{1/3}\alpha\,Z^{2/3} \simeq -0.6253\,\alpha\,Z^{2/3} \tag{3.35}$$

where α is the fine structure constant $2\pi e^2/hc$. This, too, is always a small correction.

Because the dominant contribution to the energy and pressure of the plasma is the kinetic energy of the electrons, the electron energy eigenstates are very nearly plane waves. An adequate model of the plasma therefore consists of a nearly uniform distribution of degenerate electrons with embedded classical ions. As pointed out by Salpeter (1961) the energy of the plasma can then be written as the sum of the electron kinetic energy plus correction terms, of which the Coulomb interaction is the largest:

$$E = E_e + E_C + E_{ex} + E_{TF} + E_{corr}. \tag{3.36}$$

We now turn to a discussion of the remaining terms, following Salpeter (1961).

3.3.3. Thomas–Fermi correction E_{TF}. In the evaluation of the Coulomb energy the distribution of the electrons was assumed to be homogeneous within each Wigner–Seitz 'cell'. The 'Thomas–Fermi' contribution accounts for the effect produced by the fact that the electron distribution is polarised by the positively charged ions. It could, in principle, be obtained from the equations of the Thomas–Fermi atomic model, but the solution would have to be carried through numerically for each value of Z and r_i. However, because E_C is much smaller than E_e, the perturbation of the electron density from uniformity is small, and one finds

$$E_{TF}/E_C \sim E_C/E_e. \tag{3.37}$$

It is then possible to derive this term from an expansion of the energy of the Thomas–Fermi model, with E_e and E_C as the two leading terms. The third term in this expansion is given by Salpeter (1961) as

$$E_{TF} = -\frac{162}{175}\left(\frac{4}{9\pi}\right)^{2/3}\alpha^2mc^2\,Z^{4/3}(1+x^2)^{1/2} \tag{3.38}$$

where $x = p_F/mc$ is the relativity parameter. In the extreme non-relativistic regime ($x \to 0$) this term is independent of the density (or volume) and therefore does not contribute to the pressure.

3.3.4. Exchange energy E_{ex} . This contribution arises from the fact that the electrons are indistinguishable in quantum mechanics. More precisely, one has to evaluate the interaction energy between pairs of electrons in first-order perturbation theory using antisymmetrised Dirac wave functions for the electrons. For general values of the relativity parameter this involves a complicated double integration over momentum space first carried out by Zapolski (1960), with the result

$$E_{ex} = -\left(\frac{3}{4\pi}\right)\alpha mc^2 Z\, x\, \Phi(x) \tag{3.39}$$

where

$$\Phi(x) = \frac{1}{4x^4}\left[\frac{9}{4} + 3(y^2 - y^{-2})\ln y - 6(\ln y)^2 - (y^2 + y^{-2}) - (y^4 + y^{-4})/8\right] \tag{3.40}$$

and y is given by $y = x + (1 + x^2)^{1/2}$.

3.3.5. Correlation energy E_{corr}. This is the next term after E_{ex} if the interaction energy between electrons is expanded in powers of r_i. It has been obtained by Gell-Mann and Brueckner (1957):

$$E_{corr} = (0.062\ \ln(Z^{1/3} r_i/a_0) - 0.096)\ \tfrac{1}{2}\alpha^2 mc^2 Z. \tag{3.41}$$

Salpeter (1961) discussed some other corrections — self-energy terms, the influence of internal electric fields, higher order terms in the various expansions — but generally found them to be negligible.

With the total energy thus determined (3.35), the pressure EOS is derived from

$$P = \left(\frac{\partial E}{\partial V}\right)_{N_i} = P_e + P_C + P_{TF} + P_{ex} + P_{corr}. \tag{3.42}$$

The derivative $\partial/\partial V$ can be replaced here with $\partial/\partial n_i$ or $\partial/\partial r_i$ as appropriate using (3.25) and (3.26). Explicit results for the pressure corrections are listed in Salpeter (1961) and Van Horn and Liebert (1989) and will not be repeated here.

3.4. Hamada–Salpeter zero-temperature models

The EOS derived in the previous sections was used by Hamada and Salpeter (1961) to construct zero-temperature models for white dwarfs. Because the EOS now depends explicitly on A and Z instead of μ_e only, it is necessary to specify the chemical composition of the model. According to our present understanding of the previous history we expect an interior composition of carbon and oxygen for most white dwarfs. Irrespective of this knowledge, however, the possible composition of zero-temperature models is restricted by two physical processes.

3.4.1. Pycnonuclear reactions. At sufficiently high densities the ions in a lattice can undergo nuclear reactions even at zero-temperature as a result of the quantum zero-point motions about the equilibrium lattice sites and the screening of the positive charges by the electrons. This 'pycnonuclear' regime was studied originally by Wildhack (1940), a more recent reference is Salpeter and Van Horn (1969). Formulae for the reaction rates can be found in the latter paper, and a review is given by Shapiro and Teukolsky (1983).

The critical density for the transformation of hydrogen into helium is about 1×10^6 g cm^{-3}, for C $\rightarrow$ Mg $\sim 10^{10}$; for He $\rightarrow$ C the rate is probably negligible (Shapiro and Teukolsky 1983). All these numbers are still very uncertain. For elements other than hydrogen, which is not expected in the interior of white dwarfs (Hamada and Salpeter 1961), a much faster instability occurs at about the same densities (see below). Pycnonuclear reactions are therefore not likely to be important in white dwarfs.

3.4.2. Inverse β-decays. At higher densities the Fermi energy of the electrons can exceed the mass difference between the nuclei (A, Z) and $(A + 1, Z - 1)$. It then becomes energetically favourable to 'capture' an electron onto the nucleus, transforming a proton into a neutron. The neutrinos formed in this transition can easily escape from a white dwarf. For C^{12} this instability occurs for $\rho = 3.9 \times 10^{10}$ g cm^{-3} (Wapstra and Bos 1977) and the transformation then rapidly proceeds to Ne^{24} because the intermediate nuclei have lower thresholds. Hamada and Salpeter (1961) have taken this into account by assuming that a carbon model actually consists of Ne^{24} in those regions where the density exceeds the critical value. Similarly, at very high central densities, an iron model has a central core of Cr^{56} for $\rho_c > 1.14 \times 10^9$ g cm^{-3}, and a Ti^{56} core for $\rho_c > 2.45 \times 10^{10}$ g cm^{-3}. The results of their calculations for these two model sequences in the mass–radius diagram (note that Hamada and Salpeter (1961) used slightly different values for the critical densities) are given in figure 2.

The neutronisation at extremely high densities reduces the number of free electrons and increases the molecular weight per electron μ_e, thus leading to kinks in the mass–radius relations at high masses. The Chandrasekhar limiting mass for infinite density is now replaced by a maximum mass at finite density and radius. For the 'carbon' sequence in Hamada and Salpeter's (1961) calculations this maximum mass is 1.381 $M_\odot$. It can be shown (e.g. Shapiro and Teukolsky 1983, Skilling 1968) that *homogeneous* models on the 'returning branch' with $M > M_{max}$ are dynamically unstable, although for an equilibrium equation of state maximum mass and onset of instability do not necessarily coincide exactly (Wheeler *et al* 1968, Chanmugam 1977).

3.5. Influence of general relativity

For the maximum mass carbon model, $GM/Rc^2 \simeq 1.37 \times 10^{-3}$. Even at this extreme point the effect of general relativity (GR) on the structure of white dwarfs and the shape of the mass–radius relation is very small. The mass–radius relation in GR was first derived by Kaplan (1949). GR has, however, a significant influence on the dynamical stability of high mass models. Chandrasekhar and Tooper (1964) discovered that GR leads to instability at a central density $\rho_c = 2.328 \times 10^{10}(\mu_e/2)^2$ g cm^{-3}; Shapiro and Teukolsky (1983) derive a critical value of 2.646×10^{10} $(\mu_e/2)^2$ g cm^{-3}. The radius corresponding to these densities is still much larger than the Schwarzschild radius ($\simeq$ 3.6 km). For Fe^{56} this is higher than the threshold for neutronisation, so GR is irrelevant for iron white dwarfs. For C^{12}, however, $\rho_c = 2.65 \times 10^{10}$ g cm^{-3}, lower than the neutronisation density (3.9×10^{10} g cm^{-3}), and in this case it is GR that determines

the maximum stable mass. The problem of stability will be discussed further in the section on pulsations.

It should be noted, however, that single white dwarfs are not observed with masses higher than $\simeq 1.2\ M_\odot$— they are certainly extremely rare, if they exist at all — and iron is an unlikely composition. The refinements at the high end of the mass–radius relation discussed in the preceding paragraphs are therefore at present only of theoretical interest.

3.6. Corrections at finite temperature

Zero-temperature models provide an adequate description of the overall structure of white dwarfs. However, observed white dwarfs have surface temperatures ($T_{\rm eff}$) ranging from 5000 K to over 100 000 K, and they are still losing energy, implying a temperature gradient and even higher interior temperatures. Moreover, as we will see later, their evolution is governed by their *thermal* properties. A comparison of observations with models therefore requires the calculation of finite-temperature models.

Comprehensive discussions of the EOS at finite temperatures have been given by DeWitt (1969), Kovetz and Shaviv (1970), Shaviv and Kovetz (1972), and Lamb (1974), where a thorough discussion of earlier work and many references can be found. In our presentation we will follow closely the approach taken by Lamb.

The dominant contribution to the energy and pressure at all reasonable temperatures remains that of a non-interacting Fermi gas of the electrons. The general equations have already been given in equations (3.5) through (3.8). The Coulomb contributions can be most conveniently described by two dimensionless parameters:

$$\Gamma = \frac{(Ze)^2}{r_{\rm i} kT} \qquad \text{and} \qquad \theta = \frac{\hbar\Omega_{\rm p}}{kT} = \frac{\theta_{\rm D}}{T},$$

where

$$\Omega_{\rm p} = \sqrt{\frac{4\pi n_{\rm i} Z^2 e^2}{AH}} \tag{3.43}$$

is the ion plasma frequency, and $\theta_{\rm D}$ the Debye temperature. The parameter Γ measures the Coulomb potential energy, while θ measures the importance of quantum effects. At very high temperatures the ions behave essentially as an ideal classical gas with small corrections arising from the Coulomb interactions, which for $\Gamma \leq 0.05$ can be calculated according to the Debye–Hückel theory. As the temperature falls, Γ becomes much greater than 1 and the Coulomb interactions increasingly dominate the thermal properties of the ions, forming a 'Coulomb liquid'. Eventually the ions crystallise into a solid lattice and the star approaches the zero-temperature configuration. Quantum effects become important when $\theta > 1$, and at somewhat lower temperatures the thermal energy of the ions declines rapidly until they are effectively frozen into their zero-point oscillations.

The thermodynamics in the gas/liquid and solid phases are best described by modelling their Helmholtz free energy, with the ideal Fermi energy of the electrons as the leading term and the other contributions as additive corrections. The energy and pressure can be obtained in a thermodynamically consistent way through straightforward but tedious derivation. In the following we will consider only the most important terms, which are responsible for qualitatively new effects compared

to the zero-temperature models. For a more detailed treatment, for example, the extension of the exchange and Thomas–Fermi contributions to finite temperatures, we refer the reader to Lamb (1974). The most important contributions to the free energy can be written as

$$F = F_e + F_C + F_i. \tag{3.44}$$

F_e is the electronic contribution, F_C the Coulomb potential energy, and F_i the remaining contributions of the ions, which depend on the phase.

3.6.1. Coulomb energy. The Coulomb energy can generally be written as $E_C = N_i\, kT\, f(\Gamma)$ from which the free energy can be derived using the thermodynamic relation

$$F_C = -T \int^T (E_C/T^2)\, \mathrm{d}T. \tag{3.45}$$

For sufficiently large Γ the Wigner–Seitz model gives $f(\Gamma) = -0.9\,\Gamma$. For very small Γ (< 0.05) Debye–Hückel theory (e.g. Landau and Lifshitz 1969) gives

$$f(\Gamma) = -\frac{\sqrt{3}}{2}\left(\frac{Z+1}{Z}\right)^{3/2} \Gamma^{3/2}. \tag{3.46}$$

No rigorous treatment of the intermediate range exists as yet, and it is usually treated essentially using numerical methods. As we have noted before, the distribution of the electrons is very closely homogeneous. The ions therefore behave roughly as a one-component plasma (OCP) in a uniform negatively charged background. The physics of OCPs has been studied using Monte Carlo techniques by Brush *et al* (1966), Kovetz and Shaviv (1970), Hansen (1973) and Pollock and Hansen (1973). To our knowledge the most accurate calculation to date is that of Slattery *et al* (1980). The function $f(\Gamma)$ for the intermediate range can be taken directly from these numerical experiments or fitted with analytical approximations (see e.g. Lamb 1974). Slattery *et al* (1980) give the following fit for the free energy:
In the liquid phase

$$F_C(\Gamma) = N_i kT\, (-0.89752\,\Gamma + 3.78176\,\Gamma^{1/4} - 0.71816\,\Gamma^{-1/4} + 2.19951\,\ln\Gamma - 3.30108) \tag{3.47}$$

while in the solid phase

$$F_C(\Gamma) = N_i kT\, \left(-4.29076 + 4.5\ln\Gamma - 1490/\Gamma^2\right). \tag{3.48}$$

3.6.2. Other ionic contributions. In the solid phase the temperature-dependent term in the free energy connected with the oscillations of the ion lattice, to which the zero-point contributions of Salpeter (1961) have to be added, is:

$$F_i = N_i kT \sum_\lambda \left\langle \frac{1}{2}\frac{\hbar\omega_{l\lambda}}{kT} + \ln\left[1 - \exp\left(-\frac{\hbar\omega_{l\lambda}}{kT}\right)\right]\right\rangle \tag{3.49}$$

where the $\omega_{l\lambda}$ are the frequencies of the phonon spectrum (depending on the wave vector l, tabulated for a BCC lattice by, for example, Carr (1961) and Kugler (1969)), the sum is taken over the excitation modes λ and the average over the l in the first Brillouin zone (Kovetz and Shaviv 1970, Lamb 1974). A slightly less accurate but computationally easier method uses the Debye model to describe the thermal properties of the lattice. The energy in this model is:

$$E_i = 3N_i kT D(\theta) \tag{3.50}$$

with the Debye function

$$D(\theta) = 3\theta^{-3} \int_0^{\theta} \frac{x^3 \, dx}{\exp(x) - 1} \tag{3.51}$$

and $\theta = \theta_D/T$. The free energy can be obtained as in (3.45):

$$F_i = 3N_i kT \int^{\theta_D/T} \frac{D(\theta)}{\theta} \, d\theta. \tag{3.52}$$

As is well known the energy approaches the classical limit $E_i = 3N_i kT$ for high temperatures, while for $T \to 0$ we obtain $E_i \propto T^4$ and the thermal energy rapidly decreases for $T \ll \theta_D$.

In the gas/liquid phase at high temperatures the dominant term in F_i is that for an ideal classical gas

$$F_i = -N_i kT \left[1 + \frac{3}{2} \ln \left(\frac{2\pi AHkT}{h^2} \right) + \ln V - \ln N_i \right]. \tag{3.53}$$

At high densities and low temperatures a correction for the quantum nature has also to be applied for the ions in the liquid phase, the so called 'ionic quantum correction'. It can be obtained as the first term in the Wigner (1932) expansion in terms of h^2; it is essentially an expansion in θ (Lamb 1974, Kovetz and Shaviv 1972):

$$F_{iq} = \frac{1}{24} N_i kT \theta^2 \tag{3.54}$$

which is a valid approximation for $\theta \ll 1$. Equations (3.43) through (3.54) constitute the model free energy, from which the energy, pressure and all other thermodynamic quantities can be derived.

3.6.3. Phase transitions. The transition between the liquid and the solid phase is expected to be a first-order phase transition (Lamb 1974) with an associated release of latent heat. Its location can, in principle, be obtained by equating the chemical potential (obtained from $\partial F/\partial N_i$) of the two phases. The result, however, depends sensitively on the approximations used in the EOS and various authors have obtained values of Γ_m (the Coulomb parameter at crystallisation) ranging from ~ 60 to ~ 170. Because of this uncertainty it has become customary to regard Γ_m as a free parameter, but $\Gamma_m = 160$, close to the result obtained by Lamb (1974), seems to be the preferred choice at present. This is supported by the result of Slattery *et al* (1980), who obtained 168 ± 4 from their OCP calculations. The latent heat released can then be calculated from the entropy difference of the two phases at this point.

Cesare *et al* (1973) have suggested that a similar phase transition should exist at $\Gamma \approx 1$ between the gaseous and the liquid phase. The OCP calculations, however, which should give an excellent approximation in this range, show no indication of a first-order phase transition, and Lamb (1974) has given strong theoretical arguments that a smooth transition is expected from a region exhibiting no order to one exhibiting short-range order.

The different regions relevant for the EOS in a temperature–density diagram are displayed in figure 3 together with the approximate location of white dwarfs with $M = 0.6\ M_{\odot}$ and central temperatures of 10^7 and 10^6 K.

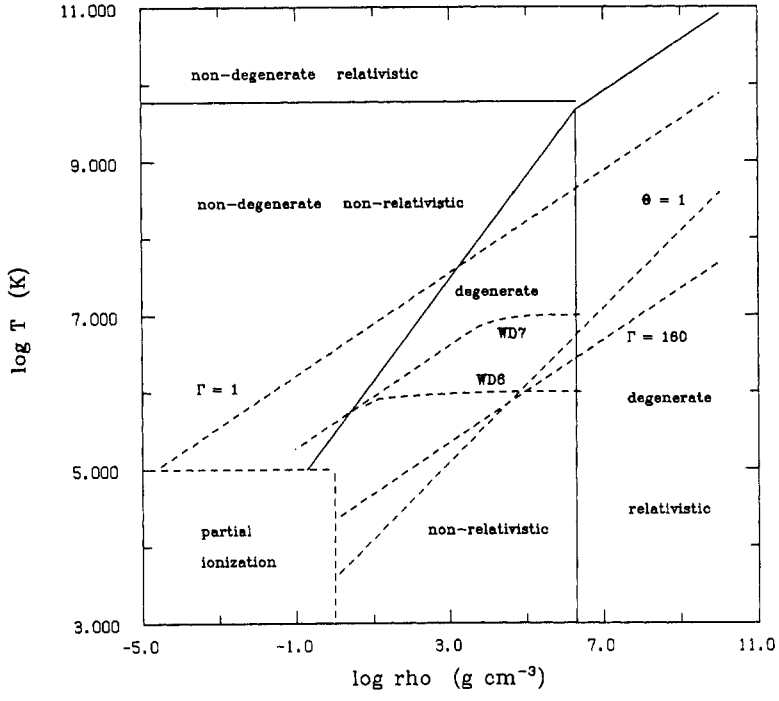

Figure 3. Temperature–density diagram for completely ionised carbon. The lower left corner, bounded approximately by the broken lines, is the region of incomplete ionisation and not considered here. The continuous straight lines are the boundaries between relativistic/non-relativistic, respectively degenerate/non-degenerate regions. Broken straight lines limit the regions where quantum ($\theta = 1$) or Coulomb ($\Gamma = 1, 160$) effects for the ions become important. The broken curved lines labelled WD6 and WD7 show the approximate structure for the interior 99% of the mass of 0.6 $M_{\odot}$ white dwarf models (the outer 1% is not shown) with central temperatures of 10^7 and 10^6 K. These calculations were done for the work in Koester (1978), but not published.

3.6.4. Construction of models at finite temperature. If the pressure is no longer a function of ρ alone but also of T, the full set of four equations describing the structure of a star has to be used (e.g. Clayton 1968). In addition to (3.15) and (3.16) these are the equations for the energy transport mechanism and energy generation. The energy

transport mechanism determines the temperature gradient:

$$\frac{dT}{dr} = \frac{3\kappa\rho}{16\sigma T^3}\frac{L_r}{4\pi r^2} \tag{3.55}$$

where L_r is the total energy flow through the sphere with radius r, and κ is the opacity coefficient. In the interior of a white dwarf heat conduction by the highly degenerate electrons is the dominant mechanism, leading to a very small temperature gradient and an almost isothermal interior, a fact exploited widely by early calculations of white dwarf evolution. Conductive opacities have been calculated by Marshak (1940), Mestel (1950), Lee (1950), Hubbard and Lampe (1969), Canuto (1970), Urpin and Yakovlev (1980), and Itoh *et al* (1983, 1984). If the electrons are not extremely degenerate, radiative energy transport becomes important. The calculation of all the relevant absorption coefficients is a formidable task that in the past has mainly been pursued by groups at the Los Alamos Laboratory (Cox and Stewart 1970, Huebner *et al* 1977).

In the outer layers of cool white dwarfs convective energy transport may become dominant and the temperature gradient has to be determined from the mixing length approximation (e.g. Böhm–Vitense 1958).

The boundary condition to (3.55) can be applied in several different forms, a typical one being

$$T(R) = T_{\rm eff} = \left(\frac{L}{4\pi\sigma R^2}\right)^{1/4} \tag{3.56}$$

at the surface.

The last equation to be used describes the energy generation in a spherical shell of inner and outer radii r, $r + dr$:

$$\frac{dL_r}{dr} = \left(\varepsilon_{\rm N} - \varepsilon_\nu - T\frac{\Delta s}{\Delta t}\right) 4\pi r^2\rho \tag{3.57}$$

where $\varepsilon_{\rm N}$ is the energy generation rate due to nuclear processes and normally negligible in white dwarfs; ε_ν is the energy loss due to neutrinos leaving the star without being absorbed again. The quantity $T\Delta s/\Delta t$ is the change in heat content of the shell from a previous model at time $t - \Delta t$. It is the most important term for white dwarf evolution as we will see later. The boundary condition for this equation is $L_r(0) = 0$ at $r = 0$.

In addition to M a second parameter, besides composition, is now necessary to specify a model, which is usually taken to be the total luminosity L. The most significant formal difference to zero-temperature models, however, is that a model now depends on the previous evolution through (3.57). An accurate treatment therefore requires the complete methods of stellar evolution calculations, starting at much earlier phases in the life of the star. Due to the heavy demands on computing power this has been attempted on a broader basis only during the last five years. In the previous twenty years it was customary to make simplifying assumptions in order to determine the temperature distribution within the model. One such possibility is to integrate equation (3.55) from the surface inwards, assuming $L_r = L =$ constant, until the temperature gradient becomes very small and can be set to zero until the centre is reached. The main emphasis in these calculations was on the evolution of white dwarfs. Koester (1978) studied the influence of finite temperatures on the mass–radius relation; his result for an interior temperature of 10^8 K is presented in figure 2.

3.6.5. Comparison with observed masses and radii. Finally, figure 2 also shows a comparison with observed data. With the exception of very few objects in binary systems (the most massive object in figure 2 is Sirius B) the most reliable masses can now be obtained from gravitational redshifts. These redshifts give the ratio M/R, the radii are obtained from effective temperatures and distances using relation (2.1) as explained in section 5. The data in the figure are from Koester (1987b), Wegner *et al* (1989), and Wegner (1989b). While they definitely rule out a hydrogen interior (the relation would be far outside the range of the figure), any discrimination between the different relations (e.g. different compositions other than hydrogen) is lost in the scatter. This scatter is very probably due to observational errors: typical uncertainties are 15% for the radius and 20% for the mass.

4. Stellar evolution and white dwarfs

The theory of stellar evolution is an immense and very active field of study and we cannot hope to report even the major results adequately in this review. Instead we will try to give a very brief description of the prehistory of a typical white dwarf and refer the reader interested in more details to the excellent reviews of some of the leading experts (Iben 1967, 1974, Iben and Renzini 1983).

The main phases in the life of a star are best visualised in the Hertzsprung–Russell diagram of figure 4. The full lines in this diagram trace the position of a star (model) as a function of time and are called 'evolutionary tracks'. The present diagram is intended only for a qualitative description. The tracks are based on actual calculations (Mengel *et al* 1979, Sweigart and Gross 1978, Schönberner 1979, Koester and Schönberner 1986); they do not, however, use exactly the same chemical abundances and input physics in the various calculations.

4.1. Prehistory of a typical white dwarf

After a star has completed its contraction from interstellar matter it enters the major phase of its life on the main sequence (MS). On the MS a star is chemically homogenous, at least at the very beginning, and derives its energy from the nuclear burning of hydrogen to helium at the centre. The part of the MS shown in the figure refers to the range of stellar masses between 0.7 $M_\odot$ (lower end) and 3.5 $M_\odot$ (high end). The evolutionary track shown is calculated for 1 $M_\odot$. Due to the high energy gained from the transformation of hydrogen to helium and the high abundance of hydrogen ($\simeq$ 90% by numbers) this is a very long lived phase and takes of the order of 8×10^9 yr for a solar mass star. During this phase the luminosity increases slowly.

When $\simeq$ 12% of the mass has been transformed to helium at the centre, a major structural change occurs. Because hydrogen is depleted at the centre, nuclear energy generation now takes place in a spherical shell surrounding the inert helium core. This change is accompanied by an expansion and cooling of the outer layers of the star: in the HRD the star moves to the right and upward to greater radii. This part of the track is therefore called the red giant branch (GB). At the top of the GB the star reaches at the centre the conditions necessary to ignite helium and start the next nuclear process, transforming helium into carbon and oxygen.

In a low mass star like our sun the density at the centre at this point is so high that the electrons are partially degenerate. In non-degenerate matter the increase in temperature caused by the new energy source would be accompanied by an increase

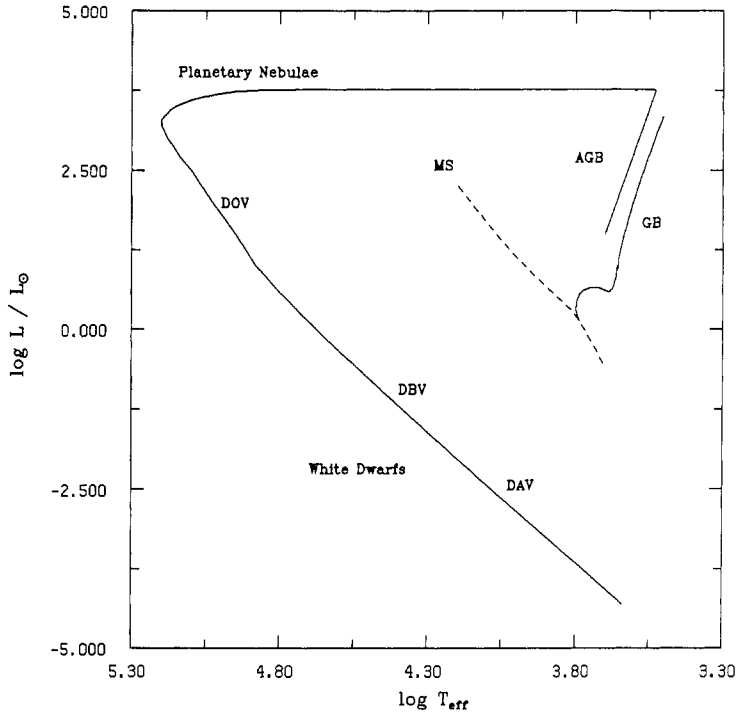

Figure 4. Qualitative description of the prehistory of a typical white dwarf.

in pressure, leading to expansion, cooling and stabilisation of the helium burning rate. However, due to the degeneracy, no significant change in pressure results; the increased temperature leads to further energy release and a thermal runaway develops. This phenomenon is called the 'helium flash'; it leads to a dynamic restructuring of the star after the degeneracy is lifted at high temperature.

When the star has adjusted to the new conditions it finds itself near the bottom of the sequence labelled AGB ('asymptotic giant branch'), quietly burning helium at the centre under non-degenerate conditions. Once helium is exhausted in the core, evolution follows a pattern similar to the departure from the main sequence: helium burns in a shell surrounding the inert carbon/oxygen core and the star moves again up and right on the AGB.

At the top of the AGB the star undergoes another instability, which leads to the expulsion of most of the remaining hydrogen-rich outer envelope (~ 0.2–$0.3\ M_\odot$). We do not yet understand this process, which might be a continuous, very strong mass loss rate sustained over a few thousand years, or a singular event. In any case, when the remaining envelope mass fraction is reduced to $\sim 10^{-3}$ the remnant star moves rapidly to the left in the HRD, on the way exciting and ionising the previously expelled matter around it because of its high surface temperature. This becomes visible as a planetary nebula, a luminous cloud of gas, with the hot central star, the previous core of the red giant (not always visible), supplying the ionising photons. When the remaining hydrogen layer is decreased to $\sim 10^{-4}\ M_\odot$ nuclear energy generation comes to a halt. The luminosity decreases rapidly and the star enters the final phase of its life as a white dwarf. At about this time the nebula around it is expanded and diluted

so much as to become unobservable.

The white dwarf is left with only gravitational and thermal energy sources available. Because the electrons are already degenerate in the interior at this stage, the radius is not far from the radius of the zero-temperature model and the remaining contraction is small. The star thus evolves roughly at a constant radius along the diagonal straight line given by equation (2.1) in the white dwarf region of the HRD.

Many important differences occur in physical details of the evolution of higher mass stars in the range $\sim$ 1–8 $M_\odot$, but the final outcome is qualitatively the same. Very high mass stars (say 10 $M_\odot$), however, have a different destiny. In these stars electron degeneracy never becomes important at the centre, the temperatures become high enough to ignite carbon and all the following nuclear burning phases up to iron, on rapidly decreasing time scales. The final fate of such a star is a supernova explosion leaving a neutron star, or possibly (in some cases) a black hole or nothing, if the star is totally disrupted.

4.2. Which stars become white dwarfs?

The maximum mass of a carbon white dwarf is $\simeq 1.4\ M_\odot$, the low mass star described above will have no difficulty in reaching this final stage. There is, however, convincing evidence today that stars with initially (on the MS) much higher masses also manage to reach this stage. Direct evidence comes from the observation of stellar clusters, groups of stars with different masses, born at the same time. The luminosity on the MS increases much more steeply than the mass; a massive star therefore needs a shorter time to consume its fuel and start the evolution towards the giant branches and the final stages. The main sequences of clusters burn away from the top in the HRD, and the most massive stars still remaining on the MS ('turn-off point' in astronomical jargon) are an indication of the age of the cluster. In the famous Hyades cluster for example, stars with $M = 2\ M_\odot$ are still on the MS; nevertheless the cluster contains about a dozen white dwarfs! These white dwarfs have typical masses of 0.6 $M_\odot$, but on the MS they must have been more massive than the turn-off point, or they would not have evolved.

The solution to this puzzle is mass loss during the evolution. Even a normal star like our sun shows a continuous mass loss (solar wind); in the red giants the observed mass loss is many orders of magnitude larger (see, e.g., Reimers 1987). This mass loss obviously is large enough to bring fairly massive stars down to the white dwarf range. What then determines the final fate of a star?

Very massive stars end their lives as supernovae, whereas low mass stars certainly form white dwarfs. In a first approximation it is therefore reasonable to assume that the initial mass on the MS is the determining parameter, with all stars below a critical mass $M_{\rm cr}$ becoming white dwarfs. One possible way to determine this critical parameter is to include mass loss (in a parametrised form, commonly that due to Reimers (1975, 1987) and Iben and Renzini (1983)) in stellar evolution calculations (the AGB branch in figure 4 includes mass loss, which reduces the original 1 $M_\odot$ to $\simeq$ 0.6 $M_\odot$ at the top of the AGB). Mass loss on the AGB was first considered by Mengel (1976) and Fusi-Pecci and Renzini (1976), and fully incorporated into the evolutionary calculations by Schönberner (1979) and many others since. A typical result for the critical mass is $\simeq 5\ M_\odot$. A difficulty of this approach is that while mass loss rates are fairly well known for the lower part of the giant branch, the extrapolation to the high luminosity region, where most mass is lost, is very uncertain.

A more empirical method compares the supernova rates (for type II supernovae, believed to originate from high mass stars) with the birth rate of massive stars. Unfortunately the supernova rate is very uncertain, and Tammann (1974) was only able to determine a range of 5 to 10 $M_\odot$ for M_{cr}. More recently, Kennicutt (1984) found $8 \pm 1\ M_\odot$ for external galaxies (of type Sc).

The most direct empirical approach is based on the consideration of stellar clusters as previously mentioned. This method was first used by van den Heuvel (1975) for the Hyades cluster, and extended by Romanishin and Angel (1980). Since then Koester and Reimers have made a systematic search for white dwarfs in young clusters with as high turn-off masses as possible (Koester and Reimers 1981, 1985, Koester 1982, Reimers and Koester 1982, 1988a,b, 1989). Their best estimate for the value of the critical mass currently is 8 (+3,−2) $M_\odot$. In addition to the maximum mass for a star that can become a white dwarf, these observations can also help to establish a relation between the initial mass on the MS and the final mass of the remnant white dwarf, thus integrating the total mass loss during the stellar life. This relation has been studied extensively by Weidemann (Weidemann and Koester 1983); recent discussions, using not only white dwarf observations, are given in Weidemann (1987) and Weidemann and Yuan (1989). The scatter in this relation, which is certainly to a large degree observational, is considerable, but it nevertheless indicates, that the remnant of a massive star is a more massive white dwarf and vice versa. Typically a 8 $M_\odot$ star seems to lead to a remnant of $\sim 1.15\ M_\odot$, a 1 $M_\odot$ star to one of $\simeq 0.5\ M_\odot$, but the relation is probably not linear for the intermediate masses (Weidemann 1987).

In conclusion, it is generally accepted today that fairly massive stars, possibly up to 8 $M_\odot$, will finally end up as white dwarfs. Comparing this limit with the mass distribution on the MS at birth, this means that certainly more than 90% of all stars will become white dwarfs.

4.3. White dwarf evolution

Following Mestel (1952), Mestel and Ruderman (1967), Van Horn (1971), Lamb and Van Horn (1975), Koester (1978) we will, in this section, study the energy balance of white dwarfs using the classical assumption that nuclear energy is no longer available. We will return later to a discussion of this point.

4.3.1. Energy balance. Using equations (3.16) and (3.57) we may write the luminosity equation:

$$\frac{\mathrm{d}L_r}{\mathrm{d}m} = -\varepsilon_\nu - T\frac{\Delta s}{\Delta t}. \tag{4.1}$$

Integrating over the whole star it follows that

$$\begin{aligned} -(L - L_\nu)\Delta t &= \int_0^M T\Delta s\,\mathrm{d}m = \int_0^M \Delta u\,\mathrm{d}m + \int_0^M P\Delta\rho^{-1}\,\mathrm{d}m \\ &= \Delta U + \int_0^M P\Delta\rho^{-1}\,\mathrm{d}m. \end{aligned} \tag{4.2}$$

Extensive thermodynamic quantities in lower case letters are defined per unit mass, those using capitals refer to the whole star, for example U and u are the internal energy. The limits in the following integrals are all 0 and M. The lefthand side must

be equal to the total energy $\Delta E = \Delta U + \Delta\Omega$ lost during the time step Δt, where Ω is the gravitational energy, thus the second term above can be identified with $\Delta\Omega$. Now, assuming the internal energy to be a function of ρ and T, we may write

$$\Delta U = \int \Delta u dm = \int \left(\frac{\partial u}{\partial T} \Delta T + \frac{\partial u}{\partial \rho} \Delta \rho \right) \mathrm{d}m. \tag{4.3}$$

Using the thermodynamic relation $-\rho^2 \partial u/\partial \rho = T\partial P/\partial T - P$ we get

$$\begin{aligned} \Delta U &= \int \frac{\partial u}{\partial T} \Delta T \, \mathrm{d}m + \int T \frac{\partial P}{\partial T} \Delta \rho^{-1} \, \mathrm{d}m - \int P \Delta \rho^{-1} \, \mathrm{d}m \\ &= \Delta U_{\mathrm{th}} + \Delta E_{\mathrm{grav}} - \Delta\Omega. \end{aligned} \tag{4.4}$$

The total energy change is thus, somewhat artificially, divided into two parts stemming from the temperature and density changes respectively:

$$\Delta E = \Delta U_{\mathrm{th}} + \Delta E_{\mathrm{grav}}. \tag{4.5}$$

A further relation between the different energy forms can be obtained from the hydrostatic equations. Multiplying by $4\pi r^3 \mathrm{d}r$ and integrating over the whole star, using the appropriate boundary conditions, we get

$$3 \int \frac{P}{\rho} \, \mathrm{d}m = -\Omega. \tag{4.6}$$

This is the virial theorem, applied to a star in hydrostatic equilibrium. In a normal star the EOS is well approximated by the ideal gas law $P \propto \rho T$, and $P/\rho = \frac{2}{3} u_{\mathrm{th}}$. In this case we have

$$\begin{aligned} &\Delta E_{\mathrm{grav}} = \int P \Delta \rho^{-1} \, \mathrm{d}m = \Delta\Omega \\ &\Delta U_{\mathrm{th}} = -\tfrac{1}{2} \Delta\Omega \\ &\Delta E = \tfrac{1}{2} \Delta\Omega = -\Delta U_{\mathrm{th}} \end{aligned} \tag{4.7}$$

a well known result: energy loss ($\Delta E < 0$) necessarily leads to gravitational contraction. One half of the released gravitational energy is radiated away, the other half increases the internal energy and temperature (because the internal energy is thermal energy in this case).

How does this picture change for white dwarfs? For simplicity we will consider here only the highly degenerate, moderately high Γ, and non-relativistic state of matter, typical of the bulk of the matter in a normal white dwarf. The ions are considered as an ideal gas and we include only the Coulomb corrections, therefore $P = P_{\mathrm{e}} + P_{\mathrm{i}} + P_{\mathrm{C}}$. From an expansion of (3.5) for $\eta \gg 1, \beta \ll 1$ we find for the electron contribution $P_{\mathrm{e}} = (2/5) Z \eta P_{\mathrm{i}}$, while at high Γ the Coulomb contribution is $P_{\mathrm{C}} = -0.3 \Gamma P_{\mathrm{i}}$. The corresponding energies are given by:

$$u_{\mathrm{e}} = \frac{3}{2} \frac{P_{\mathrm{e}}}{\rho} \qquad u_{\mathrm{i}} = \frac{3}{2} \frac{P_{\mathrm{i}}}{\rho} \qquad \text{and} \qquad u_{\mathrm{C}} = 3 \frac{P_{\mathrm{C}}}{\rho}. \tag{4.8}$$

With these assumptions we find

$$\Delta E_{\rm grav} = \int T \left(\frac{\partial P_{\rm e}}{\partial T} + \frac{\partial P_{\rm i}}{\partial T} + \frac{\partial P_{\rm C}}{\partial T} \right) \Delta \rho^{-1} \, {\rm d}m. \tag{4.9}$$

The last term in the bracket is 0, the first is of order $1/\eta^2$ and will be neglected, because the second is $O(1/\eta)$. Hence,

$$\begin{aligned} \Delta E_{\rm grav} &= \int P_{\rm i} \Delta \rho^{-1} \, {\rm d}m = \int \frac{P_{\rm i}}{P_{\rm i} + P_{\rm e} + P_{\rm C}} P \Delta \rho^{-1} \, {\rm d}m \\ &= \int \frac{P \Delta \rho^{-1} \, {\rm d}m}{1 - 0.3\Gamma + \frac{2}{5} Z\eta} = \left\langle \frac{1}{1 - 0.3\Gamma + \frac{2}{5} Z\eta} \right\rangle \Delta \Omega. \end{aligned} \tag{4.10}$$

The average is defined by this equation. In a 0.6 $M_\odot$ white dwarf at a central temperature of 10^7 K, $\Gamma \simeq 55$, $\eta \simeq 350$, and the quantity within the bracket is $\ll 1$.

How does this compare with the release of thermal energy? From the virial theorem, using our approximations for the EOS, we find

$$\Delta U_{\rm e} + \Delta U_{\rm i} + \tfrac{1}{2} \Delta U_{\rm C} = -\tfrac{1}{2} \Delta \Omega. \tag{4.11}$$

Using our knowledge of the EOS, we may also determine the changes directly. Because $\partial u_{\rm C}/\partial T = 0$, and $\partial u_{\rm i}/\partial \rho = 0$,

$$\int \Delta(u_{\rm e} + u_{\rm i}) \, {\rm d}m = \Delta U_{\rm th} + \int \frac{\partial u_{\rm e}}{\partial \rho} \Delta \rho \, {\rm d}m. \tag{4.12}$$

Up to first order in $1/\eta$, $\partial u_{\rm e}/\partial \rho = P_{\rm e}/\rho^2$, and

$$\begin{aligned} \Delta U_{\rm e} + \Delta U_{\rm i} &= \Delta U_{\rm th} - \int P_{\rm e} \Delta \rho^{-1} \, {\rm d}m \\ &= \Delta U_{\rm th} - \int P \Delta \rho^{-1} \, {\rm d}m + \int \frac{P_{\rm i} + P_{\rm C}}{P_{\rm e} + P_{\rm i} + P_{\rm C}} P \Delta \rho^{-1} \, {\rm d}m \\ &= \Delta U_{\rm th} - \left(1 - \left\langle \frac{1 - 0.3\Gamma}{1 - 0.3\Gamma + \frac{2}{5} Z\eta} \right\rangle \right) \Delta \Omega. \end{aligned} \tag{4.13}$$

Similarly

$$\int \Delta u_{\rm C} \, {\rm d}m = \int \frac{\partial u_{\rm C}}{\partial \rho} \Delta \rho \, {\rm d}m = - \int P_{\rm C} \Delta \rho^{-1} \, {\rm d}m = \left\langle \frac{0.3\Gamma}{1 - 0.3\Gamma + \frac{2}{5} Z\eta} \right\rangle \Delta \Omega. \tag{4.14}$$

Collecting the terms from the virial theorem we finally get

$$\Delta U_{\rm th} = \left(\frac{1}{2} - \left\langle \frac{1 - 0.3\Gamma}{1 - 0.3\Gamma + \frac{2}{5} Z\eta} \right\rangle - \frac{1}{2} \left\langle \frac{0.3\Gamma}{1 - 0.3\Gamma + \frac{2}{5} Z\eta} \right\rangle \right) \Delta \Omega. \tag{4.15}$$

Together with the equation for the total energy loss (4.5) and equation (4.10) this result can be interpreted in the following way:

(i) Energy loss is also accompanied by gravitational contraction in this case, and roughly one half of the gravitational energy supplies the luminosity (for $\Gamma = 0$ this would be exactly $\frac{1}{2}$).

(ii) The thermal energy and thus the temperature decrease. Because $E_{\rm grav}$ is small, equation (4.5) can be interpreted as showing that the white dwarf loses energy at the expense of its thermal energy. For this reason white dwarf evolution can be described as 'cooling'.

(iii) Unfortunately this terminology has led to much confusion in the literature and to statements of the kind: 'A white dwarf ... cannot contract and release gravitational potential energy because of the great pressure of the degenerate-electron gas. Thus its only source of energy is the thermal energy ...' (Abell *et al* 1987). This is completely wrong, as (4.15) shows. The change in gravitational energy is comparable to the total energy loss, and only the fact that $\Delta\Omega \propto \Delta R/R^2$, and that R is very small, makes the resulting radius change nearly unobservable.

The half of the gravitational energy that is not radiated away increases the internal energy as in normal stars. Very approximately, for high η, $\Gamma = 0$, we have:

$$\Delta U_{\rm i} \approx \tfrac{1}{2}\Delta\Omega \approx \Delta E \qquad \Delta E = \Delta U_{\rm i} + \Delta U_{\rm e} + \Delta\Omega \qquad \text{and} \qquad \Delta U_{\rm e} \sim -\Delta\Omega. \tag{4.16}$$

Thus, while the ionic energy decreases, the electronic (Fermi) energy increases by twice that amount and the total internal energy increases by $-\frac{1}{2}\Delta\Omega$.

4.3.2. White dwarf cooling. Equation (4.5) and the fact that $\Delta E_{\rm grav}$ is $O(1/\eta)$ suggest a very simple approach to the evolution of white dwarfs, proposed originally in a pioneering paper by Mestel (1952). If we neglect the gravitational energy release and the neutrino emission, and assume that the thermal heat content can be described as a function of $T_{\rm C}, M, A$, we have

$$L = -\frac{{\rm d}U_{\rm th}}{{\rm d}t} = -\frac{\partial U_{\rm th}}{\partial T_{\rm C}}\,\frac{{\rm d}T_{\rm C}}{{\rm d}t} = -\langle c_v\rangle\, M \frac{{\rm d}T_{\rm C}}{{\rm d}t}. \tag{4.17}$$

Here the average $\langle c_v\rangle$, as defined by the above equation, can be calculated from the temperature and density structure of a model.

To solve this equation we need another relation between L and $T_{\rm C}$, which can be obtained from an integration of the structure equations as described in the previous section. Using an analytic approximation for the opacity (Kramer's law) Mestel (1952) found:

$$\frac{L}{M} = a\, T_{\rm C}^{b} \simeq 1.138\ 10^{-27}\, T_{\rm C}^{3.5} \quad L_\odot/M_\odot. \tag{4.18}$$

Later papers using better opacity approximations and taking into account convection in the outer layers have usually obtained slightly smaller values for the exponent, e.g. 2.3 (Ostriker and Axel 1969), 2.7 (Van Horn 1968), 1.8–2.6 (Lamb and Van Horn 1975). Koester (1976) gives the following fit:

$$\frac{L}{M} = 9.743\ 10^{-21}\, T_{\rm C}^{2.56} \quad L_\odot/M_\odot. \tag{4.19}$$

With such a relation at hand the simple differential equation (4.17) can be solved easily, assuming $\langle c_v\rangle$ = constant:

$$t - t_0 = \frac{\langle c_v\rangle M^{1-1/b}}{a^{1/b}} \left(L^{1/b-1} - L_0^{1/b-1}\right). \tag{4.20}$$

Here $t - t_0$ is the time needed to cool from luminosity L_0 to L, the so called 'cooling age'. Mestel's (1952) fundamental result can be derived from this with the following simplifications:

(i) the electronic contribution to c_v, which is $O(1/\eta)$ is neglected and the ions are treated as an ideal gas with $c_v = \frac{3}{2}k/AH$; and

(ii) the luminosity L_0 at $t_0 = 0$ is assumed much higher than L such that the second term can be neglected.

With these assumptions the result is:

$$t = \text{constant} \times L^{-5/7}. \tag{4.21}$$

Using (4.18) and the specific heat for $A = 12$ one finds typical cooling ages for the faintest observed white dwarfs ($L \sim 10^{-4.5}\ L_\odot$) of 10^{10} yr. With similar assumptions, but a and b from Koester (1976), the cooling time is

$$t = \frac{10^8}{A}\left(\frac{M}{M_\odot}\right)^{0.609}\left(\frac{L}{L_\odot}\right)^{-0.609} \quad \text{yr.} \tag{4.22}$$

The time spent in the white dwarf phase thus turns out to be a major phase in stellar life, longer than the MS life time for all but the smallest masses that have had time to evolve.

Mestel and Ruderman (1967) were the first to realise that the inclusion of Coulomb effects and crystallisation must have a significant effect on cooling times. Because in the lattice phase $c_v \simeq 3k/AH$, cooling ages at the same luminosity would be increased by a factor of two. On the other hand, if T_C drops below the Debye temperature, $c_v \propto T^3$ and the decrease in heat capacity should lead to much more rapid (Debye) cooling. Similar calculations, following Mestel (1952) and Mestel and Ruderman (1967), have been made by a large number of authors, using increasingly sophisticated treatment of the outer layers important for the $L(T_C)$ relation and the interior EOS (c_v) (Van Horn 1968, Koester 1972, 1976, Sweeney 1976, Lamb and Van Horn 1975, D'Antona and Mazzitelli 1979). While these calculations greatly improved our understanding of white dwarf evolution, especially of the processes in the outer, non-degenerate layers, they suffer from several drawbacks, if the desired degree of reality is set ever higher. The problems with the simple approximations are:

(i) The release of gravitational energy depends on the previous history of the star, especially strongly in the very early phases at high luminosities. If these are to be described adequately a very realistic starting model is needed. This can only be obtained by following the complete evolutionary history, ideally from the MS, but at least from the bottom of the AGB.

(ii) The basic structure expected in a white dwarf consists of a carbon/oxygen core (the remains of helium burning) surrounded by a helium layer (left behind by the hydrogen burning shell) and an outer, largely unchanged hydrogen-rich envelope. The masses and chemical composition in these outer shells have a significant influence on the subsequent evolution, but again, they can only be determined from realistic stellar evolution calculations.

It thus became apparent in the last five years that progress can now only be made by using the full apparatus of stellar evolution theory and calculating the complete track through the AGB and the planetary nebula stage, including mass loss and a detailed EOS as learned over the past two decades. Such calculations were initiated by

Iben and Tutukov (1984), and followed by Iben and MacDonald (1985, 1986), Koester and Schönberner (1986), and Mazzitelli and D'Antona (1986). Two examples for cooling curves $L(t)$ taken from these papers, with the sources, are given in figure 5. All curves are for a 0.6 $M_\odot$ white dwarf and the times have been renormalised to give (arbitrarily) 10^6 yr at $L = 10\ L_\odot$. At first sight it is truly remarkable how well the most modern calculations agree with the simple Mestel result. This agreement is, however, somewhat accidental because several of the improvements in theory have opposite effects on the cooling curves and tend to cancel when averaged over the whole evolutionary time span. Let us look somewhat more closely at the differences between Mestel (1952) and the modern results.

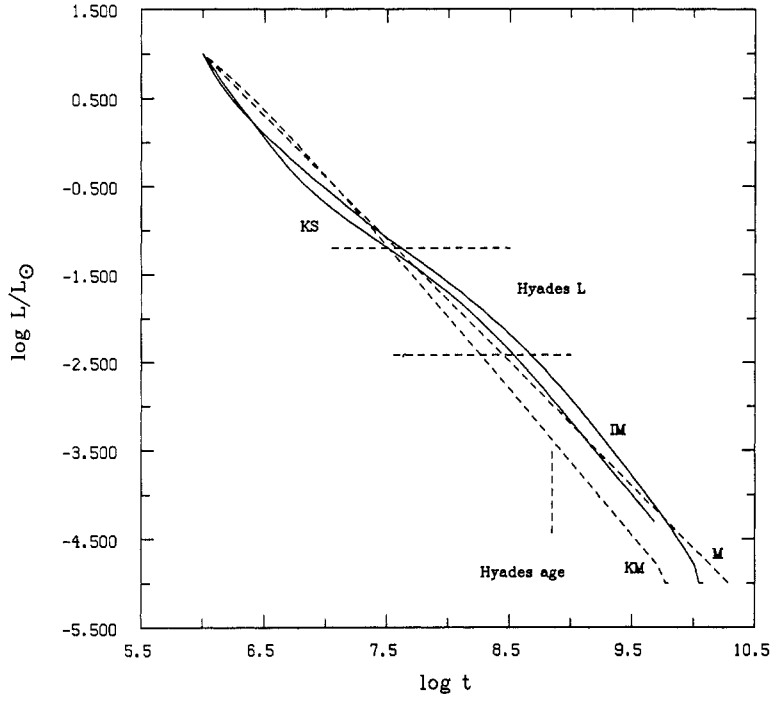

Figure 5. Cooling of white dwarfs with 0.6 $M_\odot$. Continuous lines: IM, Iben and MacDonald (1985); KS Koester and Schönberner (1986). Broken lines: simple models based on Mestel (1952) (M) and equation (4.20) with numbers a and b from Koester (1976). See text for further explanations.

At high luminosities and central temperatures energy is lost from the star not only in the form of photons, but also through the emission of neutrinos and for $\log L/L_\odot > -1$ this is the dominant mechanism. There are four processes that lead to the emission of neutrinos at high densities and temperatures: photo, pair, plasma and bremsstrahlung neutrino processes. Under the conditions prevailing in hot white dwarfs the plasma–neutrino process is usually dominant. In a plasma a photon may be considered, as a result of collective interactions with the plasma, to gain an effective mass ('plasmon') so that it decays into an e^+e^- pair and subsequently into a $\nu_e\overline{\nu}_e$ pair. Itoh (1989) has recently discussed the energy loss rates in a review paper, which also contains many references and formulae.

Because neutrino emission provides an additional energy loss mechanism its effect is to accelerate the cooling and thus steepen the $L(t)$ relation. This effect is only partly compensated for by energy sources not taken into account by Mestel: electronic thermal energy and gravitational energy release $E_{\rm grav}$.

Below $\log L/L_\odot \sim -1$ neutrino losses become negligible and the cooling slows down, 'overtaking' the Mestel curve. For $\log(L/L_\odot)$ between -2 and -3 Coulomb interactions become more and more important, increasing c_v, until below $\log L/L_\odot \sim -3$ the crystallisation starts at the centre, moving outward in a crystallisation front as the temperature drops. The final steep drop below $\log L/L_\odot \sim -5$ marks the onset of the 'Debye cooling' phase. From here on evolution would proceed rapidly, but it is doubtful whether any white dwarf has yet reached this stage.

4.3.3. The role of nuclear burning. Iben and Tutukov (1984) drew attention to the fact that the common neglect of nuclear energy generation might not be justified. The role of hydrogen burning as a major energy source ceases long before the beginning of the sequences in figure 5. However, it never stops completely and although the rate drops continuouslly, the other sources drop faster. Thus, in the phase between 10^8 and 2×10^9 yr, hydrogen burning again becomes the dominant energy source (Iben and Tutukov 1984). Similar results were obtained by Mazzitelli and D'Antona (1986), while Koester and Schönberner (1986) found this contribution to be always below 12%.

These differences can be traced back to differences in the mass of the remaining hydrogen-rich layer. It is well known that the hydrogen-burning rate drops significantly once the hydrogen-mass has decreased to the order of $10^{-4}\ M_\odot$ (e.g. D'Antona and Mazzitelli 1979), because the density and temperature at the base of the hydrogen envelope become too low. The precise rate, however, depends strongly on the exact amount of hydrogen left. In Iben and Tutukov (1984) this is $1.5 \times 10^{-4}\ M_\odot$, while Koester and Schönberner (1986) find $0.9 \times 10^{-4}\ M_\odot$. This tiny difference is responsible for the different role of hydrogen burning.

The hydrogen-envelope mass thus turns out to be a very important parameter. Unfortunately it is not only changed by nuclear burning from the interior but also by mass loss — during the formation of the planetary nebula and in later phases. The formation of the nebula is very poorly understood and we do not know whether the modelling in stellar evolution calculations is very realistic. Some central stars of planetary nebula show very high mass-loss rates in the range 10^{-10}–$10^{-7}\ M_\odot$ yr (Hamann *et al* 1984, Perinotto 1987, Hutsemékers and Surdej 1989), and mass loss is also inferred from observations of hot white dwarfs (Bruhweiler and Kondo 1983) but the dependence on stellar parameters is not known. It is, therefore, doubtful, in our opinion, whether evolutionary calculations can predict the remaining envelope with any reliability.

On the other hand there are three independent arguments — pulsational stability, EUV observations of white dwarfs, and the number ratio of hydrogen versus helium dominated atmospheres — that all indicate hydrogen masses less than or equal to $10^{-7}\ M_\odot$. These arguments will be discussed in later sections. If we accept these arguments as convincing, nuclear energy generation is negligible for white dwarfs with $L \leq 10\ L_\odot$.

4.3.4. Crystallising carbon/oxygen mixtures. While our simplest models were constructed assuming a pure carbon interior, evolutionary calculations predict a mixture

of carbon and oxygen, with the precise ratio depending mainly on the treatment of convection and the adopted rate of the $C^{12}(\alpha,\gamma)\ O^{16}$ reaction (Mazzitelli and D'Antona 1986) and rather uncertain at present. This ratio is important in view of another uncertainty concerning the behaviour of the mixture during crystallisation. The question is whether carbon and oxygen remain completely miscible in the solid state or whether oxygen, which freezes first, sinks towards the centre of the star. The resulting release of gravitational energy could lengthen the evolutionary time scale at low luminosities by up to 5×10^9 yr (Mochkovitch 1983, Garcia-Berro *et al* 1988a, b, Isern *et al* 1989). The phase diagram of a carbon/oxygen mixture has been studied by Stevenson (1980) and Barrat *et al* (1988) with ambiguous results. The latter study suggests that carbon and oxygen remain completely miscible, but that upon freezing a change in concentration occurs. The lengthening of the time scale is only moderate ($0.5 - 0.75 \times 10^9$ yr) in this case.

4.3.5. Observational tests of cooling ages. We have already noticed that the cooling ages of the faintest white dwarfs are of the order of 10^{10} yr; these are long but they are compatible with the age of our galaxy. It is possible, however, to make more detailed comparisons between theory and observations.

One relatively direct method is to compare the luminosities of white dwarfs in galactic clusters with the ages of the clusters. As an example we have in figure 5 indicated the range of luminosities for seven white dwarfs in the Hyades cluster. These values were calculated from the radii and effective temperatures given in Wegner *et al* (1989). The age of the cluster (7×10^8 yr, Maeder and Mermilliod 1981) is also indicated by the vertical bar. All white dwarfs are younger than the cluster, but the faintest come close to the total age. Their MS life time cannot have been very long, which means they have had relatively high progenitor masses.

A more powerful, though less direct method, compares the distribution of observed white dwarfs over luminosity (in a normalised volume around the sun) with theoretical predictions. This distribution function, $n(\log L)$, is called the 'luminosity function', and $n(\log L)\mathrm{d}\log L$ gives the number of white dwarfs at $\log L$ in the interval $\mathrm{d}\log L$. Assuming a cooling curve $t = f(\log L)$, we can write the time interval spent by a cooling white dwarf in $\mathrm{d}\log L$ as:

$$\mathrm{d}t = \frac{\mathrm{d}f(\log L)}{\mathrm{d}\log L}\,\mathrm{d}\log L. \tag{4.23}$$

The predicted number of white dwarfs in $\mathrm{d}\log L$ is proportional to $\mathrm{d}t$, if the birthrate $\dot{n}$ is constant:

$$n(\log L)\,\mathrm{d}\log L = \dot{n}\,\mathrm{d}t = \frac{\mathrm{d}f}{\mathrm{d}\log L}\,\dot{n}\,\mathrm{d}\log L. \tag{4.24}$$

If the observed and theoretical distribution can be fitted, we will then automatically get the birthrate. We can also derive the total number of white dwarfs

$$N = \int_o^t \dot{n}\,\mathrm{d}t = \int_{L_{\max}}^{L_{\min}} n(\log L)\,\mathrm{d}\log L. \tag{4.25}$$

The actual comparison is slightly complicated by the fact that not all white dwarfs have the same mass, and that the birthrate cannot have been constant. But these

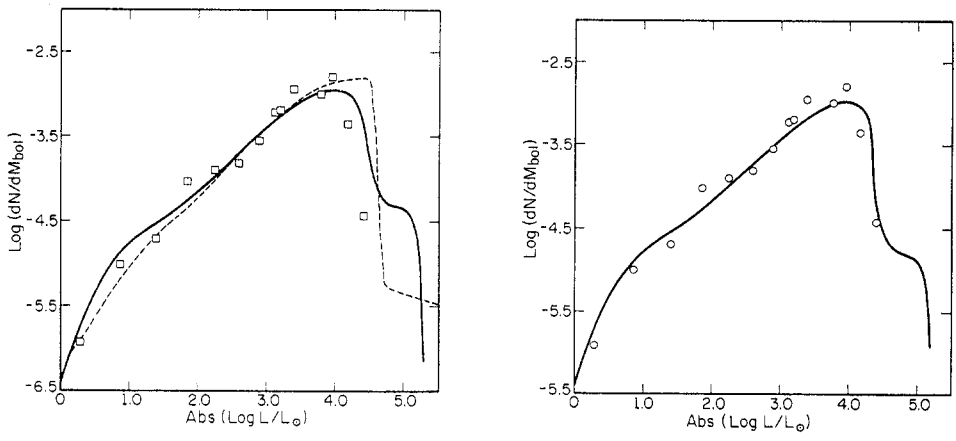

Figure 6. Observed and theoretical luminosity functions from Iben and Laughlin (1989, figure 14). Open symbols are the observed values after Liebert *et al* (1988), continuous curves are theoretical calculations by Iben and Laughlin (1989), while the broken curve is from Winget *et al* (1987a). The left panel is for a disk age of 9×10^9 yr, the right for 8×10^9 yr. The variable on the vertical axis in the figure is proportional to log(n) in our notation.

complications can be taken into account. This comparison has over the years been attempted by many authors, from the pioneering work by Weidemann (1967) to the most recent attempt by Iben and Laughlin (1989). Our figure 6 is taken from the latter paper and shows the observed luminosity function (Liebert *et al* 1988) together with some theoretical results.

The Mestel (1952) cooling function would correspond to a straight line in this diagram with a slope roughly equal to that in the central part of the figure. The deviation from the straight line at high L is easily explained with the accelerated evolution due to neutrino losses. The deviations at the cool end have presented a more severe problem. The faintest observed white dwarfs have $\log L/L_\odot \simeq -4.6$ (Liebert *et al* 1988). The cooling times down to this luminosity are $\leq 10^{10}$ yr, less than the current best estimate of the age of the galaxy from globular clusters ($\simeq 1.5 \times 10^{10}$ yr, Iben and Renzini 1984). If white dwarf formation has occurred for more than 10^{10} yr, we would expect more and fainter white dwarfs ('Debye cooling', for some time suspected to be responsible for this 'red deficit' becomes important only at even lower luminosity). A possible effect that might theoretically prolong the life of white dwarfs are pycnonuclear reactions discussed in §3. With our current knowledge of white dwarf structure and masses this possibility can be ruled out: the densities in the interior are not high enough for the C $\rightarrow$ Mg transformation.

Extremely faint white dwarfs are difficult to detect and their numbers may be affected by severe selection effects. But continued effort (see, e.g., Liebert 1980, Sion 1986) has discovered only one new object (Ruiz *et al* 1986) and the falloff of the observed luminosity function is now considered to be real (Liebert *et al* 1988).

In a bold strike Winget *et al* (1987a) therefore reversed the arguments: if the oldest white dwarfs have cooling ages of $9 \pm 1.8 \times 10^9$ yr, as in their calculations, they conclude that star formation in the galactic disk did not occur much earlier. The correction for the MS life time of the progenitors adds only $0.3(+0.8, -0.1) \times 10^9$ yr to this number, thus the final conclusion is that the age of the galactic disk is $9.3 \pm 2 \times 10^9$

years. Iben and Laughlin (1989) in similar calculations improved the corrections due to the mass distribution of white dwarfs, but arrive at almost identical conclusions: the luminosity function of white dwarfs is best fitted with total cooling times for the faintest objects between 8 and 9×10^9 yr.

4.3.6. Reliability of theoretical ages. The conclusions discussed above depend heavily on the accuracy of theoretical ages at the low luminosity end. Unfortunately, a closer look at the results obtained by different groups within the last four years reveals large discrepancies, with the age at $L/L_\odot = -4.5$ ranging from 5 to 13×10^9 yr (Winget and Van Horn 1987). These authors have studied the differences in detail and found that they can all be attributed to differences in input physics and model parameters. The most important variables are the conductive opacities, carbon/oxygen ratio in the core, latent heat, hydrogen and helium layer thicknesses, and heavy element abundances in the outer layers. If they correct differentially for all these differences to bring all model calculations in accord with 'standard' assumptions they find that all ages agree at $8.2 \pm 0.5 \times 10^9$ yr. While this demonstrates that the differences between the groups can be understood it is not clear in all cases what the 'true' assumptions are. Clearly, the best available data for opacities etc should be used, but in other cases (carbon/oxygen ratio, carbon/oxygen crystallisation, remaining hydrogen and helium layers) theory does not predict unambigous results.

In conclusion: the general agreement between theoretical cooling curves and the observed luminosity function is satisfactory. It is highly probable that the drop-off in the luminosity function is real and connected to the beginning of star formation in the galactic disk $\sim 10^{10}$ yr ago. The actual numbers given for the age of the disk should, however, be regarded with some caution.

The total white dwarf number density calculated from the luminosity function is 0.0032 pc^{-3} (Liebert *et al* 1988); considering the possible uncertainties (e.g. undetected white dwarfs obscured by a much brighter companion) it could be a factor of two higher (Liebert *et al* 1989). This is only 1% of the dynamically estimated total mass density in the solar neighbourhood (Bahcall 1984a,b). With a total cooling age for the faintest of 9×10^9 yr this corresponds to a white dwarf birthrate, time averaged over the history of the galactic disk, of 3.6×10^{-13} pc^{-3} yr^{-1}.

5. The visible surface: spectra and colours

Most of our knowledge about white dwarfs is derived from the light emitted at the surface. The spectral energy distribution is determined by the temperature structure (characterised by the effective temperature), the pressure stratification (determined by the surface gravity g) and the chemical composition of the atmospheric layers. It is the task of the theory of stellar atmospheres to construct theoretical models of the outer layers using the laws governing radiative and convective energy transfer, improve them until they fit the observations and then derive these parameters.

In this section we will give a short summary of these observations and their interpretation. This summary can by no means be complete, the main emphasis is on setting the stage for the next section. For more details we refer the reader to review papers (e.g. Liebert 1980) and the original literature.

The first step towards an understanding is, as with normal stars, to classify the observed spectra using empirical criteria. The classification scheme currently in use

is that defined by Sion *et al* (1983). The major spectral types and their classification criteria are (McCook and Sion 1987; as a reminder: 'metals' are all elements heavier than helium):

DA: Only Balmer lines; no He I or metals present

DB: He I lines; no hydrogen or metals present

DC: Continuous spectrum; no lines deeper than 5% in any part of the electromagnetic spectrum

DO: He II strong; He I or hydrogen present

DZ: Metal lines only; no hydrogen or helium lines

DQ: Carbon features; either atomic or molecular in any part of the electromagnetic spectrum

In figure 7 we give a few example spectra. Historically, the letter 'D' in these designations stands for 'dwarf'. Some of the second letters have counterparts in the classification scheme of normal MS stars, although their meaning is quite different in the white dwarf case. In some cases the designations can be combined, for example 'DZA' stands for a spectrum dominated by metal lines but showing also weak hydrogen lines. If a temperature estimate is available a one digit temperature indicator (0...9) can be appended, being defined as the integer part of $50400/T$. The use of the whole electromagnetic spectrum in this classification reflects the tremendous observational progress in the last decade, mainly due to the IUE satellite, which made the whole range from 1200 to 3200 Å easily accessible.

5.1. Brief summary of spectroscopic results

The basic observational facts are:

(i) No white dwarf has a chemical composition that even remotely resembles that of the sun. The differences are not factors of order unity, but many orders of magnitude.

(ii) White dwarf spectra generally fall into two well-defined groups: those with hydrogen-dominated atmospheres (spectral type DA) versus helium-dominated atmospheres (DO, DB, DC, DZ, DQ). Usually, though not in all cases, the dominating element is at least a factor of 1000 more abundant than all other elements together.

One of the most persistent problems in the field of white dwarfs is the distribution of these two basic types over the temperature range. At the highest temperatures we find the following:

DO: This class is characterised by helium-dominated atmospheres in the range 45 000 to over 100 000 K. Hydrogen is present with number abundances $\geq 1\%$ (Wesemael *et al* 1985).

DA: This class is by far the largest and observed over almost the whole range of temperatures where the Balmer lines can be visible, from 6000 to $\simeq$ 70 000 K. Balmer lines should be visible at even higher temperatures, but no such DA has so far been observed. The DAO ($T_{\rm eff} \sim 60\,000$ K) has helium abundances of the order of 1% (Wesemael *et al* 1985). In all other cases it is probably much less abundant, although 1% is about the limit that can be determined from optical observations. Much lower fractions ($\sim 10^{-5}$) can be obtained from the analysis of EUV observations obtained with the Einstein and Exosat satellites (Kahn *et al* 1984, Petre *et al* 1986, Jordan *et al* 1987, Paerels and Heise 1989). Atmospheric parameters for large numbers of DAs have been determined by Shipman (1979), Koester *et al* (1979), Shipman and Sass (1980), Weidemann and Koester (1984), McMahan (1989) and especially for the hottest DA by Holberg *et al* (1986) and Finley *et al* (1989).

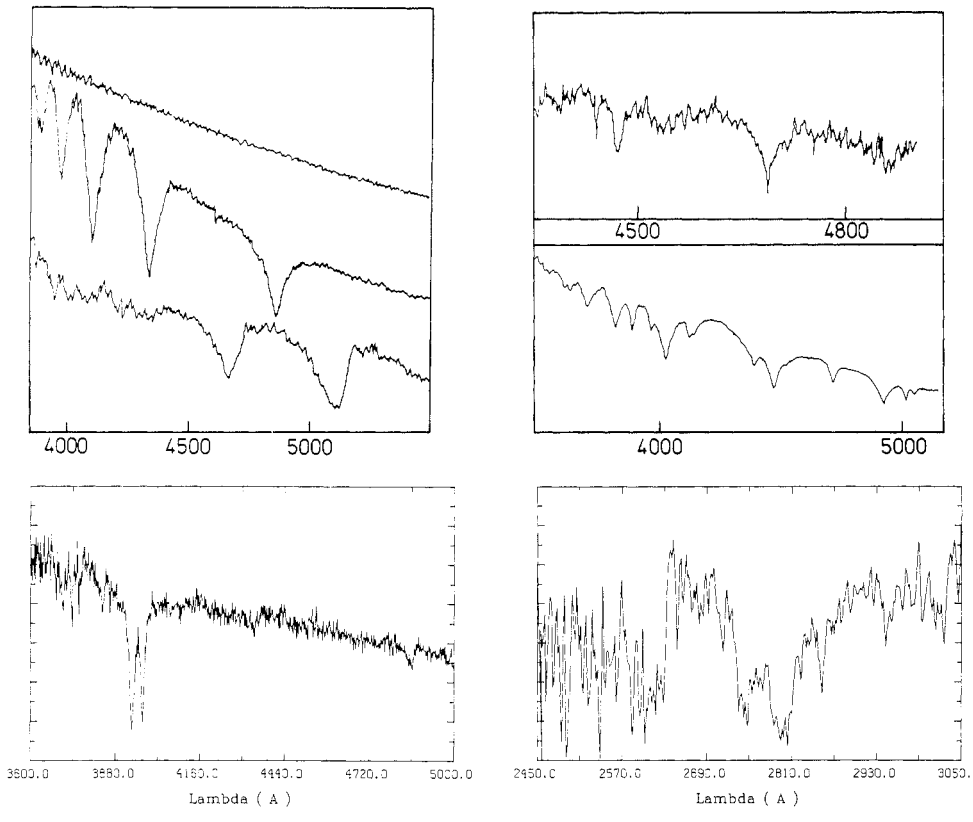

Figure 7. Example spectra showing the wide variety of spectral types. The two left panels show from top to bottom: L97-3 (DQ, former DC), LDS455A (DA), L870-30 (DQ), and K789-37 (DZA, from Koester *et al* 1989). The right panels show: HZ21 (DO, from Wesemael *et al* 1985), GD353 (a variable DB, from Koester *et al* 1985), and the ultraviolet spectrum of K789-37 as a demonstration of the large amount of additional information provided by UV observations (also from Koester *et al* 1989).

DB: This class shows only He I lines and is observed between 12 000 and 30 000 K, but mysteriously completely absent in the range 30 000 to 45 000 K, where the He I lines should be very strong, but no helium-rich object is observed. Improved observations have recently discovered a number of DBs showing weak hydrogen lines (DBA), with abundances of the order of 10^{-4}, and Shipman *et al* (1987) estimate that these objects might make up as much as 20% of the DB class. Recent analyses of members of the DB class are given in the papers by Wickramasinghe and Reid (1983), Oke *et al* (1984), Liebert *et al* (1986), and Wegner and Nelan (1987).

The picture gets even more confusing at low temperatures (< 12 000 K). Whereas for $T_{\rm eff}$ between 10 000 and 50 000 K the number ratio of hydrogen versus helium-dominated atmospheres is roughly 4 : 1, this ratio drops below one at the low temperature end (Fontaine and Wesemael 1987, Shipman 1989). The main helium-rich classes at low temperatures are:

DC: Historically most cool helium-rich spectra below the DB range (< 12 000 K) were classified DC, because helium lines are no longer visible and only optical spectra were available. A real breakthrough was provided by IUE, which showed that all accessible DC white dwarfs (only very few unfortunately!) had strong CI resonance

lines in their UV spectra and were thus reclassified DQ (Weidemann *et al* 1981, Vauclair *et al* 1981a, Wegner 1981, 1983). Whether this is true for all objects in this class is an open question.

DQ: Originally classified after the Swan bands of the C_2 molecule, all of the approximately twenty members of this class accessible to UV observations also show the CI resonance lines. Atmospheric parameters for many members of the DC and DQ classes have been derived by Koester *et al* (1982), Wegner and Yackovich (1984), and Wegner and Koester (1983), and references to the observations can be found in these papers. Typical carbon abundances in these objects range from 10^{-7} to 10^{-3} (Wegner and Yackovich 1984).

DZ: (approximately thirty members) As optical observations improved it turned out that several of the cooler non-DA stars formerly classified DC, DB or DBA showed CaII resonance lines (and in a few cases weak lines of Mg, Fe) and were given the designation DZ. Here again IUE observations made a breakthrough: some of the first of these (Cottrell and Greenstein 1980) revealed strong features of Mg, Fe and Si in the UV spectra. A number of observations were analysed by Zeidler-K.T. *et al* (1986); Liebert *et al* (1987a) used new and improved optical data to derive abundances. A summary of abundance determinations is given in the next section. The metal abundances, relative to helium, are always much lower than the solar values.

5.2. Photometry

Obtaining spectra for faint white dwarfs is very time consuming and needs large telescopes, especially if large samples are desired. One way around this is to sacrifice high spectral resolution and observe the star through filter systems, with photomultiplier tubes, or more recently, CCDs as detectors. For historical reasons these measurements are called 'magnitudes' in astronomy, their relation to a more physical quantity such as energy flux $f(\lambda)$ (outside the earth's atmosphere, which has to have the appropriate correction) is, for example:

$$V = -2.5 \log \int_0^\infty S(\lambda) f(\lambda)\, \mathrm{d}\lambda + \text{constant} \tag{5.1}$$

where V stands for visual magnitude and $S(\lambda)$ is the combined sensitivity function of the filter and the telescope optics. The constant in this equation is fixed by defining some well-observed stars as 'standards' for a particular system. The differences between magnitudes in different spectral regions are called 'colours', which are essentially intensity ratios. The most widely used system is the Johnson system UBV, with broad band filters of widths $\sim$ 1000 Å in the UV, blue and visual range of the spectrum. For white dwarfs the Strömgren system uvby with much smaller bandwidths has proven immensely useful. Observed colours in a two-colour diagram, e.g. u–b versus b–y, can be compared with theoretical predictions from model atmosphere calculations to determine the parameters T_{eff} and $\log g$ (an example is the work by Koester *et al* (1979) for DAs previously mentioned.).

5.3. Derivation of fundamental parameters

The primary observational objective is to determine the spectral energy distribution for a star $f(\lambda)$, corrected for the influence of the earth's atmosphere. The theoretical analysis then gives, at least in principle, the atmospheric parameters T_{eff}, $\log g$ and

composition. The theoretical study of white dwarfs and their evolution on the other hand is concerned with their physical parameters mass, radius and luminosity. What is the connection between the two parameter sets?

5.3.1. Luminosity. The spectral energy distribution $f(\lambda)$ depends on the mean intensity $I(\lambda)$ of the stellar disk, which can never be resolved for white dwarfs, and the solid angle ω subtended by the star:

$$f(\lambda) = I(\lambda)\,\omega = I(\lambda)\,\frac{\pi R^2}{d^2} \tag{5.2}$$

assuming that no absorption occurs in the interstellar medium along the line of sight. Here R and d are the radius and distance of the star. The mean intensity is connected to the energy flux $F(\lambda)$ per unit area at the stellar surface by $I(\lambda) = F(\lambda)/\pi$ (e.g. Mihalas 1978). For the total energy flux, the luminosity, we then get

$$L = 4\pi R^2 \int_0^\infty F(\lambda)\,\mathrm{d}\lambda = 4\pi d^2 \int_0^\infty f(\lambda)\,\mathrm{d}\lambda. \tag{5.3}$$

The determination of luminosities thus requires two steps: the extrapolation of the energy distribution to longer and shorter wavelengths not covered by the observations; and the distance. The first step must use theoretical models, which are more accurate the broader the observed wavelength range. Fortunately most white dwarfs are relatively close to the sun and for ~ 250 of them distances are known, mainly through trigonometric parallaxes (the apparent motion relative to distant stars caused by the yearly motion of the earth around the sun).

5.3.2. Radii. The most reliable method to determine radii utilises equation (2.1) with the effective temperature from an analysis of spectra or colours and the luminosity obtained as described above.

5.3.3. Masses. With the exception of seven objects (van Maanen 2, 40 Eri B, Stein 2051 B, Sirius B, Procyon B, G107-70B, BD+16°516) where the classical methods of binary orbit determination can be used, the determination of masses rests on the use of relations between mass and radius as obtained by some observational data or theory:

(i) The surface gravity as obtained from atmospheric analysis depends on mass and radius as $g = GM/R^2$.

(ii) The gravitational redshift as predicted by general relativity gives the relation $\Delta\lambda/\lambda = GM/c^2R$.

(iii) A third relation is provided by the theoretical mass–radius relation, either Hamada and Salpeter (1961), or one taking into account the effects of finite temperatures, if available.

Surface gravities can have large errors up to a factor of two and are useful mainly for statistical purposes. The most accurate determinations today use the gravitational redshift plus the theoretical relation, but are applicable only to a restricted number of bright white dwarfs in wide binary systems or clusters, because high resolution is necessary and the individual space motion has to be known from the companion or the cluster (Koester 1987b, Wegner 1989a). Any two of the above relations can be used to derive the radius in addition to the mass, even if the distance is not known.

A recent example is the study by McMahan (1989), who obtained masses and radii from the surface gravity and the mass–radius relation.

The mass distribution of DA white dwarfs is fairly well known today from statistical analyses of large samples by Koester *et al* (1979), Shipman and Sass (1980), Weidemann and Koester (1984) and McMahan (1989). This distribution is surprisingly narrow with two-thirds of all DA falling in an interval of 0.2 $M_\odot$. The mean mass is $\simeq 0.58 M_\odot$. McMahan (1989) finds a slightly lower average mass, but this is probably due to his use of surface gravities, which in our opinion are less accurate and may be affected by systematic errors, whereas the former authors preferred to use distances and derived radii plus the Hamada–Salpeter relation to define the average. For helium-rich objects the mass distribution is much less certain, but Oke *et al* (1984) found no significant difference from the DAs.

6. Physical processes in the non-degenerate envelope

The basic mechanism responsible for the pure, mono-elemental composition in the atmospheres of most white dwarfs was identified a long time ago by Schatzman (1949, 1958): gravitational separation of heavier and light elements in the extremely strong gravitational fields ($g \sim 10^8\ \mathrm{cm\,s^{-2}}$). The lightest element present floats to the top and forms the observable atmosphere, if no other competing mechanism exists to prevent this. The process leading to this distribution is diffusion, and ideally the diffusion equations should be solved simultaneously with the equations describing the evolution (cooling) of the white dwarfs. Such calculations have been started only recently by Iben and MacDonald (1985,1986), and with more emphasis on the chemical evolution of the outer layers by a group at Montreal (Pelletier *et al* 1986, 1989, Dupuis *et al* 1989, and references in these papers).

As we will see below the diffusion time scales are always much shorter than evolutionary time scales and the basic results for the outer layers can be obtained by neglecting the evolution as was done in the papers by Fontaine and Michaud (1979), Vauclair *et al* (1979), Alcock and Illarianov (1980a) and Muchmore (1984).

Diffusion in multi-component, non-uniform gases has been studied in detail by Chapman and Cowling (1970) and Burgers (1969) by solving the set of coupled Boltzmann equations for each species. An excellent review of the applications of this theory to element distributions in stars has been presented by Vauclair and Vauclair (1982). We will now derive the basic equation in a very simple, intuitive way and compare the final result with the more accurate derivation.

6.1. The diffusion equation

Let us assume a mixture of two species, distinguished by the indices 1 and 2, with partial pressures P_i, densities ρ_i, and masses m_i. If there is no interaction between the species, the equations of motion are:

$$\begin{aligned} \rho_1 \dot{v}_1 &= -\nabla P_1 + \rho_1 F_1 \\ \rho_2 \dot{v}_2 &= -\nabla P_2 + \rho_2 F_2 \end{aligned} \tag{6.1}$$

where ∇P_i stands for the radial gradient of the partial pressures P_i and the F_i are external forces (per mass) due to gravitational and electric fields (and possibly other effects).

If a relative motion exist between the species we expect interactions proportional to the relative velocity, which on dimensional grounds we write purely phenomenologically as a 'viscosity force'

$$F_v = \frac{\rho_1 \rho_2 (v_1 - v_2)}{\rho \tau} \tag{6.2}$$

with a typical collision time scale τ. We then have

$$\begin{aligned} \rho_1 \dot{v}_1 &= -\nabla P_1 + \rho_1 F_1 - \frac{\rho_1 \rho_2}{\rho \tau}(v_1 - v_2) \\ \rho_2 \dot{v}_2 &= -\nabla P_2 + \rho_2 F_2 + \frac{\rho_1 \rho_2}{\rho \tau}(v_1 - v_2). \end{aligned} \tag{6.3}$$

Subtraction of the two equations leads to

$$(\dot{v}_1 - \dot{v}_2) + \frac{v_1 - v_2}{\tau} = \left(-\frac{1}{\rho_1}\nabla P_1 + F_1\right) - \left(-\frac{1}{\rho_2}\nabla P_2 + F_2\right). \tag{6.4}$$

Solutions of this type of differential equation show an initial phase with exponential increase of the relative velocity of duration $\sim \tau$. After this short time a stationary state is reached asymptotically with

$$v_1 - v_2 = \tau \left(-\frac{1}{\rho_1}\nabla P_1 + \frac{1}{\rho_2}\nabla P_2 + F_1 - F_2\right). \tag{6.5}$$

Using the hydrostatic equation this can be transformed into:

$$v_1 - v_2 = \frac{\tau k T}{\langle m \rangle}\left(-\frac{1}{c_2}\nabla \ln c_1 + \frac{m_1 F_1 - m_2 F_2}{kT}\right) \tag{6.6}$$

$$\text{with} \qquad \langle m \rangle = \frac{m_1 m_2}{c_1 m_1 + c_2 m_2} \qquad \text{and} \qquad c_i = n_i/n. \tag{6.7}$$

The exact solution using the Boltzmann equations (Chapman and Cowling 1970) can be brought into the form:

$$v_1 - v_2 = D_{12}\left(-\frac{1}{c_2}\nabla \ln c_1 + \frac{m_1 F_1 - m_2 F_2}{kT} + \alpha_T \nabla \ln T\right). \tag{6.8}$$

Here, D_{12} is the binary diffusion coefficient; its order of magnitude can be estimated from a comparison of (6.8) and (6.6):

$$D_{12} \sim \tau k T/m \sim \tfrac{1}{3}\tau v_{\rm th}^2 \sim \tfrac{1}{3} l v_{\rm th} \tag{6.9}$$

where $v_{\rm th}$ is the thermal velocity and l the mean free path. The actual calculation of D_{12} requires the calculation of a collision integral which depends on the nature of the particle interaction potential. The most accurate results available for stellar plasmas are currently those of Paquette *et al* (1986b). The additional term on the right hand side is the thermal diffusion due to a temperature gradient, with the thermal diffusion coefficient $D_{12}\alpha_T$. This term is taken into account in numerical computations, but is

only of minor importance according to the results of Paquette *et al* (1986a) and will be neglected in our simple considerations.

In the equilibrium state the relative velocity vanishes and the concentration gradient is given by the right hand side of (6.8) . In order to understand the nature of the external forces let us, as an example, identify the species 1 and 2 with protons and electrons. Because the gravitational force is stronger on the protons gravity tends to separate electrons and protons, creating an electric field E which counteracts the separation. As a starting point we assume that the matter remains very closely neutral ($n_p = n_e$). The concentration gradient therefore vanishes and in equilibrium we have:

$$m_p g + eE = m_e g - eE \tag{6.10}$$

$$E = -\frac{m_p + m_e}{2e}\, g \simeq -\frac{m_p}{2e}\, g. \tag{6.11}$$

The electric force is thus of the same order of magnitude as the gravitational force. Is this consistent with our assumption about neutrality? From Poisson's equations we have:

$$\nabla \cdot \boldsymbol{E} = -4\pi e(n_p - n_e) = -\frac{m_p}{2e}\, \nabla \cdot \boldsymbol{g} = \frac{m_p}{2e}\, G\, 4\pi n_p m_p \tag{6.12}$$

or

$$-\frac{n_p - n_e}{n_p} = \frac{G m_p^2}{2e^2} \sim 4 \times 10^{-37}. \tag{6.13}$$

The charge separation is indeed extremely small, justifying our assumption (cf Rudkjøbing 1952). The total force on electrons and protons per unit volume is:

$$F = n_p(m_p g + eE) + n_e(m_e g - eE) = n\,\frac{m_p + m_e}{2}\, g \tag{6.14}$$

which means that we are justified in neglecting the electric field in the hydrostatic equation as long as we take the mean mass of a particle to be $(m_p + m_e)/2$.

In the realistic white dwarf problem we are confronted not with binary, but at least ternary mixtures: two ionic species plus electrons. Because the velocity of the electrons is, however, much higher, it is a good approximation to assume that they have always reached their equilibrium distribution. The electric field can then be determined from

$$\frac{\partial P_e}{\partial r} = -n_e\,(m_e g + eE) \tag{6.15}$$

and (6.8) describes the diffusion of the two ionic species in the neutralising background of the electrons. It should be clear from the preceding discussion that this diffusion must always occur in an initially homogeneous stratification because equilibrium between electric and gravitational forces cannot in general be obtained for two ions with different (Z, A). The heavier ion always diffuses downwards and vice versa until equilibrium ($v_1 - v_2 = 0$) is achieved. In equilibrium the two species are completely separated at a transition zone, where the composition changes drastically over a few pressure scale heights $\sim 1/(\partial \ln P/\partial r)$. Only the presence of more effective mixing processes can prevent the separation. In order to clarify the importance of competing processes we need more quantitative estimates.

6.2. Diffusion velocities and time scales

Koester (1989a) has recently estimated the relative diffusion velocities in a hydrogen/helium mixture using the new diffusion coefficients (Paquette *et al* 1986b). Table 1 shows the results (v_{12} in cm s^{-1}) at a depth below the surface corresponding to $\Delta M = 10^{-17}$ to 10^{-10} $M_\odot$ for white dwarfs with different effective temperatures. The second line for each mass entry gives a diffusion time scale L/v_{12} in yr, where L is the typical length scale of the outer layers. This time can therefore be interpreted as the time necessary to achieve complete hydrogen/helium separation. For comparison the last line gives approximate cooling ages at that effective temperature.

Table 1. Hydrogen/helium diffusion velocities in cm s^{-1} (upper line for each entry) and time scales (lower line, in yr) evaluated at different depths below the surface (given as fractional mass).

	$T_{\rm eff}$				
$\log \Delta M/M_\odot$	60 000	50 000	40 000	30 000	20 000
−10	1.6×10^{-5}	1.4×10^{-5}	1.2×10^{-5}	9.8×10^{-6}	7.3×10^{-6}
	1387	1457	1538	1635	1798
−11	4.9×10^{-5}	4.2×10^{-5}	3.6×10^{-5}	2.9×10^{-5}	2.2×10^{-5}
	298	316	336	362	393
−12	1.5×10^{-4}	1.3×10^{-4}	1.1×10^{-4}	8.7×10^{-5}	6.5×10^{-5}
	63	68	73	79	87
−13	4.7×10^{-4}	4.0×10^{-4}	3.4×10^{-4}	2.7×10^{-4}	2.0×10^{-4}
	13	14	15	17	19
−14	1.5×10^{-3}	1.3×10^{-3}	1.0×10^{-3}	8.2×10^{-4}	5.9×10^{-4}
	2.8	3.0	3.3	3.6	4.1
−15	4.7×10^{-3}	4.0×10^{-3}	3.3×10^{-3}	2.6×10^{-3}	1.8×10^{-3}
	0.6	0.6	0.7	0.8	0.9
−16	1.5×10^{-2}	1.3×10^{-2}	1.0×10^{-2}	8.1×10^{-3}	5.7×10^{-3}
	0.1	0.1	0.1	0.2	0.2
−17	4.9×10^{-2}	4.1×10^{-2}	3.3×10^{-2}	2.6×10^{-2}	1.8×10^{-2}
	0.02	0.03	0.03	0.03	0.04
Cooling age	1.6×10^{6}	2.7×10^{6}	5.3×10^{6}	1.5×10^{7}	7.9×10^{7}

The interpretation is the following: the diffusion velocities seem rather small (although they are much larger than in MS stars due to the high g). However, *the derived time scales are much shorter than the cooling ages.* The fundamental result is therefore that in the absence of competing processes we should expect the equilibrium situation with only the lightest element present (hydrogen in this case) visible at the surface. This is in agreement with the time-dependent studies of the diffusion process by Pelletier *et al* (1989) and also with the majority of observations.

At the high temperature end of the white dwarf sequence, however, some objects (DO, DAO) show both helium and hydrogen in their optical spectra. Moreover, the interpretation of Einstein and Exosat observations in the EUV region has demonstrated that even the DAs, with a pure hydrogen spectrum in the optical range, must have traces (10^{-3} to 10^{-5}) of helium in their atmospheres (see previous section). Why did the helium not disappear long ago?

6.3. Competing processes

Detailed calculations of diffusion in the presence of other processes (see below) have

not yet been made. For the purpose of estimating their influence we may, however, estimate typical velocities associated with these processes and compare them with diffusion velocities. If they are much smaller the process can probably be neglected safely, whereas at the other extreme diffusion should be inhibited. Recent discussions under this aspect have been presented by Michaud (1987) and Koester (1989a).

6.3.1. Meridional circulation. It has long been known that the rotation of a star should lead to large-scale internal motions, the Eddington–Vogt meridional circulation (Eddington 1925, Vogt 1925). Tassoul and Tassoul (1983) found a stationary solution for the flow pattern in a cooling white dwarf with the assumption that viscous stresses exactly balance the transport of angular momentum in the surface boundary layer. They discussed a 0.8 $M_\odot$ white dwarf with $L = 10^{-2}\ L_\odot$ and found time scales for mixing by circulation currents greater than the Hubble time. Since circulation velocities increase with luminosity and decrease with mass they could, however, be substantially larger for a 60000 K (with $L \sim L_\odot$) white dwarf of 0.6 $M_\odot$. Also, Tassoul and Tassoul (1983) estimate that the time scale to reach the stationary solution is $\sim 10^{10}$ yr, much longer than the cooling ages of hot white dwarfs. It cannot, therefore, be completely ruled out at present that rotation might have an effect in the surface layers of very hot white dwarfs (Koester 1989a), considering the observed helium/hydrogen ratios in the hot DO and DAO objects. On the other hand, white dwarfs are observationally found to be very slow rotators (Greenstein and Peterson 1973, Pilachowski and Milkey 1984, 1987, Koester and Herrero 1988), which would tend to make the effects of rotation less important.

6.3.2. Mass loss. The possibility of mass loss in hot DAs has been inferred from the presence of shortward-shifted absorption components of highly ionised species in their UV spectra (Bruhweiler and Kondo 1983). The interaction of diffusion with mass loss has been discussed in detail by Michaud (1987). Because of the continuity of the flow, mass loss leads to a systematic velocity in the transition region which is superposed on the diffusion velocity. It is easy to estimate with the numbers in table 1 that these velocities are comparable if the mass loss is of the order of $10^{-15}\ M_\odot\ \mathrm{yr}^{-1}$. With somewhat different assumptions about the original abundance distribution Michaud (1987) derived $10^{-14}\ M_\odot\ \mathrm{yr}^{-1}$ as the critical rate at which diffusion becomes ineffective.

We have already mentioned that there are strong arguments that at least a large fraction of the DA white dwarfs have very thin outer hydrogen layers, probably $\leq 10^{-14}\ M_\odot$. Such a thin layer would be stripped off by a mass loss of this magnitude in a very short time, which is not observed. It might well be, however, that mass loss in previous evolutionary phases has led to these thin hydrogen layers and stopped when it came close to the hydrogen/helium transition zone, although at the moment this is pure speculation. For the remainder therefore let us simply assume that mass loss, if present, is small enough not to interfere with diffusion.

6.3.3. Accretion of interstellar matter. Accretion is the flow of matter from outside the star onto the surface, and except for the sign of the flow the estimate for the critical rate is the same as in the case of mass loss. The accretion rate necessary ($\sim 10^{-15}\ M_\odot\ \mathrm{yr}^{-1}$) to compete with diffusion is much higher than expected on theoretical grounds for an isolated hot white dwarf in the tenuous interstellar medium, although it could be much higher when the white dwarf traverses a cloud, a region of higher density. However, from the distribution of these clouds, the time between encounters

is estimated as $\sim 5 \times 10^7$ yr, larger than the age of the hottest DAs and much larger than diffusion times. For the helium/hydrogen ratio in hot white dwarfs accretion therefore seems to be unimportant. This process plays, however, a crucial role in our current interpretation of the DZ objects at much lower temperature.

6.3.4. Radiative levitation. In our simple derivation of the diffusion equation we have neglected the radiation pressure on the ionic species in the consideration of external forces. Depending on the ionisation state and absorption cross sections the absorption of photons within the outer layers of the star, and the associated transfer of momentum to the absorbing particle, results in an outward force that decreases the effective gravitational acceleration felt by the ions. Because absorption efficiencies can vary over many orders of magnitude for different ions this force is highly selective and therefore can lead to relative diffusion.

In their pioneering paper Vauclair *et al* (1979) have shown that radiation forces in some cases can support carbon, nitrogen and oxygen ions in the atmosphere against the effect of gravitational separation. This concept has been extended in recent years in work by Morvan *et al* (1986), Vauclair (1989), and Chayer *et al* (1989), who demonstrated that the elements mentioned above (and silicon) can be supported in the form of 'metal clouds' in the outer layers, although the present attempts to interpret the silicon and carbon observed in three DAs in terms of this model are so far not completely successful (Koester 1989a).

Selective radiation pressure on helium had been invoked (Petre *et al* 1986, Shipman 1987) as an explanation for the helium seen in DAO and DA. However, Vennes *et al* (1989) have recently shown that this effect is not strong enough to explain the observed abundances.

6.3.5. Convection. Whenever the temperature gradient $\mathrm{d}\ln T/\mathrm{d}\ln P$ in a star becomes steeper than the adiabatic gradient $(\mathrm{d}\ln T/\mathrm{d}\ln P)_{\mathrm{ad}}$ the stratification becomes unstable (Schwarzschild criterion) and macroscopic motion or convection sets in. Because no convection theory exists that is applicable under the conditions in stars (extremely high Reynolds numbers), the energy transport is usually calculated in the 'mixing-length' approximation (Böhm-Vitense 1958).

The importance of convection in the envelopes of white dwarfs was first pointed out by Böhm (1968). The more efficient energy transport decreases the temperature gradient and changes the relation between the surface and interior temperatures. Far more important, however, is the role of convection for the interpretation of the element distribution in the outer layers and its possible change during the cooling history. The flow velocities in convection zones are much higher than diffusion velocities and the flow is highly turbulent. Within a convection zone, matter will therefore be completely mixed and no concentration gradient can develop (Vauclair and Vauclair 1982). If the concentration of a species is lower below the convection zone, diffusion can still occur at the bottom of the zone; in this case the whole mass in the zone acts as a 'reservoir' and the time scales for the disappearance of elements out of the atmosphere may become much longer.

6.4. Spectral types and spectral evolution

The interpretation of spectral types and atmospheric abundances in white dwarfs is at the forefront of current research; even review papers appear at the rate of several per year (Vauclair 1989, Koester 1987a, Shipman 1989, Shipman 1987, Fontaine and

Wesemael 1987, Liebert *et al* 1987b, Sion 1986, Vauclair and Liebert 1987). It is not possible to report all speculations in this review, we will instead concentrate on a few major problems and our current understanding, following the papers by Fontaine and Wesemael (1987), Koester (1987a) and Shipman (1989).

6.4.1. Hydrogen versus helium-dominated atmospheres. The main observational facts that need explanation are:

(i) the absence of hydrogen atmospheres with $T_{\rm eff} \geq 70\,000$ K, whereas helium-rich objects are observed well over 100 000 K (the PG1159 objects, a subgroup of the DO);

(ii) the absence of DBs in the gap between 30 000 and 45 000 K; and

(iii) the change in the number ratio of hydrogen versus helium atmospheres from $\simeq 4:1$ at higher temperatures to ≤ 1 below 10 000 K.

Because the change in luminosity and surface temperature of cooling white dwarfs is a continuous function of time, the above facts strongly suggest that white dwarfs can change their atmospheric composition and even spectral type during their evolution. This does not exclude, however, the possibility that different progenitor channels exist, with some stars entering the white dwarf phase without any hydrogen left, while others retain a small hydrogen envelope. This point of view was strongly emphasised by Shipman (1989). An argument in favour of this view is that observations of the central stars of planetary nebulae show a strong variation of helium/hydrogen ratios (Mendez *et al* 1986, 1988). On the theoretical side Iben (1984) has argued that it might depend on the exact phase, between helium-shell flashes, when a star leaves the AGB whether it retains a hydrogen envelope or not.

While the possibility of more than one birth channel cannot be excluded it cannot by itself explain the observed gaps. Fontaine and Wesemael (1987) have therefore taken the opposite view and tried to explain the relevant facts assuming a single channel. In their view, the extremely hot helium-rich PG1159 objects and the somewhat cooler DO are the progenitors of all white dwarfs. They argue that the mass loss on the AGB and in the planetary nebula phase strips the star of all matter outside the hydrogen-burning shell. It thus enters the white dwarf stage with a helium-rich atmosphere. However, a small amount of hydrogen is hidden in the deeper layers and floats to the top, until enough hydrogen ($\sim 10^{-16}\ M_{\odot}$) is accumulated that the star appears as a DA. This could explain the mixed abundances in the DO and DOA, and it could be responsible for the fact that all white dwarfs are DAs when reaching $T_{\rm eff} \simeq 45\,000$ K.

During further cooling a convection zone develops in the helium layer underneath the hydrogen, and around 30 000 K it can mix with the hydrogen and transform the star into a DB, if the hydrogen layer thickness is $\leq 10^{-15}\ M_{\odot}$. This explanation of the DB gap was first proposed by Liebert *et al* (1986, 1987b). If the hydrogen layer is larger the star remains a DA. This scenario requires that a substantial fraction of the hot DAs have extremely thin hydrogen layers (MacDonald 1989), in conflict with the results of traditional stellar evolution calculations.

Michaud *et al* (1984) recently suggested an interesting theoretical possibility. They assumed that the tail of the carbon distribution from the core and of the hydrogen distribution from the top meet at the intermediate layer, leading to quiet hydrogen burning, which could reduce the hydrogen mass to $10^{-7}\ M_{\odot}$. The detailed calculations by Iben and MacDonald (1985), however, did not support this conclusion.

Fortunately there are several observational clues that can give information about the deeper layers in DA white dwarfs. We have already mentioned that the EUV

observations of $\sim$ 20 DA white dwarfs require the presence of an absorbing element below 200 Å, which is usually assumed to be helium. Most of the analyses so far have assumed a homogenous helium/hydrogen mixture in the atmosphere and determined helium abundances of the order of 10^{-3} to 10^{-5}. If we believe instead that the DAs have very thin hydrogen layers we would have to use stratified atmosphere models, where the transition between hydrogen and helium is determined from the diffusion equilibrium and the total hydrogen mass present. The hydrogen opacity decreases strongly at shorter wavelength below 912 Å, and the emerging spectrum originates from deeper and deeper layers. The presence of helium can therefore become 'visible' in the EUV, although the star appears as a normal DA without any helium features in the optical spectrum.

Such atmospheric models and synthetic spectra were published by Jordan and Koester (1986) and applied to the interpretation of Exosat observations by Koester (1989a, 1989b) and Vennes *et al* (1989). These papers demonstrate that the EUV observations can indeed be interpreted with stratified models and the required hydrogen layers are very thin, ranging from 4×10^{-14} to $4 \times 10^{-16} M_{\odot}$. The one channel/mixing scenario of Fontaine and Wesemael (1987) thus looks quite promising, but several severe problems remain:

(i) The PG1159 and DO groups can account for only $\sim$ 20% of all cooler white dwarfs, unless the assumed evolutionary time scales at high temperatures are completely wrong (Weidemann and Yuan 1989).

(ii) In his detailed study of stratified atmospheres Koester (1989a) was not able to find models that would look like a DA above 30 000 K and turn into a DB around this value. The model grid was relatively coarse, but if this transition is to occur at 30 000 K for about 20% of all DAs, it certainly requires an extreme fine-tuning of the mass in the hydrogen layer.

The situation seems to be much clearer at the low temperature end regarding the change in the number ratio of hydrogen versus helium atmospheres. At about 15 000 K a hydrogen atmosphere develops a convection zone below the surface, which increases dramatically in depth below 10 000 K. If this zone reaches into the helium zone, the much higher densities there lead to a complete dilution of the surface hydrogen and turn the star into a helium-dominated object. Following original suggestions by Strittmatter and Wickramasinghe (1971) and Baglin and Vauclair (1973) the evolution of convection zones and the mixing process has been studied in detail by Koester (1976) and Vauclair and Reisse (1977). Both groups found that mixing would occur below 10 000 K, if the hydrogen layer mass is less than $\sim 10^{-10}\ M_{\odot}$. This process is now generally believed to be responsible for the changing number ratio, and the strong implications are that a large fraction of the DAs must indeed have thin hydrogen envelopes of the order of this value or even smaller. In §7 we will encounter yet another argument for the existence of very thin layers.

6.4.2. The DBA white dwarfs. With the discovery of six new DBs with traces of hydrogen in their spectra from the Palomar–Green survey (Shipman *et al* 1987) the DBA now constitute a well established subclass. Shipman *et al* (1987) estimate that about 25% of all DBs might show hydrogen abundances in the range 10^{-3} to 10^{-5}. Koester (1987a) gives a table of recent abundance determinations for these objects. It is tempting to connect these observations with the above DB/DA scenario, assuming that the hydrogen is primordial and mixed within the helium convection zone around $T_{\rm eff} = 30\,000$ K. However, the mass in this convection zone is $\sim 10^{-6}\ M_{\odot}$; with a

typical observed hydrogen abundance of 10^{-4} this means a total hydrogen mass of 10^{-10}! Such hydrogen layers (although low compared to 'evolutionary' masses) are much too thick to mix with the helium above $T_{\rm eff} \simeq 10\,000$ K — these objects would remain pure DAs throughout most of their life.

The only explanation we are left with seems to be accretion of interstellar matter onto stars with helium atmospheres. Since hydrogen is lighter than helium, it remains within the convection zone, whereas all heavier elements can leave this zone at the bottom by diffusion. Reasonable accretion rates in dense clouds are $10^{-15}\ M_\odot\ {\rm yr}^{-1}$, a typical crossing time for a cloud 10^5 to 10^6 yr, which could easily produce the required amount of hydrogen.

6.4.3. Metals in DZ white dwarfs. This class of about thirty objects shows metal lines, predominantly CaII, in the optical range, in rare cases also magnesium and iron. Table 2 shows the present status of abundance determinations.

Table 2. Metal abundances in DZ, DBZ, DBAZ and DZA.

		Log($N_{\rm metals}/N_{\rm He}$)					
Object	$T_{\rm eff}$	Ca	Mg	Si	Fe	H	Source
GD303	19000	−10.0				≤−5.5	SAK
GD378	16000	−10.0				−4.0	SAK
GD61	15000	−10.0				−3.8	SAK
GD85	15000	≤−10.0				≤−5.0	SAK
G200-39	14500	−10.3				−4.0	KSSA, KW
GD40	14000	−7.4	−7.2	< −6.7	−7.2	≤−5.2	SGB, S, SG
GR488	13500	−9.0				−4.0	KSSA
GD408	13000	−10.0				≤−5.0	SAK
PG2322+119	12000	−8.7				−5.2	LWG
CBS78	12000	−8.0				<−4.7	SSWLS
GD124	12000	≤−10.0				≤−5.0	SAK
K789-37	9500	−8.8	−8.1	<−9.0	−8.0	−3.8	KWK
L119-34	9300	−9.1	−7.7	−9.2	−8.1		ZWK
Ross640	8800	−9.1	−7.2	−7.3	−8.3	−3.5	ZWK
GD401	8800	−8.0	<−8.0	<−8.5	<−8.2	<−3.4	CG, L, K
G105-B2B	8800	−9.5	<−7.2	<−7.5			ZWK
GD95	8200	−9.6	−7.2		−8.5		LWG
L745-46A	7800	−10.4	−9.0	−9.5	< −11.0	−5.9	ZWK, K
G165-7	7500	−7.2				<−4.0	WL
G163-28	6500	−10.7	<−8.0				ZWK
G157-35	6000	−10.5	−8.7		−9.2		ZWK
vMa2	6000	−10.6	−8.8		−8.8		LWG, ZWK
Solar ratios to hydrogen		−5.70	−4.58	−4.48	−4.40		
Solar ratios to calcium			1.12	1.22	1.30		

Sources for abundances: CG, Cottrell and Greenstein 1980; K, Koester 1987a KSSA, Kenyon *et al* 1988; KW, Koester and Weidemann 1989; KWK, Koester *et al* 1989; L, Liebert 1987 (Hα< 2Å); LWG, Liebert *et al* 1987a; S, Shipman 1984; SAK, Sion *et al* 1988a; SG, Shipman and Greenstein 1983; SGB, Shipman *et al* 1977; SSWLS, Sion *et al* 1986; WL, Wehrse and Liebert 1980; ZWK, Zeidler-K T *et al* 1986.

What can we learn from these data? The abundances are always very low, much lower than the solar ones. That they can be detected at all these levels is due to the extreme transparency of helium at these temperatures. Clearly these elements cannot be primordial, because the diffusion times ($\sim 10^6$ yr) are orders of magnitudes smaller than the age of these white dwarfs ($>10^9$ yr). There is also no chance that these elements could have been mixed up again from deep below, the convection zones are not deep enough.

Again, the only solution seems to be accretion. In the basic scenario, the convection zone is regarded as a homogeneously mixed reservoir. Matter is added through accretion at the outer boundary, predominantly during a passage through an interstellar cloud, and diffuses out of this zone at the bottom. The time scales for this diffusion are defined by the mass contained in the convective zone divided by the diffusive flux; typical times are 10^5 to 10^6 yr. The typical accretion rates that are needed under these circumstances to produce the observed metal abundances are 10^{-16} to 10^{-14} $M_\odot$ yr^{-1}. With these simplifications, the equation governing the time evolution of abundances in the convection zone is extremely simple and leads immediately to the following conclusions:

(i) Hydrogen as the lightest element does not diffuse, but always stays in the convection zone. If the accreted matter has solar composition, this sets an upper limit to the total accreted mass (from the observed hydrogen abundances or upper limits).

(ii) If accretion times are very long, an equilibrium is reached, where the abundances are solely determined by the accretion rate and the diffusion time scales. If significant accretion, however, is possible only in dense interstellar clouds, this equilibrium stage would never be reached, because the crossing time for a cloud, of the order of 5×10^5 yr (Petre *et al* 1986), is not long compared to the diffusion time scales. We would then expect that the atmospheric composition shortly after the encounter should reflect the composition of the accreted matter (with the exception of helium).

(iii) When accretion stops, elements (except hydrogen) disappear with an e-folding time determined by their diffusion time scales. The ratio of, for example, calcium/hydrogen can thus only decrease from the original value.

(iv) Diffusion time scales for magnesium are always longer than those of calcium (Paquette *et al* 1986a), meaning that the abundance ratio of calcium/magnesium can only decrease from the value in the accreted matter.

(v) The diffusion time scale for iron in the relevant temperature range is only slightly longer than that of calcium, the ratio of iron/calcium should therefore roughly reflect the accretion abundances.

In interpreting the observations in view of this scenario we have to keep in mind that the determined abundances have uncertainties of typically a factor of two to three and the diffusion velocities of about a factor two. To facilitate the conclusions, table 2 also contains the solar ratios of the observed elements to hydrogen and to calcium.

If we assume a conservative upper limit of 10^{-4} for the hydrogen abundance in the six cooler objects where calcium is observed, but hydrogen is not, there are 21 cases with calcium/hydrogen determinations or lower limits. Taking the data at face value the ratio in 11 of them would be larger than that for solar abundances. This problem has been known for several years and the inevitable conclusion seems to be that matter cannot be accreted with solar abundances in these cases. There is no indication that the predictions of the diffusion theory can be that much in error, but since much less is known about the accretion process it seems easier to blame it and assume that the accretion of hydrogen is prevented.

There is indeed a process that might do just that: the so called 'propeller mechanism' proposed originally by Illarionov and Sunyaev (1975) and applied to white dwarfs by Wesemael and Truran (1982). In this mechanism, a rotating white dwarf with a small magnetic field might screen out protons and other light charged particles, while heavier elements might be accreted, especially if they are locked up in dust grains. In order for this mechanism to work the hydrogen near the star must be ionised, and this only happens if the effective temperature is high enough, $\geq$ 10 000 K. Liebert *et al* (1987a) were the first to point out that the slightly cooler objects K789-37 and Ross640, which in fact show about the solar calcium/hydrogen ratio, seem to provide empirical evidence for a critical temperature of 10 000 to 11 000 K for the accretion of hydrogen. This could be an acceptable explanation, however, the most likely explanation for the DBA phenomenon requires just the opposite, accretion of hydrogen, in exactly the same range of effective temperatures. Moreover, the even cooler objects GD401, L745-46A, and G165-7 also show a calcium/hydrogen ratio above the solar value although the 'propeller mechanism' is not supposed to work at these temperatures.

The evidence against solar accretion of hydrogen is weakened considerably if we allow an uncertainty of a factor of ten in the ratio. That would leave only four contradictory cases, with only one of them (G165-7) below 10 000 K. Sion *et al* (1988a) have used their results for the DBZ as a strong argument *in favour* of solar accretion.

For GD40, GD401 and K789-37 there is also a contradiction with the predictions for the magnesium/calcium ratio, which is a factor of three to ten smaller than the solar ratio, although, taking all possible uncertainties together, this does not seem to be as severe as in the hydrogen problem.

Summarising the discussion of metal abundances, we could state that the basic accretion-diffusion-mixing scenario is supported at least by part of the observations and is probably correct. The details, however, present some puzzles, which will only be solved if we understand the accretion mechanism, especially the accretion of dust grains and the possible deviations from solar abundances in the accreted matter (Alcock and Illarionov 1980b).

6.4.4. Carbon in DQ. What is different with carbon compared to other elements? If we believe in gravitational settling as the basic mechanism working in the outer layers of white dwarfs, we would, in helium-rich objects, expect that the thin helium layer floats on top of the next heavy element (carbon), built up by helium burning in previous stages of evolution. This provides the base for the current explanation of the DQs, first proposed by Koester *et al* (1982) and studied in much more detail by Fontaine *et al* (1984) and Pelletier *et al* (1986). We assume that there is a smooth transition between helium and carbon layers, with a structure given by the diffusion equilibrium. If the convection zone in the helium layer reaches down to the tail of the carbon distribution it can bring up traces of carbon to the surface without transforming the outer layers into almost pure carbon, as would be the case for an infinitely sharp transition layer. The detailed calculations predict a maximum carbon abundance in the range 11 000 to 12 000 K, due to a combined effect of extent of convection zones and the physics of pressure ionisation. This correlation is indeed present in the observations as was first noted by Wegner and Yackovich (1983). This theory even allows, at least in principle, an empirical determination of the thickness of the helium layer: $\log M_{\rm He}/M$ must be between -3.5 and -4.0 in order to fit the observations (Pelletier *et al* 1986), a result, which again is in conflict with the current

predictions of pre-white dwarf evolution (Mazzitelli and D'Antona 1986, Iben and Tutukov 1984, Iben and MacDonald 1985).

7. Pulsating white dwarfs

The luminosity of an isolated star may vary because the star is oscillating about its equilibrium state. Examples for this phenomenon are RR Lyrae and Cepheid variables, where the entire star expands and contracts radially with a well-defined period. The study of the pulsational properties of stars has a long history and excellent reviews may be found in Rosseland (1949), Ledoux (1958), Ledoux and Walraven (1958), Cox (1980) and Van Horn (1984).

The principal aim of stellar pulsation theory is to study the reaction of a stellar model in hydrostatic equilibrium to various types of perturbations. The simplest but as it turns out most important of these are small, adiabatic, radial perturbations, which determine whether the star is dynamically stable or not, on a dynamical time scale $\sim (G\rho)^{-1/2}$. This is the shortest of the various instability time scales in stellar models (Ledoux and Walraven 1958).

7.1. Radial oscillations

The radial oscillations of white dwarfs were first studied by Sauvenier-Goffin (1949) in the Newtonian approximation. The differential equation describing such oscillations obtained by linearising the basic equations of momentum, energy and mass conservations with respect to small radial perturbations $\xi(r) = \delta r/r$ (Cox 1980) is:

$$r\ddot{\xi} = 4\pi r^2 \xi \frac{\mathrm{d}}{\mathrm{d}m}\left[(3\Gamma_1 - 4)\,P\right] + \frac{1}{r}\frac{\partial}{\partial m}\left(16\pi^2\Gamma_1 P \rho r^6 \frac{\partial \xi}{\partial m}\right) \tag{7.1}$$

where r, P, m, ρ, Γ_1 refer to the equilibrium solution and Γ_1 is the adiabatic index $(\mathrm{d}\ln P/\mathrm{d}\ln\rho)_{\mathrm{ad}}$. As a simple example consider a motion where ξ and Γ_1 are spatially constant, i.e. independent of m so that

$$\ddot{\xi} = -(3\Gamma_1 - 4)\frac{Gm}{r^3}\xi. \tag{7.2}$$

Hence, for solutions with $\xi \propto \exp(\mathrm{i}\sigma t)$,

$$\sigma^2 = (3\Gamma_1 - 4)\frac{Gm}{r^3} \tag{7.3}$$

and an oscillatory solution with a period $\Pi = 2\pi/\sigma$ exists if $\Gamma_1 > 4/3$. For $\Gamma_1 < 4/3$, we have $\sigma^2 < 0$, and the star is dynamically unstable on a time scale $\tau \sim (G\rho)^{-1/2}$.

It can be shown that these conclusions remain valid for a general stellar model with the changes that Γ_1 is replaced by an appropriate average over the star and the single frequency σ is replaced by an eigenvalue spectrum, with the lowest frequency given by a relation similar to (7.3). The detailed numerical calculations of Sauvenier-Goffin (1949) confirmed the dimensional estimates derived from (7.3) that the fundamental pulsation periods of white dwarfs should be 10 s or somewhat less.

The dynamical stability of spherical stars within the framework of general relativity was studied by Chandrasekhar (1964), who found that the stability criterion is modified to

$$\langle\Gamma_1\rangle > \frac{4}{3} + \frac{2KGM}{Rc^2} \tag{7.4}$$

where K is positive and ~ 1. Hence general relativistic effects may be important for neutron stars, where $GM/Rc^2 \sim 0.1$. For the (ideal) degenerate electron gas in the interior of white dwarfs, $\Gamma_1 \simeq 5/3$ if the electrons are non-relativistic, and $\Gamma_1 \simeq 4/3$, if they are highly relativistic. Thus although $GM/Rc^2 \leq 10^{-3}$ for white dwarfs, general relativistic effects can play an important role for the highest density white dwarfs.

The dynamical stability of high mass white dwarfs had been of considerable interest about two decades ago. Finzi and Wolf (1967) had suggested that Type I supernovae may form because of the collapse of a white dwarf which contracts slowly due to electron capture reactions. Baglin (1968) argued that white dwarfs with reasonable compositions have a limiting mass of 1.2 $M_\odot$ corresponding to $\rho_C \simeq 7.8 \times 10^8$ g cm^{-3} and that white dwarfs with $M > 1.2\ M_\odot$ would become dynamically unstable not because of electron capture but because of general relativistic effects.

On the other hand an analysis by Wheeler *et al* (1968) showed that white dwarfs with $1.8 \times 10^9 \leq \rho_C \leq 4 \times 10^{10}$ g cm^{-3} could exist for various assumptions regarding μ_e and that for typical compositions with average atomic weights A given by $12 \leq A \leq 40$ general relativistic effects are not the prime cause of the instability. The difference in the results arose from the Wheeler *et al* (1968) assumption that, because the dynamical time scale is shorter than the electron capture time scale, the composition of the star may not change during the oscillation. This leads to a larger value of Γ_1 (Meltzer and Thorne 1966, Chanmugam 1977).

The discovery of the first radio pulsars with a period of 1.3 s (see Smith 1977 and references therein) led to speculations that it might be a radially oscillating white dwarf star, since the shortest periods for such radial oscillations in the fundamental mode are $\simeq 2$ s (Wheeler *et al* 1968, Faulkner and Gribbin 1968, Skilling 1968, Chanmugam 1977) and occur for white dwarfs near the limiting mass with the highest central density. The discovery of the Crab pulsar with a period of 0.033 s, however, confirmed instead that pulsars are rotating neutron stars. At present, no white dwarfs with high central densities have yet been discovered, so that a Newtonian description is adequate.

Besides the determination of the stability and the frequency spectrum the aim of stellar pulsation theory is to study whether radial oscillations can be excited. For this purpose it is necessary to study the 'vibrational stability' of the star (Ledoux and Walraven 1958), which includes thermal effects and energy transport so that energy dissipation can be included in the analysis. In the fully non-adiabatic treatment σ becomes complex, with the imaginary part proportional to the work done by pressure and gravitational forces during one cycle. The magnitude of this energy integral can be estimated in the linear, quasi-adiabatic approximation using the adiabatically derived eigenfunctions. In this case radial oscillations are excited if the energy integral $C < 0$, where

$$C = \int_0^M \left(\frac{\delta T}{T}\right)_{\text{ad}} \delta\left(\varepsilon_N - \frac{1}{\rho}\nabla \cdot \boldsymbol{F}\right) \mathrm{d}m \tag{7.5}$$

and ε_N is the energy generation rate due to nuclear burning, $\boldsymbol{F}$ the radiative flux and the suffix ad means that $(\delta T/T)$ is calculated in the adiabatic approximation.

In general the principal mechanisms that can excite oscillations are related to the two terms in brackets: the 'ε-mechanism' caused by a certain temperature dependence of the energy generation, and, more importantly, variations in the energy transport caused by the temperature and density dependence of the stellar opacity ('κ-mechanism'). In this mechanism, radiation travelling through a partial ionisation zone is more easily absorbed when the star is compressed, because the opacity increases. This energy is then released when the star expands so that the pulsation is driven.

Vauclair (1971a, see also Ledoux and Sauvenier-Goffin 1950) has considered the effects of a hydrogen burning shell, the classical κ-mechanism in the He II ionisation zone, and the increase in the luminosity perturbations in the inner parts of the isothermal core due to opacity variations etc. He found that the κ-mechanism can drive the oscillations of both the fundamental and first overtone (Vauclair 1971b) for DA white dwarfs with $T_{\rm eff} \sim 10\,000$ K. This instability against radial oscillations was confirmed in all subsequent calculations (Cox *et al* 1980, 1987, Saio *et al* 1983, Starrfield *et al* 1983).

7.1.1. Discovery of the first variable white dwarf. The calculations by Sauvenier-Goffin (1949) had motivated searches for variable white dwarfs with periods of the order of 10 s, but these searches for over a decade failed to reveal any examples of variability (e.g. Lawrence *et al* 1967). Because white dwarfs had shown no evidence for variations they became useful examples of 'standard' stars whose luminosities do not vary with time. However, observations of one such white dwarf 'standard' (HL Tau 76) in December 1965 by Landolt (1968) revealed that its brightness varied with a period of 750 s. This is, as is so often the case in astronomy, another example of a major discovery, which was totally unexpected and serendipitous. This again stimulated searches for variability and soon other variable white dwarfs with periods between $\sim$ 100 and $\sim$ 1000 s were discovered (Lasker and Hesser 1969, 1971). These periods were puzzling, however, because they were substantially larger than the expected periods for the radial oscillations. In spite of continued searches no radial variability in the short period range has yet been discovered (Robinson 1984, and references therein).

7.2. Non-radial oscillations

Extensive theoretical studies of non-radial oscillations in stars had been carried out a long time ago although, unlike the case of radial oscillations, there were no observational examples of stars exhibiting such oscillations. These studies showed that the possible pulsation frequencies split up broadly into three distinct classes of oscillations, the g- (or gravity) modes, the p- (or pressure) modes, and the f-mode which exists when the spherical harmonic index $l \geq 2$ (Cowling 1941). The p-modes correspond to oscillations where the restoring force is due to pressure so that they are essentially accoustic waves. They have periods which are $\leq (G\rho)^{-1/2}$, with the higher modes having shorter periods. Calculations of non-radial oscillations of highly luminous white dwarfs by Harper and Rose (1970) (see also Baglin and Schatzman 1969) showed that g-mode oscillations had periods of $\sim$ 50 s. On the other hand, these periods scale roughly $\propto 1/T$, where T is the core temperature (Baglin and Heyvaerts). This led Chanmugam (1972), and Warner and Robinson (1972), to propose that if the variable white dwarfs were cooler they could exhibit g-mode non-radial oscillations consistent with the observed periods $\geq$ 100 s.

Consider a spherically symmetric Newtonian model of a star which is perturbed so that the Lagrangian perturbation $\delta r = \delta r\, e_r + r\delta\theta\, e_\theta + r\sin\theta\,\delta\phi\, e_\phi$, where (r, θ, ϕ) are spherical polar coordinates and e_r, e_θ, e_ϕ are orthogonal unit vectors in the radial and transverse directions (see Cox 1980). If the perturbation has a time dependence $\propto \exp(i\sigma t)$ and the angular part is expanded in spherical harmonic functions, then the linearised mass, energy and momentum equations and Poisson's equation $\nabla^2\psi = 4\pi G\rho$ may be written as follows in the adiabatic approximation (Cox 1980):

$$
\begin{aligned}
u &= r^2\delta r \\
y &= P'/\rho \\
\frac{dy}{dr} &= \frac{\sigma^2 + Ag}{r^2}\, u - Ay - \frac{d\psi'}{dr} \\
\frac{du}{dr} &= \frac{\rho g}{\Gamma_1 P}\, u + \left(\frac{l(l+1)}{\sigma^2} - \frac{r^2\rho}{\Gamma_1 P}\right) y + \frac{l(l+1)}{\sigma^2}\, \psi' \\
\frac{1}{r^2}\frac{d}{dr}\left(r^2\frac{d\psi'}{dr}\right) &= -\frac{4\pi G\rho A}{r^2}\, u + \frac{4\pi G\rho^2}{\Gamma_1 P}\, y + \frac{l(l+1)}{r^2}\, \psi'.
\end{aligned}
\tag{7.6}
$$

Here primes denote Eulerian perturbations and u, y and ψ' are functions only of r, g is the local acceleration of gravity, l is the spherical harmonic index, while

$$
A = \frac{1}{\rho}\frac{d\rho}{dr} - \frac{1}{\Gamma_1 P}\frac{dP}{dr}. \tag{7.7}
$$

These equations may then be solved by using appropriate boundary conditions at the centre and the surface of the star. The eigenvalues corresponding to the angular oscillation frequencies are given by σ^2_{nl} with $n = 1,2,3,\ldots$. The spectra of the oscillation frequencies show that the g-modes may be subdivided into two further classes called g^+- and g^--modes. The g^+-modes are stable and correspond to $\sigma^2_{nl} > 0$ while the g^--modes are unstable and correspond to $\sigma^2_{nl} < 0$. The f-mode and p-modes have $\sigma^2_{nl} > 0$ and are stable. For $\sigma^2_{nl} > 0$, σ^2_{nl} increases with both n and l. A schematic diagram, based on Smeyers (1967), of the different modes is shown in figure 8, taken from Cox (1980).

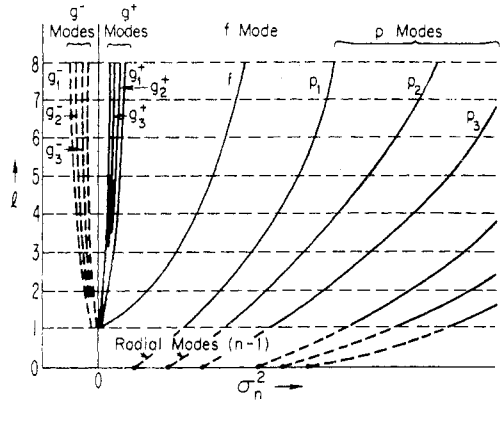

Figure 8. Eigenvalues σ^2_{nl} of linear, adiabatic, non-radial oscillations for various modes n versus the angular spherical harmonic index l (schematic) from Cox (1980). The four types of non-radial oscillations (p, f, g^+ and g^-) are shown.

The quantity A plays an important role in showing the connection between non-radial oscillations and convective instability. Consider a stratified fluid in which the physical quantities depend only on the radial coordinate r. If a fluid element is displaced from r to $r + \delta r$ the buoyancy force per unit volume acting upwards on the element is $\rho g A \delta r$ (Cox 1980). The fluid element will tend to return to its original position if $A < 0$, in which case the fluid is said to be convectively stable and vice versa. If there is no friction or heat exchange with the fluid element and the fluid is convectively stable, it will undergo oscillations about the equilibrium position with an angular frequency N, known as the Brunt–Väisäila frequency, where $N^2 = -Ag$. If $|A|$ is sufficiently small it may be shown that for g-modes $\sigma_{nl}^2 \propto \langle -A \rangle$.

For a zero-temperature degenerate electron gas $A = 0$ so that there are no g-modes with non-zero frequencies. However, if the thermal corrections to the equation of state of a degenerate electron gas are included it may be shown that $A \propto T^2$ so that $\sigma_{nl} \propto T$ (Baglin and Heyvaerts 1969). Hence, simple dimensional analysis shows that the periods for g-mode non-radial oscillations of a white dwarf increase as the star cools (Chanmugam 1972).

Detailed numerical calculations of non-radial oscillations of white dwarfs composed of iron confirmed that the g-mode periods increase monotonically as the star cools and evolves (Osaki and Hansen 1973). Furthermore, they showed that a 0.398 $M_\odot$ white dwarf with a luminosity $L = 7.38 \times 10^{-5}\ L_\odot$ would have non-radial quadrupole oscillations ($l = 2$) for $n = 1$ and 2 of 209.8 and 291.1 s respectively, reasonably close to the basic periods of 212 and 273 s then reported for R548. Similar results were also obtained by Brickhill (1975).

The major unsolved problem at that time was to understand why the particular g-modes with low values of l would be excited. The resolution of this problem took almost a decade and was aided by a number of observations of these variable white dwarfs.

7.3. Observations of variable DA *(*DAV*) white dwarfs*

Searches for low amplitude (≤ 0.1 magnitudes) luminosity variations in white dwarfs were significantly helped by the development of the two-star high-speed photometer by Nather (1973). This enabled high-speed photometric observations to be carried out on a star with simultaneous observations of a nearby 'standard' so that atmospheric fluctuations could be subtracted out and real variations in the luminosity more accurately determined. The use of the two-star photometer soon led to the discovery of additional variable DA white dwarfs, a class which became known as ZZ Ceti stars and is now called DAV. It also showed that some earlier reports of variable white dwarfs were spurious, while others were verified. Instead of recalling the whole history of variable white dwarf discoveries, we give in table 3 an up-to-date list of all presently known variables with references to the discovery papers.

In several cases multiple periods were observed. Thus, for example, R548 has two pairs of observed periods (table 3), which were interpreted (Stover *et al* 1980) as due to splitting by the rotation of the star with a period of 1.5 days. For a star oscillating with a frequency σ_{nl} the $(2l + 1)$ fold degeneracy is lifted by rotation giving the m modes:

$$\sigma_{nlm} = \sigma_{nl} \pm m(1 - c_l)\Omega, \tag{7.8}$$

with $m = -l, -l + 1, \ldots, l$, where Ω is the rotational frequency of the star and c_l is a constant depending on the internal structure of the star (Ledoux 1958) with $c_l \simeq$

Table 3. Observations of variable white dwarfs.

Object	Periods (s)	References
Variable PNN		
K1-16	1520, 1730	GB
Longmore 4	1800	BC
Variable DO (DOV)		
PG1159-035	390–833	MSLG
PG1707+427	447.16, 448.95, 334.6	BGGL
PG2131+066	450	BGGL
PG0122+200	614, 467, 449, 435, 400, 380, 364, 336	BG
Variable DB (DBV)		
GD358	142.3–952	WRNF
PG1654+160	148.5–851	WRN
PG1351+489	489.5	WNH
PG1115+158	1000	WNH
PG1456+103	423–854	GBGL
CBS114	650	WC
KUV05134+2605	350–900	GWGL
Variable DA (DAV)		
HL Tau 76	746.2, 494.2	L
R548 = ZZ Ceti	212.77, 213.13, 274.25, 274.77	LH
G29-38	613, 677, 931, 1016	SK
G38-29	1024, 938	MR75
BPM31594	308, 617	M76
G117-B15A	107.6, 119.8, 126.2, 215.2, 271.0, 304.4	RU
Ross808	769, 1250	MR76
GD99	??	MR76
BPM30551	606.8, 682.7, 744.7, 840.2	HLN
G207-9	739, 557, 318, 292	RM
L19-2	192.4	M77
GD154	780, 1186	RSNM
GD385	256.13, 256.33, 128.11	FMCLPV
G191-16	865	MFDGLS
G185-32	200	MFDGLS
G255-2	685, 830	VDC81
G226-29	109.3 triplet	GM
GD66	197, 256, 273, 304	DVC
G238-53	685, 830	FW
PG2303+243	900.5, 794.5, 623.4, 397.3, 349.3 ...	VDC87

References: BC, Bond and Ciardullo 1989; BG, Bond and Grauer 1987; BGGL, Bond *et al* 1984; DVC, Dolez *et al* 1983; FMCLPV, Fontaine *et al* 1980; FW, Fontaine and Wesemael 1984; GB, Grauer and Bond 1984; GBGL, Grauer *et al* 1988; GM, Gustafson and McGraw 1980; GWGL, Grauer *et al* 1989; HLN, Hesser *et al* 1976; L, Landolt 1968; LH, Lasker and Hesser 1971; M76, McGraw 1976; M77, McGraw 1977; MFDGLS, McGraw *et al* 1981; MR75, McGraw and Robinson 1975; MR76, McGraw and Robinson 1976; MSLG, McGraw *et al* 1979; RM, Robinson and McGraw 1976; RSNM, Robinson *et al* 1978; RU, Richer and Ulrych 1974; SK, Shulov and Kopalskaya 1971; VDC81, Vauclair *et al* 1981b; VDC87, Vauclair *et al* 1987; WC, Winget and Claver 1989; WNH, Winget *et al* 1987b; WRN, Winget *et al* 1984; WRNF, Winget *et al* 1982b.

0.25 for white dwarfs (Hansen *et al* 1977). The recent observations of GD358 (a DBV), which was considered the most convincing case for rotational splitting, have, however, cast some doubt on this interpretation (Hill 1987). Hill showed that the splitting changed or even disappeared completely between two observations, which hardly can be reconciled with an interpretation due to rotation of the star.

The most important step towards the solution for the excitation mechanism was, however, the realisation that the structure of the outer layers as discussed in the previous sections plays a crucial role in it.

7.4. Excitation mechanisms

In 1981 several groups independently proposed excitation mechanisms in white dwarfs involving ionisation zones in realistically stratified outer layers, corresponding to diffusion equilibrium. These calculations required the fully non-adiabatic solution of the non-radial pulsation equations. Dziembowski and Koester (1981) showed that the κ-mechanism operating in a He^+ ionisation zone could drive the oscillations. Calculations of white dwarf models with a helium layer of 10^{-4} $M_\odot$ showed that g-modes with periods $\sim$ 100 to 1000 s could be driven if the mass of the hydrogen layer is less than $1.2 \times 10^{-13} M_\odot$.

Dolez and Vauclair (1981) in similar calculations also found driving by the hydrogen ionisation zone for slightly more massive hydrogen layers up to $\sim 10^{-11}$ $M_\odot$. Winget (1981), and Winget *et al* (1981) carried out the most comprehensive study of the effects of hydrogen and helium ionisation zones in exciting non-radial oscillations in evolving white dwarfs with masses of 0.6 and 0.8 $M_\odot$. These authors and Starrfield *et al* (1982) showed that models with *relatively* thick surface layers M_H in the range 10^{-14} to 10^{-8} $M_\odot$ could provide the appropriate periods in the observed DAV white dwarfs. Calculations of the radial part of the eigenfunctions $\delta r/r$ showed that in specific cases it is trapped in the hydrogen layer (see figure 9).

Thus, as may be seen in figure 9, the g_{11} mode, which has relatively negligible amplitude in the inner parts, can be easily excited. These studies clearly showed that the manner in which the outer envelope is stratified plays a crucial role in selecting a particular mode of oscillations. An implication of this effect, on the other hand, is that the observations in combination with theoretical calculations might be used to empirically probe the stratifications of white dwarfs below the visible surface.

This success for the variable DAs led Winget *et al* (1982a) to suggest that DB white dwarfs may also exhibit non-radial oscillations driven by a partial helium ionisation zone.

7.5. DBV, DOV and PNN variables

The prediction that the helium white dwarfs would also show g-mode oscillations was soon verified when Winget *et al* (1982b) made the exciting discovery of pulsations from the DB white dwarf GD358. Since then six more DB variables have been discovered (see table 3). Several of these variables show very complex frequency spectra displaying many periods, with GD358, the prototype, having over 20. In this and similar cases table 3 only gives the dominant periods or period ranges, because the periods are not always stable from one observing run to the next, probably due to beating between closely spaced and unresolved frequencies.

In addition to the DAV and DBV white dwarfs two other classes of variable white dwarfs (or pre-white dwarfs) have been reported. One of these is a subclass of the DO

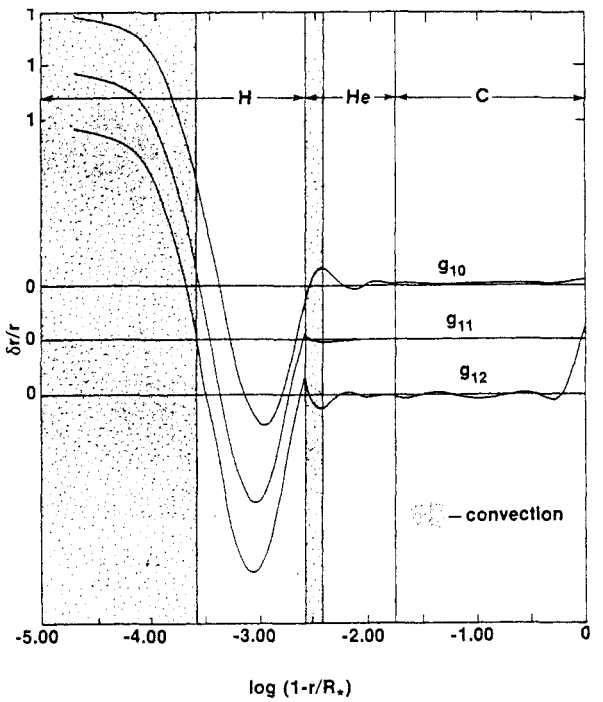

Figure 9. The radial part of the eigenfunctions $\delta r/r$ (as a function of the fractional radius r/R_* and normalised to unity at the surface) for the g_{10}, g_{11}, and g_{12} modes for compositionally stratified white dwarf models. The scales are displaced for clarity. Note the trapping of the modes in the hydrogen layer. From Winget *et al* 1981.

stars and was originally named PG1159 variables after the first member (PG1159-035) to be discovered (McGraw *et al* 1979). The DOV stars (or GW Vir stars as they are also called) are extremely hot ($> 10^5$ K, Werner *et al* 1989), but the temperatures are not well known. The PNN class presently consists of two members that are central stars of planetary nebulae; the prototype K1-16 was discovered recently by Grauer and Bond (1984). They are less evolved and more luminous than the DOVs and their observed periods are slightly longer. The excitation mechanism for the two hot variable classes is poorly understood; the various possibilities are discussed in detail by Kawaler (1987).

7.6. Instability strips, period changes and white dwarf 'seismology'

The determination of the regions in the HRD where pulsational instability occurs, the 'instability strips', is hampered for the two hot classes by the lack of adequate spectral analyses and temperature determinations.

7.6.1. Instability strips. McGraw and Robinson (1976) made the important observation that the DAV stars have very similar effective temperatures between 10 000 and 15 000 K. The range of instability was subsequently studied by McGraw (1979), Greenstein (1982), Weidemann and Koester (1984), Fontaine *et al* (1985), Wesemael *et al* (1986) and Lamontagne *et al* (1987, 1989). The estimates seem at present to

have converged on the values 11 500–13 000 K for the red and blue edges. Furthermore, it appears that essentially all white dwarfs in this temperature range are variable (Fontaine *et al* 1982). When comparing this observational fact to the theoretical predictions two main conclusions emerge (e.g. Winget *et al* 1981, 1982a, Bradley *et al* 1989):

(i) The thickness of the outer hydrogen layer must be in the range from 10^{-13} to 10^{-8} $M_\odot$. If the layer is thicker than $\sim 10^{-8}$ $M_\odot$ the blue edge of the instability strip drops rapidly to 8000 K, incompatible with the observations.

(ii) Energy transport in the convection zone must be much more effective than is usually assumed. In the mixing-length approximation different efficiencies are modelled by changes of the free parameter α, the ratio of mixing-length to pressure scale height. Agreement with the observed instability strip is only obtained for $\alpha = 3$, whereas most stellar evolution calculations use values between 1 and 2.

The first conclusion, which is in sharp disagreement with predictions of stellar evolution calculations, has been challenged recently by Pesnell (1987) and Cox *et al* (1987). They proposed a new driving mechanism called 'convection blocking' based on a different treatment of the interaction of pulsations with convection and find pulsational instability even with thick hydrogen layers of the order of 10^{-4} $M_\odot$. The final decision about this mechanism may have to wait until a theory of time-dependent convection is available, although a comparison of convection and pulsation time scales casts some doubt on the realism of their assumptions (Koester 1987a). They were, however, unable to find unstable modes above $T_{\rm eff} = 11\,500$ K, which is clearly not in agreement with the empirical instability strip.

The instability strip for the DB variables is less well known, because the determination of effective temperatures for hot DBs is extremely difficult in general. Koester *et al* (1985) found $T_{\rm eff} = 24\,000 \pm 1000$ K for the prototype GD358 from an analysis of UV and very good optical data. The calculations of Winget *et al* (1983) had predicted instability in the range 16×10^3 to 19×10^3 K assuming the standard mixing-length theory, and up to 26×10^3 to 29×10^3 K with more efficient convection. Liebert *et al* (1986) found somewhat higher temperatures for the hot DBs from UV observations and determined 24×10^3–28×10^3 K for the instability strip, with an uncertainty of 2000 K for the red and blue edges. In any case both determinations agree on the conclusion that convection must be very efficient if the theoretical calculations are correct. Contrary to the DAV case not all DBs in the instability strip seem to be variable. The location of the instability strip in the HRD are indicated in figure 4.

7.6.2. Period changes. In the cooler DBV and DAV white dwarfs cooling dominates the evolution. Because $\sigma_{nl} \propto T$ in this case (Baglin and Heyvaerts 1969) one can deduce that periods of g-mode oscillations increase with time roughly as

$$\frac{\dot{\Pi}}{\Pi} \propto -\frac{\dot{T}}{T} \propto \frac{1}{\tau_c} \tag{7.9}$$

where τ_c is the cooling time scale and T the core temperature. Current predictions for $\dot{\Pi}$ from numerical models for the DAVs are in the range 2 to 7.5×10^{-15} (Bradley *et al* 1989), while the best available observations are upper limits of 9.6×10^{-15} for R548 (Tomaney 1987) and 1.25×10^{-14} for G117-B15A (Kepler *et al* 1989). It will take a few more years of observations before meaningful comparisons become feasible.

Predicted period changes for the DBV white dwarfs are larger, $\sim 10^{-13}$ (Kawaler *et al* 1986). However, in spite of extensive observations of the best candidate

PG1351+489 the analysis so far has not given conclusive results. Kawaler and Hansen (1989) suggest that non-linear effects might be responsible, while Goupil *et al* (1988) claim that this object might be on the way to displaying chaotic behaviour.

Due to their much younger age and correspondingly faster evolutionary time scales the situation is more promising for the hot DOVs. Because these objects are not yet completely degenerate, their period changes should show the combined effect of contraction and cooling. While cooling *increases* the period, contraction *decreases* it. Theoretical computations (Kawaler *et al* 1985) indicated that cooling dominates and that the periods should increase by $\sim 10^{-11}$. From observations of PG1159-035 spanning five years Winget *et al* (1985) found a secular period change of the expected magnitude; however, the period was *decreasing* with time. The reason for this discrepancy is not understood and stellar rotation, non-adiabatic effects, magnetic fields, or excitation of modes with significant amplitudes in the core (where cooling dominates) have been proposed as possible solutions (Kawaler and Hansen 1989).

7.6.3. Mass determinations from pulsation spectra. The mean period spacing over several modes for successive values of n is fairly constant, at least for higher values of n, with deviations less than 10% in the models (Kawaler 1987). This period spacing for g-modes in DOVs is very insensitive to the internal composition or the luminosity but depends very strongly on the total stellar mass. The identification of constant period spacing in two objects enabled Kawaler (1987) to determinate the masses of PG1159-035 to be 0.6 $M_{\odot}$ and that of PG0122+200 to be 0.73 $M_{\odot}$. This interpretation depends on the correct identification of modes but has the potential of becoming a very accurate 'seismological' tool.

8. Magnetic white dwarfs

The possible existence of strong magnetic fields ($\sim$ 1 MG) in white dwarfs was suggested by Blackett (1947), who argued that the magnetic moment of a star is proportional to its angular momentum and that angular momentum was conserved during stellar evolution, which is not the case (see below). Ginzburg (1964) and Woltjer (1964) suggested that if the surface magnetic flux ($\propto BR^2$), where B is the surface magnetic field and R the radius, is conserved during the lifetime and collapse of a normal (i.e. non-degenerate) star then the magnetic field of the white dwarf or neutron star produced would be very high. For typical initial values of $B \sim 100$ G and $R \sim 10^{11}$ cm for the normal star, a neutron star with a radius $\sim 10^6$ cm would then have a field $\sim 10^{12}$ G, while a white dwarf with $R \sim 10^9$ cm would have a field $\sim 10^6$ G. The discovery of pulsars, which are believed to be rotating neutron stars with magnetic fields $\sim 10^{12}$ G (Smith 1977) appeared, therefore, to confirm this suggestion and inspired searches, using Zeeman spectroscopy, for strong magnetic fields in white dwarfs (Preston 1970). This requires an understanding of the behaviour of atoms in strong magnetic fields, to which we now turn.

8.1. Spectroscopy in high magnetic fields

The behaviour of atoms in strong magnetic fields has been discussed by a number of authors (see for example the review by Garstang 1977, and references therein). We briefly summarise here some of the essential features relevant for our discussion, following Garstang (1977).

The Hamiltonian for an atom in a magnetic field, neglecting terms involving the nuclear spin (i.e. hyperfine structure), is given by

$$H = H_{\rm KE} + H_{\rm C} + H_{\rm spin} + H_{\rm magI} + H_{\rm magII} \tag{8.1}$$

where $H_{\rm KE}$ denotes the kinetic energy of the electrons, $H_{\rm C}$ the Coulomb interaction between the electrons and the nucleus and between the electrons, $H_{\rm spin}$ the electron spin–orbit term, $H_{\rm magI}$ the term linear in the magnetic field $\boldsymbol{B}$ which gives rise to the linear Zeeman effect and $H_{\rm magII}$ the quadratic Zeeman term. For a uniform magnetic field with the vector potential $\boldsymbol{A} = (\boldsymbol{B} \times \boldsymbol{r})/2$ where $\boldsymbol{B} = \nabla \times \boldsymbol{A}$ and $\nabla \cdot \boldsymbol{A} = 0$, it follows that

$$H_{\rm magI} = e\boldsymbol{B} \cdot (\boldsymbol{L} + g_{\rm e}\boldsymbol{S})/2mc \tag{8.2}$$

where, for a many-electron atom, the total orbital ($\boldsymbol{L}$) and spin ($\boldsymbol{S}$) angular momenta are given by $\boldsymbol{L} = \sum \boldsymbol{l}_i$ and $\boldsymbol{S} = \sum \boldsymbol{s}_i$, and the sums are over the individual electrons i. Here $g_{\rm e} \simeq 2$ is the electronic g-factor.

If $\boldsymbol{B}$ is taken to be along the $\theta = 0$ axis in spherical polar coordinates (r, θ, ϕ),

$$H_{\rm magII} = (e^2B^2/8mc^2) \sum r_i^2 \sin^2 \theta_i \tag{8.3}$$

where the summation is over the atomic electrons i.

For sufficiently weak magnetic fields, $B \ll 5 \times 10^4$ G, except for light atoms, $H_{\rm magII}$ may be neglected and $H_{\rm magI} \ll H_{\rm spin}$ where the inequalities symbolically represent the corresponding typical matrix elements. Then the principal effects of the magnetic field arise through the linear Zeeman effect and the first-order effect on an atomic level characterised by $|SLJM\rangle$ is given by $\Delta E = \Delta E_0 + (e\hbar/2mc)Bg_JM$, where g_J is the Landé g-factor (Garstang 1977) and ΔE_0 is the transition energy in the absence of the field.

For stronger magnetic fields where $H_{\rm C} \gg H_{\rm magI} \gg H_{\rm spin} \gg H_{\rm magII}$, the magnetic interaction is large enough to break the spin–orbit coupling and the states are labelled by $|SM_SLM_L\rangle$. In this case the Paschen–Back effect is important and

$$\Delta E = \Delta E_0 + (e\hbar/2mc)B\Delta M_L \tag{8.4}$$

where, for electric dipole transitions, $\Delta M_L = 0, \pm 1$ (with $\Delta M_S = 0$).

For higher magnetic fields (≥ 0.1 MG), or at lower fields for large n, the quadratic Zeeman term $H_{\rm magII}$ could become more important. For a one-electron atom with the unperturbed state $|nlm_lm_s\rangle$ the first-order energy shift, assuming a nucleus of charge Z, is given by

$$\Delta E_{\rm Q} = \frac{e^2B^2a_0^2}{8mc^2Z^2} n^2 \frac{[(5n^2 + 1 - 3l(l+1))]\,[l^2 + l - 1 + m_l^2]}{(2l-1)(2l+3)} \tag{8.5}$$

where a_0 is the Bohr radius. For transitions between two levels $\Delta l = 0, \pm 2$, while Δn can take any value (see Hamada and Nakamura (1973) and Garstang and Kemic (1974) for improved calculations of the quadratic Zeeman effect using perturbation theory).

For magnetic fields in excess of 100 MG the magnetic terms in the Hamiltonian can become comparable to the Coulomb energy. This regime is intermediate to the

Paschen–Back (and quadratic Zeeman) regimes and the Landau regime where the magnetic field is so strong that the Coulomb interaction is small compared to the magnetic term (Garstang 1977). The intermediate field regime is very much more difficult to understand because it is not possible to use perturbation methods easily. By contrast the high field (Landau) regime is relatively easier to study (Yafet *et al* 1956). Variational calculations for the intermediate field have been carried out by a number of authors (e.g. Smith *et al* 1972), for B less than about 7×10^{11} G (see also Praddaude 1972). More recently, extensive calculations for the intermediate regime have been performed by research groups at Louisiana State University (LSU, Henry and O'Connell 1984, 1985) and at the University of Tübingen (Rösner *et al* 1984, Forster *et al* 1984, Wunner *et al* 1985, 1987). These calculations are in general agreement with one another in regions where they overlap.

8.2. Search for magnetic white dwarfs

Because white dwarfs have in general very broad spectral features, or none at all, it is difficult to detect their magnetic fields using Zeeman spectroscopy. Preston (1970) attempted to detect strong magnetic fields ($\gg$ 1 MG) in white dwarfs by looking for the effects due to the quadratic Zeeman shift in the spectra of DA white dwarfs with strong Balmer lines. For the case of large n, neglecting terms of order n^2, the quadratic Zeeman term is given by

$$\Delta\lambda_{\mathrm{Q}} = -4.9654\ 10^{-23} Z^{-2}\ \lambda^2 B^2 n^4 (1 + m_l^2) \quad \text{Å} \tag{8.6}$$

for an s–np transition. Note that $\Delta\lambda_{\mathrm{Q}} \propto \lambda^2 n^4$ and not λ as in the case of the Doppler effect. This would allow the separation of the magnetic shift from that due to the space motion of the star along the line of sight. Furthermore, the shift in the σ component ($m_l = \pm 1$) is twice that of the π component ($m_l = 0$), so that the centroid of the triplet is shifted appropriately. Preston (1970) used this together with the radial velocities of several white dwarfs obtained by Greenstein and Trimble (1967) to place upper limits of about 0.5 MG for the average field over the stellar disk.

A novel approach for detecting magnetic fields in hot objects emitting an essentially featureless spectrum was proposed by Kemp (1970) with his magnetoemission model. He argued that the emitted radiation would nevertheless be circularly polarised and that its measurement could lead to the identification of the magnetic field. He noted that the Zeeman components of spectral lines have left and right circularly polarised components when viewed along the magnetic field. If the lines are significantly broadened so that they overlap and the spectrum becomes continuous, the radiation contains a hidden fractional circular polarisation. In order to show this he considered a simple model where the system consisted of three-dimensional harmonic oscillators distributed continuously with different natural angular frequency per unit angular frequency interval. Then the radiation at a frequency ω arises either from the transition from the $m = +1$, or the $m = -1$ state, to the ground state from two different oscillators, which have natural frequencies $(\omega \pm \omega_{\mathrm{c}}/2)$ respectively, in the absence of a field. Here $\omega_{\mathrm{c}} = eB/mc$ is the cyclotron frequency. Since the magnetic field does not change the wave function to first order the transition probabilities are inversely proportional to $(\omega \pm \omega_{\mathrm{c}}/2)$. Hence the intensities of the two components, which are left and right circularly polarised, are different and the radiation at the frequency ω is circularly polarised with fractional circular polarisation $V/I = -\omega_{\mathrm{c}}/2\omega$ for $\omega \gg \omega_{\mathrm{c}}$,

where I, Q, U, V are Stokes parameters. These results were experimentally confirmed, qualitatively, for thermal light sources in the laboratory (Kemp *et al* 1970a).

The first magnetic white dwarf to be discovered was Grw+70° 8247. It has an extraordinary spectrum whose main features defied identification for nearly half a century. Minkowski (1938) obtained several spectra of it which showed that it was not featureless as previously thought and that it had wide shallow absorption features at 4135 and 4475 Å. These together with another at 3910 Å discovered by Greenstein (1956) became known as Minkowski bands. Subsequent high resolution spectroscopy revealed a number of additional features (Wegner 1971).

In 1970, following the development of the magnetoemission model, Kemp discovered circularly polarised light from Grw+70° 8247 with a relatively small telescope, the 24 in of the University of Oregon. After observing the fractional circular polarisation as a function of wavelength Kemp *et al* (1970b) claimed a mean projected magnetic field of 10 MG for Grw+70° 8247. Because there were significant deviations from the simple linear relationship between circular polarisation and wavelength predicted by the magnetoemission model, and because the theoretical results were derived using a perturbation expansion in the magnetic field, there was some uncertainty in the interpretation. Nevertheless, the overall results were essentially unchanged, when the harmonic oscillator model was solved exactly (Chanmugam *et al* 1972).

After the discovery of the optical polarisation from Grw+70° 8247 attempts were made to understand the spectral features as those due to various atoms and molecules in strong magnetic fields (Mullan 1971, Angel 1972, Landstreet and Angel 1975, Wickramasinghe 1972, Greenstein 1970). Thus, for example, the discovery of a feature at 5835 Å raised the possibility that it was a Zeeman shifted He I 5876 Å line. However, Kemic (1974) presented calculations of the Hα–Hδ and He I lines, and showed that none of the features could be explained with magnetic fields of less than 100 MG and hence Angel (1979) suggested that the features might be explained by hydrogen atoms in even higher magnetic fields.

Subsequent observations of Grw+70° 8247 with the IUE satellite showed a feature at 1347 Å in the ultraviolet which was interpreted by Greenstein (1984b) as due to the Lyman α line 1s0–1p1 in a magnetic field of 200–400 MG, retaining the labelling of energy levels by their zero field quantum numbers nlm. Calculations by Henry and O'Connell (1984) showed that this σ-transition corresponded to a maximum wavelength of 1342.6 Å for $B \simeq 500$ MG, while similar results were obtained by Rösner *et al* (1984) and Forster *et al* (1984), who found the maximum to occur at 1343 Å. The discrepancy with the observations of 4 Å is probably due to uncertainties of the IUE wavelength scale (Greenstein *et al* 1985).

A difficulty in determining the magnetic field spectroscopically is that the magnetic field varies across the surface of the white dwarf leading to different shifts for different parts of the stellar surface thus smearing out all spectral features. However, as conjectured from earlier calculations by Praddaude (1972), Greenstein (1984b) pointed out that the features may remain visible at those wavelengths, where the variation of the shift with field strengths becomes stationary. By searching for these stationary regions in the calculations of the Tübingen and LSU groups it became possible to identify the features in Grw+70° 8247 with transitions of hydrogen in a magnetic field of about 320 MG, which is much higher than the original estimate from the magnetoemission model (Greenstein *et al* 1985, Angel *et al* 1985, Wickramasinghe and Ferrario 1988). Observed spectra of Grw+70° 8247 and the position of spectral features in different fields are displayed in figure 10. However, the correct understanding of variations in

the circular polarisation as a function of wavelength can only be obtained in detail if one takes into account the transfer of radiation through an atmosphere containing atoms in such strong magnetic fields (see below).

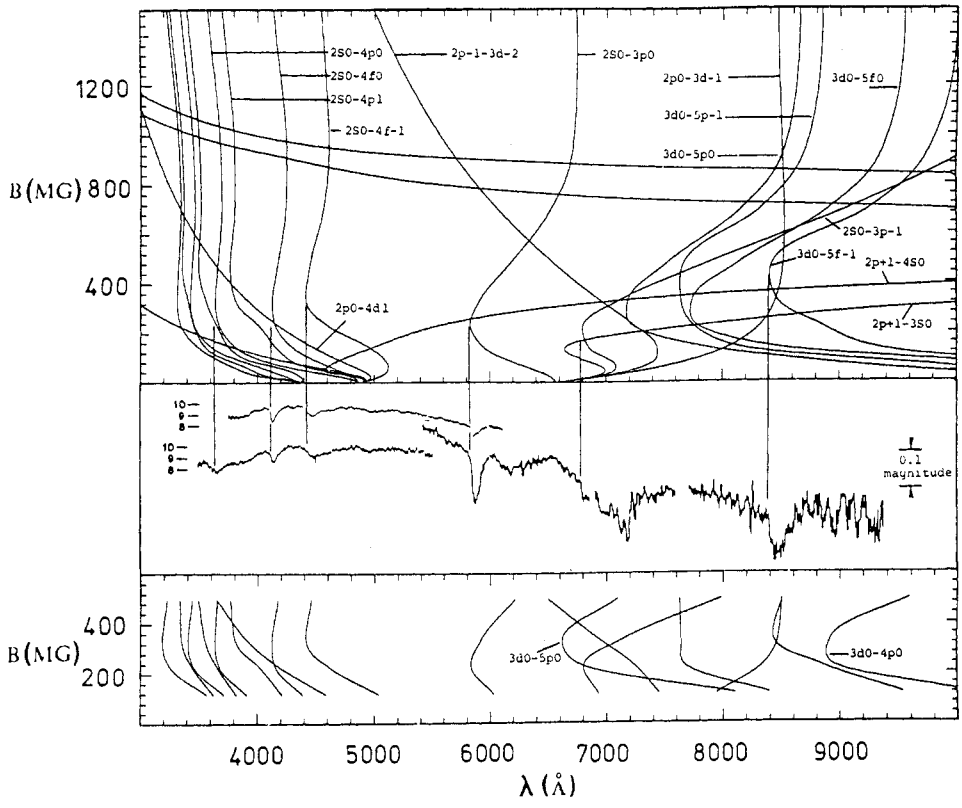

Figure 10. Observations of Grw+70° 8247 by Angel *et al* (1985) (centre) compared with the field–wavelength dependence of Zeeman components of hydrogen based on calculations by the Tübingen (upper) and LSU (lower) groups. The blue spectral region is on a flux scale (F_ν), and the red spectral region is on a magnitude scale ($-2.5 \log F_\nu$ + constant). Reproduced from Wickramasinghe and Ferrario (1988).

The search for magnetic white dwarfs was continued after the discovery of polarisation in Grw+70° 8247, and 27 objects with magnetic fields, in most cases smaller than in Grw+70° 8247, have now been detected, either from polarisation measurements, or from the Zeeman splitting of spectral features. These results and references to the discoveries are collected in table 4.

For many white dwarfs, which showed no detectable fields, upper limits have been determined. A sensitive method was used by Angel and Landstreet (1970) who searched for polarisation in the wings of the Hγ line. If the mean longitudinal field over the stellar disk is B_l and $I(\lambda)$ is the observed line intensity profile then the fractional circular polarisation is given by (Angel *et al* 1973):

$$V/I = 4.67\ 10^{-13} z (B_l/\lambda^2) \mathrm{d} \ln I / \mathrm{d} \ln \lambda \qquad (8.7)$$

Table 4. Observations of magnetic fields in isolated white dwarfs. Adapted from Schmidt (1989).

Object	T	Spectral features	Period	Polarisation (%) linear	circular	Polar field (MG)	References
PG0136+251	45000	H				2	LSGSM
PG1658+440	28000	H				3.5	LSGSM, PMWG
G141-2	5600	H				5	G86
GD90	9700	H			<0.15	9	ACSBH, WM, OD
G99-37	6200	C2, CH		<0.1	0.8	10	AL, A
KUV03292+0035	15000	H				12	WMB
GD356	7500	H(em)			<0.05	15	GM
HS1254+3430	15000	H				18	HGEHTR, J
KPD0253+5052	17600	H	4.1h		0.2	18	DM
WD1136-014		H				24	FL
G99-47	5600	H		<0.1	0.4	25	LAL, OD
KUV813-14	10400	H			0.25	29	SLSS, LSSSGB
PG1533-057	17000	H				31	LSSSGB
Feige 7	17800	H, He	2.2h		0.3	35	LASSB, MW
BPM25114	8600	H	2.8d		1	36	WB, WM
PG1313+095	15000	H	5.4h		1	≈50	GSL
GD116	16000	H				65	WSLS, SLWSS
GD229	16000	H		4	<0.2	25–60	LA, OSRW
ESO439-162	6300	C2				≈100	RM
G195-19	8000	none	1.3d	<0.13	0.8	≈100	AIL
PG1015+015	9900	H	1.6h		1	120	A, WC
G227-35	7000	?		0.25	2	≈150	HS, AHL
LP790-29	8600	C2		1	6	200	LS
G240-72	6000	?		1	0.5	≈200	AHSM
Grw+70°8247	12000	H		2	3	320	KSLA, G84, GHO, ALS, WF
PG1031+234	15000	H	3.4h	4	8	500	SWLGS, LSG

References: A, Angel 1978; AHL, Angel *et al* 1975; AHSM, Angel *et al* 1974b; AIL, Angel *et al* 1972; AL, Angel and Landstreet 1974; ALS, Angel *et al* 1985; ACSBH, Angel *et al* 1974a; DM, Downes and Margon 1983; FL, Foltz and Latter 1988; G84, Greenstein 1984b; G86, Greenstein 1986; GHO, Greenstein *et al* 1985; GM, Greenstein and McCarthy 1985; GSL, Green *et al* 1986; HGEHTR, Hagen *et al* 1987; HS, Hintzen and Strittmatter 1974; J, Jordan 1989; KSLA, Kemp *et al* 1970b; LA, Landstreet and Angel 1974; LAL, Liebert *et al* 1975; LASSB, Liebert *et al* 1977; LS, Liebert and Strittmatter 1977; LSG, Latter *et al* 1987; LSGSM, Liebert *et al* 1983; LSSSGB, Liebert *et al* 1985; MW, Martin and Wickramasinghe 1986; OD, O'Donoghue 1980; OSRW, Östreicher *et al* 1987; PMWG, Pravdo *et al* 1986; RM, Ruiz and Maza 1989; SLSS, Sion *et al* 1984; SLWSS, Saffer *et al* 1989; SWLGS, Schmidt *et al* 1986; WB, Wickramasinghe and Bessell 1976; WC, Wickramasinghe and Cropper 1988; WF, Wickramasinghe and Ferrario 1988; WM, Wickramasinghe and Martin 1979; WMB, Wegner *et al* 1987; WSLS, Wagner *et al* 1988. Most of the temperature determinations are from Sion *et al* (1988b).

where λ is measured in Å and $z \simeq 1$ (Babcock 1958). This technique has been used to place upper limits typically of about 0.05 MG in several DA white dwarfs with the lowest upper limit being of the order of 1000 G for 40 Eri B (Angel *et al* 1981).

Even more sensitive is the search for Zeeman broadening in the narrow core of Hα in DAs with high resolution spectroscopy, made possible by technological progress. This method has been used recently (Koester and Herrero 1988) to determine upper

limits of typically 25 000 G for a number of brighter DA white dwarfs.

8.3. Theoretical modelling of magnetic atmospheres

The detection of circularly and linearly polarised optical radiation from white dwarfs confirms that they possess strong magnetic fields (Kemp *et al* 1970b). Qualitatively, the polarisation may be thought to arise as a result of circular dichroism or the existence of different opacities for the different modes of propagation of the observed radiation through the white dwarf's atmosphere (Angel *et al* 1981). For optically thin emission along the field at a frequency ω the fractional circular polarisation is given by

$$V/I = a(\omega_c/\omega) \tag{8.8}$$

where the constant $a = 2.0$ for the free–free opacity in a magnetic field (Kemp 1970, 1977) and bound–free transitions of hydrogen and helium in a magnetic field, with somewhat different values for H^- and He^- (Lamb and Sutherland 1974, Angel *et al* 1981). However, the observed circular polarisation does not increase linearly with wavelength as equation (8.8) predicts.

More extensive attempts have been made more recently to solve the complete transfer equations for the radiation from white dwarf atmospheres in the presence of a magnetic field by, for example, Martin and Wickramasinghe 1978, O'Donoghue 1980, Jordan 1989, and reviewed by Wickramasinghe (1987). In these calculations the effects of the Lorentz force on the atmospheric structure have been neglected, because the currents caused by the ohmic decay of the magnetic field (Landstreet 1986) are small (Jordan 1989) and hence the atmosphere is essentially force-free. The effects of the magnetic fields on the line and continuum opacities and on the equations of radiative transfer have been taken into account. In general the calculations have been performed for a plane parallel atmosphere, stratified in the z direction, which has a uniform magnetic field. The basic equations for radiative transfer are then given by:

$$\begin{aligned}
\mu\frac{dI}{dz} &= -\kappa_I(I-\mathcal{B}) - \kappa_Q Q - \kappa_V V \\
\mu\frac{dQ}{dz} &= -\kappa_Q(I-\mathcal{B}) - \kappa_I Q + r_R U \\
\mu\frac{dU}{dz} &= -r_R Q - \kappa_I U + r_W V \\
\mu\frac{dV}{dz} &= -\kappa_V(I-\mathcal{B}) - r_W U - r_I V.
\end{aligned} \tag{8.9}$$

Here, $\mathcal{B}$ is the Planck function for black body radiation, μ the cosine of the angle between the outward normal and the direction of propagation of the radiation and r_R and r_W the Faraday mixing coefficients (Pacholczyk 1976). These equations are essentially those due to Unno (1956) but include terms which allow for Faraday effects (Hardorp *et al* 1976, Wickramasinghe and Ferrario 1988). The absorption coefficients for the various Stokes parameters are given as follows in terms of κ_L and κ_R, which correspond to the absorption coefficients for left and right circularly polarised radiation travelling parallel to the magnetic field, with κ_P the absorption coefficient for linearly

polarised radiation travelling perpendicular to the field with the electric vector parallel to the magnetic field:

$$\kappa_I = \tfrac{1}{2}\kappa_P \sin^2\xi + \tfrac{1}{4}(\kappa_L + \kappa_R)(1 + \cos^2\xi)$$
$$\kappa_Q = \tfrac{1}{2}\kappa_P - \tfrac{1}{4}(\kappa_L + \kappa_R)\sin^2\xi$$
$$\kappa_V = \tfrac{1}{2}(\kappa_R - \kappa_L)\cos\xi. \tag{8.10}$$

Here ξ is the angle between the magnetic field and the direction of propagation of the radiation. By a suitable choice of the coordinate system κ_U is set equal to zero. The radiative transfer equations may be solved using various iterative techniques for an atmosphere in local thermodynamic equilibrium.

The continuum opacities in the presence of a strong magnetic field have been calculated by Lamb and Sutherland (1974), who showed that the bound–free opacity of hydrogen in a magnetic field can be deduced from the zero-field case because of the rigidity of the wave functions. They showed that these opacities can be expressed as

$$\kappa_q(\omega) = \frac{\omega}{\omega - q\omega_L}\, g(\omega - q\omega_L) \tag{8.11}$$

where $\omega_L = \omega_c/2$ is the Larmor frequency, $q = 0, +1, -1$ which correspond to κ_P, κ_R, κ_L respectively, and $g(\omega)$ the zero-field opacity.

Calculations of the circular polarisation and intensity as a function of wavelength have been performed for GD90 by Wickramasinghe and Martin (1979), see also O'Donoghue (1980), for centred and off-centred dipole magnetic fields and by Martin and Wickramasinghe (1984) for a quadrupole magnetic field with a polar field of 12 MG. Reasonably good fits to the data , with some discrepancies, have been obtained for the off-centred dipole and the quadrupole.

Wickramasinghe and Martin (1979) obtained good fits to the spectrum of BPM25114, which varies with a 2.8 d period, assuming a centred dipole field with a polar value of 36 MG. This value has been recently confirmed by Jordan (1989), who obtained a better fit by using the new line opacities obtained by the Tübingen group.

The magnetic white dwarf Feige 7 has both hydrogen and helium lines in its spectrum, which together with its polarisation varies with a period of 2.2 hr (Liebert *et al* 1977). Attempts to fit the observations with a centred dipole failed to produce the observed shifts of up to 10 Å in the field-dependent components with phase (Martin and Wickramasinghe 1936). Furthermore the period of the variations of the calculated circular polarisation is half the observed period. Off-centred dipoles also fail to fit the data and Wickramasinghe (1987) suggests that the star may contain a magnetic spot in addition to the centred dipole as suggested for PG1031+234 (Schmidt *et al* 1986).

More recently Wickramasinghe and Ferrario (1988) (see figure 10) have used the calculations of the spectra of hydrogen in magnetic fields greater than 100 MG by the LSU and Tübingen groups to model the spectrum of Grw+70° 8247. They show that the wavelengths, shapes and strengths of the features at 4135, 4480 and 5885 Å are in good agreement with a model in which the white dwarf has a centred dipole with a polar field of 320 ± 20 MG and a viewing angle with the field of 0 to 30 degrees and an effective atmospheric temperature of 14 000 K. The agreement is less satisfactory at long wavelengths (6200–9000 Å) and in the UV (2000–3000 Å), which they suggest may be due to departures from the assumed dipolar magnetic field. Their

calculations confirm that the long unidentified Minkowski bands are due to hydrogen, the simplest and most abundant element in the universe, in a strong magnetic field of about 320 MG. Slightly better fits for Grw+70° 8247 have been obtained recently by Jordan (1989) using improved opacities.

The spectrum and polarisation of PG1031+234 have been analysed by Schmidt *et al* (1986) and Latter *et al* (1987) without solving the radiative transfer equations by assuming that the local field and geometry qualitatively determine them. They provide convincing evidence that the field strength in this white dwarf is of order 500 MG and that it may contain a magnetic spot with a field approaching 10^9 G. This white dwarf has the strongest magnetic field of any white dwarf known and its field strength is comparable to that in the millisecond pulsars, which have fields ($\sim 10^8$ G) substantially weaker than those found in typical pulsars ($\sim 10^{12}$ G, White and Stella 1988).

Fits to the flux of PG1015+014, which shows variable circular polarisation with a period of 99 min, have been obtained by Wickramasinghe and Cropper (1988) assuming a polar field of 120 MG. Their model shows that, as in the case of Feige 7, the magnetic dipole axis is perpendicular to the rotation axis. Wickramasinghe (1987) speculates that magnetic white dwarfs prefer to be either perpendicular rotators or aligned rotators as in the cases of Feige 7 and PG1015+014. Then systems such as Grw+70° 8247, which show no evidence for polarisation variations may be parallel rotators. This implies that these fields must show a high degree of symmetry, which is difficult to justify.

Despite the significant progress and apparent success in fitting the observed spectra of Grw+70° 8247 it should be emphasised that the continuum opacities due to Lamb and Sutherland (1974), which have been used, are certainly not valid at such high field strengths above about 100 MG. More accurate calculations for this high field regime are badly needed.

8.4. Origin of magnetic fields

Of all the isolated white dwarfs that have been surveyed only about 3–5% have observable magnetic fields (Angel *et al* 1981, Schmidt 1989). These have magnetic fields in the range of 1–500 MG (Schmidt 1989). Because it is not easy to detect magnetic fields weaker than about 1 MG and because complete surveys below this value have not been made, it is unclear, whether the fraction of white dwarfs with fields below 1 MG is the same as that above it.

The absence of detectable magnetic fields in the overwhelming majority of white dwarfs is puzzling in view of the arguments discussed at the beginning of this section, and the possibility that they are born with strong magnetic fields which subsequently decay has been explored. The time scale for the ohmic decay of the magnetic field of a conducting sphere of uniform electrical conductivity σ and radius R is given by $\tau \sim 4\sigma R^2/\pi c^2$, if the length scale of variation of the field is roughly R. By using this expression and a simple estimate for the electrical conductivity (Mestel 1965) found that $\tau \sim 10^{10}$ yr. The electrical conductivity, however, is both a function of the density and temperature in the star and hence varies both as a function of the radial distance r from the centre of the star and also increases with time as the star cools. Detailed numerical calculations were performed by Chanmugam and Gabriel (1972), who used the electrical conductivity due to Canuto and Solinger (1970). They found that, for a symmetric dipolar magnetic field, the longest living mode decays on a time scale $\tau_0 \sim 10^{10}$ yr with the higher modes decaying increasingly faster.

More elaborate calculations were performed by Fontaine *et al* (1973), who used the Hubbard and Lampe (1969) values for the conductivity and found that $\tau_0 \simeq 3 \times 10^9$ yr. More recently these calculations have been further extended by Wendell *et al* (1987) who used the expressions for the conductivity due to Yakovlev and Urpin (1980) in the interior of the star. They found that the decay time exceeds the stellar age throughout the cooling sequence for a 0.6 $M_\odot$ carbon white dwarf and the field decays by a factor of only about 2 in 10 billion yr. These results are closer to those of Chanmugam and Gabriel (1972), than those of Fontaine *et al* (1973), and imply there is no justification for assuming that the longest living modes of white dwarfs would have decayed away.

The magnetic fields of white dwarfs may (or may not) be related to those of pulsars. An interesting feature of the white dwarfs is that their surface magnetic fluxes ($\sim BR^2 \sim 10^{24}$–5×10^{26} G cm^2 for white dwarfs of radius 10^9 cm. By comparison the overwhelming majority of radio pulsars, which are believed to be rotating neutron stars with radii of $\sim 10^6$ cm, have magnetic fields $\sim 10^{11}$–10^{13} G and hence have surface magnetic fluxes $\sim 10^{23}$–10^{25} G cm^2, which is within an order of magnitude or so comparable to that of the magnetic white dwarfs. This has led to the suggestion that most pulsars and magnetic white dwarfs have a similar origin in the sense that they are descendants from red giant stars with similar magnetic fields produced during an earlier evolutionary phase. Magnetic flux is assumed to be conserved during the subsequent evolution, producing either a neutron star or a white dwarf (Ruderman and Sutherland 1973, Levy and Rose 1974). Note, however, that alternative origins for the magnetic fields of neutron stars have been proposed, where the fields are produced after the neutron star is formed by thermoelectric effects (Urpin and Yakovlev 1980, Blandford *et al* 1983). If such a model is correct then a separate origin for the white dwarf magnetic fields must be found since white dwarfs, unlike neutron stars, do not have hot crusts for a similar mechanism to work.

The rotation periods of seven isolated magnetic white dwarfs have been determined from the variations of their optical polarisation and range from 1.65 hr, for PG1015+015, to 2.8 days for BPM25114 (see table 4, and Schmidt 1989). In three cases (G240-72, GD229 and Grw+70° 8247) there is no evidence of variations in the position angle of the linear polarisation implying that either their rotation periods are greater than 100 yr or that the magnetic field is symmetric about the rotation axis. The magnetic white dwarfs appear to be slow rotators (cf Blackett 1947) in the sense that their rotational energy is much smaller than their gravitational energy and hence does not influence their structure significantly. On the other hand, since the moment of inertia $I \propto R^2$, their values are roughly 10^6 times that of neutron stars and hence five of the magnetic white dwarfs with known rotation periods have angular momenta, which are comparable to pulsars with rotation periods of 7 ms to 0.3 s (Angel 1978, Brecher and Chanmugam 1978), suggesting that at least some magnetised white dwarfs and some pulsars may have had progenitors with similar angular momenta. There is no correlation between the rotation period and the surface temperature of the star (table 4) suggesting that they do not spin down with age (Schmidt 1987).

The rotation periods for five magnetic white dwarfs are a few hours, which corresponds to the orbital periods of cataclysmic binaries, which contain accreting white dwarfs. A subclass of the latter are known as AM Her binaries, which contain white dwarfs with magnetic fields of 20–50 MG rotating synchronously (Liebert and Stockman 1985). Binaries with fields larger than 50 MG are absent and Schmidt *et al* (1986) speculate that any such system would evolve relatively quickly so that the

secondary is whittled down because of mass transfer to the white dwarf and mass ejection from the system so that it either does not exist anymore or is too faint to be seen. They suggest that the isolated magnetic white dwarfs may have unseen small companions. Hameury *et al* (1989) point out that for field strengths $\geq$ 40 MG such systems end up as detached binaries with low mass degenerate companions and orbital periods $\leq$ 7 hr. Thus such systems could provide an explanation for the short-period, apparently isolated, white dwarfs.

Greenstein and Oke (1982), from an accurate trigonometric parallax of Grw+70° 8247, have found its mass to be greater than 1 $M_{\odot}$. This is consistent with the evidence presented by Liebert (1988) that magnetic white dwarfs have masses which are on average slightly larger than non-magnetic white dwarfs, implying more massive and younger progenitors. This conclusion is supported by the space motions of the magnetic stars (Sion *et al* 1988b). Since pulsars have massive progenitors and similar surface magnetic fluxes (and in some cases angular momenta) as the magnetic white dwarfs it may well be that the fields of these degenerate stars are related by flux conservation to the fields of their progenitors. Thus, in the absence of a satisfactory theory for the origin of the magnetic fields of degenerate stars, flux conservation remains, because of its simplicity, an attractive hypothesis.

9. Summary of present knowledge and unsolved problems

Enormous progress has been made in the past two decades in our understanding of the structure of white dwarfs and their relationship to the evolution of stars in general. Thus, it had been a puzzle for a long time to understand, how stars with masses much larger than a typical white dwarf could evolve into one. We now realise that mass loss is extremely important and that stars with masses up to 8 $M_{\odot}$ can become white dwarfs. The evolution of white dwarfs is understood in principle, and it is plausible that in the near future calculated ages of the oldest visible white dwarfs will lead to consistent results, thus opening up the possibility to infer the age of the galactic disk with more certainty than is currently possible. Important questions regarding the masses of the hydrogen and helium layers in white dwarfs, the behaviour of a carbon/oxygen mixture in the crystalline phase, as well the precise abundance ratio of these elements, remain to be solved.

The relationship between the different spectral types, though studied very actively today, remains somewhat speculative. This is especially true for the basic dichotomy between hydrogen-rich and helium-rich spectral types. It is believed that the important processes, diffusion, convection, accretion and mass loss, are identified. How important mass loss really is, or what happens during the accretion of interstellar matter of solar composition, remains uncertain.

The variable white dwarfs are believed to be undergoing non-radial oscillations. The mechanisms exciting such oscillations in the DAVs and DBVs have been found, although it is controversial whether they require, in the case of the DAVs, an extremely thin hydrogen layer. The empirical location of the instability strip of the DBVS is uncertain by a few 1000 K, which is unfortunate because better knowledge could offer a means to calibrate the mixing-length approximation for convection. The red edge of the instability strip of the DAVs is probably caused by the interaction of pulsation with convection. The lack of a time-dependent theory of convection currently prevents a complete understanding.

The magnetic white dwarfs, with their extremely high fields, provide a test for the behaviour of hydrogen atoms in such fields. A severe problem in the theoretical modelling of spectra is the lack of accurate calculations of the bound–free opacity in strong fields. On the observational side, further efforts to detect field strengths below 1 MG and to search for a possible relationship between rotation and magnetic fields, are necessary.

Although white dwarfs are not very exotic like neutron stars and black holes, they nevertheless offer unique opportunities for studies with close connections to many branches of physics and astronomy.

Acknowledgments

We have greatly benefited from being able to see parts of a preliminary version of the monograph currently being prepared by Van Horn and Liebert and want to thank Hugh Van Horn for this opportunity. We also gratefully acknowlege financial support through grants AST8814711 (DK) and AST8822954 (GC) from the National Science Foundation.

References

Abell G O, Morrison D, and Wolff S C 1987 *Exploration of the Universe* (Philadelphia: CBS College Publishing) p 559
Abrikosov A A 1961 *Sov. Phys.-JETP* **12** 1254
—— 1962 *Sov. Phys.-JETP* **14** 408
Adams W S 1915 *Publ. Astron. Soc. Pacific* **27** 236
—— 1925 *Proc. Nat. Acad. Sci.* **11** 382
Alcock C and Illarionov A 1980a *Astrophys. J.* **235** 534
—— 1980b *Astrophys. J.* **235** 541
Anderson W 1929 *Z. Phys.* **54** 433
Angel J R P 1972 *Astrophys. J.* **171** L17
—— 1978 *Ann. Rev. Astron. Astrophys.* **16** 487
—— 1979 *White Dwarfs and Variable Degenerate Stars* IAU Coll. No. **53** ed H M Van Horn and V Weidemann (Rochester: University of Rochester Press) 313
Angel J R P, Borra E F and Landstreet J D 1981 *Astrophys. J. Suppl.* **45** 457
Angel J R P, Carswell R F, Strittmatter P A, Beaver P A and Harms R 1974a *Astrophys. J.* **194** L47
Angel J R P, Hintzen P and Landstreet J D 1975 *Astrophys. J.* **196** L27
Angel J R P, Hintzen P, Strittmatter P A and Martin P G 1974b *Astrophys. J.* **190** L71
Angel J R P, Illing R M E and Landstreet J D 1972 *Astrophys. J.* **175** L85
Angel J R P and Landstreet J D 1970 *Astrophys. J.* **160** L147
—— 1974 *Astrophys. J.* **191** 457
Angel J R P, Liebert J and Stockman H S 1985 *Astrophys. J.* **292** 260
Angel J R P, McGraw J T and Stockman H S 1973 *Astrophys. J.* **184** L79
Auluck F C and Mathur V S 1959 *Z. Astrophys.* **48** 28
Babcock H W 1958 *Astrophys. J.* **128** 228
Baglin A 1968 *Astrophys. Lett.* **1** 143
Baglin A and Heyvaerts J 1969 *Nature* **222** 1258
Baglin A and Schatzman E 1969 *Low Luminosity Stars* ed S S Kumar (New York: Gordon and Breach)
Baglin A and Vauclair G 1973 *Astron. Astrophys.* **27** 307
Bahcall J N 1984a *Astrophys. J.* **276** 156
—— 1984b *Astrophys. J.* **276** 169

Barrat J L, Hansen J P and Mochkovitch R 1988 *Astron. Astrophys.* **199** L15
Bath G T 1985 *Rep. Progr. Phys.* **48** 483
Blackett P M S 1947 *Nature* **159** 658
Blandford R, Applegate J and Hernquist L 1983 *Mon. Not. R. Astron. Soc.* **204** 1025
Böhm K H 1968 *Astrophys. Space Sci.* **2** 375
Böhm-Vitense E Z 1958 *Astrophysics* **46** 108
Bond H E, and Ciardullo R 1989 *White Dwarfs* IAU Coll. No. **114** ed G Wegner (Berlin: Springer) 473
Bond H E and Grauer A D 1987 *Astrophys. J.* **321** L123
Bond H E, Grauer A D, Green R F and Liebert J 1984 *Astrophys. J.* **279** 751
Boss L 1910 *Preliminary General Catalogue* (Washington: Carnegie Institution)
Bradley P A, Winget D E and Wood M A 1989 *White Dwarfs* IAU Coll. No. **114** ed G Wegner (Berlin: Springer) 286
Brecher K and Chanmugam G 1978 *Astrophys. J.* **221** 969
Brickhill A J 1975 *Mon. Not. R. Astron. Soc.* **170** 405
Bruhweiler F and Kondo Y 1983 *Astrophys. J.* **269** 657
Brush S G, Sahlin H L and Teller E J 1966 *Chem. Phys.* **45** 2102
Burgers J M 1969 *Flow Equations for Composite Gases* (New York: Academic)
Canuto V 1970 *Astrophys. J.* **159** 641
Canuto V and Solinger A B 1970 *Astrophys. Lett.* **6** 141
Carr W J Jr 1961 *Phys. Rev.* **122** 1437
Cesare L de, Forlani A and Platania G 1973 *Astrophys. Space Sci.* **21** 461
Chandrasekhar S 1931 *Astrophys. J.* **74** 81
—— 1935 *Mon. Not. R. Astron. Soc.* **95** 207
—— 1939 *An Introduction to the Study of Stellar Structure* (Cambridge: University of Cambridge Press)
—— 1964 *Astrophys. J.* **146** 417
Chandrasekhar S and Tooper R F 1964 *Astrophys. J.* **139** 1396
Chanmugam G 1972 *Nature* **236** 83
—— 1977 *Astrophys. J.* **217** 799
Chanmugam G and Gabriel M 1972 *Astron. Astrophys.* **16** 149
Chanmugam G, O'Connell R F and Rajagopal A K 1972 *Astrophys. J.* **175** 157
Chapman S and Cowling T 1970 *The Mathematical Theory of Non-Uniform Gases* (Cambridge: Cambridge University Press)
Chayer P, Fontaine G and Wesemael F 1989 *White Dwarfs* IAU Coll. No. **114** ed G Wegner (Berlin: Springer) 253
Clayton D D 1968 *Principles of Stellar Evolution and Nucleosynthesis* (Chicago: University of Chicago Press)
Cottrell P L and Greenstein J L 1980 *Astrophys. J.* **283** 941
Cowling T G 1941 *Mon. Not. R. Astron. Soc.* **101** 367
Cox A N 1986 *Highlights of Astronomy* **7** 229
Cox A N, Hodson S W and Starrfield S G 1980 *Non-radial and Non-linear Stellar Pulsations* ed H A Hill and W Dziembowski (Berlin: Springer) 453
Cox A N, Starrfield S G, Kidman R B and Pesnell W D 1987 *Astrophys. J.* **317** 303
Cox A N and Stewart J N 1970 *Astrophys. J. Suppl.* **19** 261
Cox J P 1980 *Theory of Stellar Pulsations* (Princeton: Princeton University Press)
Cox J P and Giuli R T 1968 *Principles of Stellar Structure* (New York: Gordon and Breach)
D'Antona F and Mazzitelli I 1979 *Astron. Astrophys.* **74** 161
—— 1990 *Ann. Rev. Astron. Astrophys.* in press
DeWitt H E 1969 *Low Luminosity Stars* ed S S Kumar (New York: Gordon and Breach)
Dirac P A M 1926 *Proc. R. Soc.* A **112** 660
Dolez N, Vauclair G and Chevreton M 1983 *Astron. Astrophys.* **121** L23
Dolez N and Vauclair G 1981 *Astron. Astrophys.* **102** 375
Downes R A and Margon B 1983 *Publ. Astron. Soc. Pacific* **95** 358
Dupuis J, Pelletier C, Fontaine G and Wesemael F 1989 *White Dwarfs* IAU Coll. No. **114** ed G Wegner (Berlin: Springer) 359
Dziembowski W and Koester D 1981 *Astron. Astrophys.* **97** 16
Eddington A S 1925 *Observatory* **48** 73

—— 1926 *Internal Constitution of the Stars* (Cambridge: Cambridge University Press)
Eggen O 1985 *Publ. Astron. Soc. Pacific* **97** 1029
Einstein A 1907 *Jahrbuch Radioakt.* **4** 411
Faulkner J and Gribbin J R 1968 *Nature* **218** 734
Fermi E 1926 *Z. Phys.* **36** 902
Finley D S, Basri G and Bowyer S 1989 *White Dwarfs* IAU Coll. No. **114** ed G Wegner (Berlin: Springer) 139
Finzi A and Wolf R A 1967 *Astrophys. J.* **150** 115
Foltz C B and Latter W B 1988 preprint referenced in Schmidt (1989)
Fontaine G, Bergeron P, Lacombe P, Lamontagne R and Talon A 1985 *Astron. J.* **90** 1094
Fontaine G, McGraw J T, Coleman L, Lacombe P, Patterson J and Vauclair G 1980 *Astrophys. J.* **239** 898
Fontaine G, McGraw J T, Dearborn D S P, Gustafson J and Lacombe P 1982 *Astrophys. J.* **258** 651
Fontaine G and Michaud G 1979 *Astrophys. J.* **231** 826
Fontaine G, Thomas J H and Van Horn H M 1973 *Astrophys. J.* **184** 911
Fontaine G, Villeneuve B, Wesemael F and Wegner G 1984 *Astrophys. J.* **277** L61
Fontaine G and Wesemael F 1984 *Astron. J.* **89** 1728
—— 1987 *The Second Conference on Faint Blue Stars* IAU Coll. No. **95** ed A G D Philip, D S Hayes and J Liebert (Schenectady: L Davis Press) 319
Forster H, Strupat W, Rösner W, Wunner G, Ruder H and Herold H 1984 *J. Phys.* B **17** 1301
Fowler R H 1926 *Mon. Not. R. Astron. Soc.* **87** 114
Fusi-Pecci F and Renzini A 1976 *Astron. Astrophys.* **46** 447
Garcia-Berro E, Hernanz M, Isern J and Mochkovitch R 1988a *Astron. Astrophys.* **193** 141
—— 1988b *Nature* **333** 644
Gatewood G D and Gatewood C V 1978 *Astrophys. J.* **225** 191
Garstang R H 1977 *Rep. Progr. Phys.* **40** 105
Garstang R H and Kemic S B 1974 *Astrophys. Space Sci.* **31** 103
Gell-Mann M and Brückner K A 1957 *Phys. Rev.* **106** 364
Giclas H L, Burnham R Jr and Thomas N G 1980 *Lowell Obs. Bull. No.* **166**
Ginzburg V L 1964 *Sov. Phys. Dokl.* **9** 329
Goupil M J, Auvergne M and Baglin A 1988 *Astron. Astrophys.* **196** L13
Grauer A D and Bond H E 1984 *Astrophys. J.* **277** 211
Grauer A D, Bond H E, Green R F and Liebert J 1988 *Astron. J.* **95** 879
Grauer A D, Wegner G, Green R F and Liebert J 1989 *preprint*
Green R F, Schmidt M and Liebert J 1986 *Astrophys. J. Suppl.* **61** 305
Greenstein J L 1956 *Proc. 3rd Berkeley Symp.* ed J Neyman (Berkeley: University of California Press)
—— 1970 *Astrophys. J.* **162** L55
—— 1982 *Astrophys. J.* **258** 661
—— 1984a *Astrophys. J.* **276** 602
—— 1984b *Astrophys. J.* **281** L47
—— 1986 *Astrophys. J.* **304** 334
Greenstein J L, Henry R W and O'Connell R F 1985 *Astrophys. J.* **289** L25
Greenstein J L and McCarthy J K 1985 *Astrophys. J.* **289** 732
Greenstein J L and Oke J B 1982 *Astrophys. J.* **252** 285
Greenstein J L, Oke J B and Shipman H L 1971 *Astrophys. J.* **169** 563
—— 1985 *Quart. J. R. Astron. Soc.* **26** 279
Greenstein J L and Peterson D M 1973 *Astron. Astrophys.* **25** 29
Greenstein J L and Trimble V 1967 *Astrophys. J.* **149** 283
Gustafson R G and McGraw J T 1980 *Bull. Am. Astron. Soc.* **12** 863
Hagen H J, Groote D, Engels D, Haug U, Toussaint F and Reimers D 1987 *Astron. Astrophys.* **183** L7
Hamada T and Nakamura Y 1973 *Publ. Astron. Soc. Japan* **25** 527
Hamada T and Salpeter E E 1961 *Astrophys. J.* **134** 683
Hamann W R, Kudritzki R-P, Mendez R H and Pottasch S R 1984 *Astron. Astrophys.* **139** 459
Hameury J M, King A R and Lasota J P 1989 *Mon. Not. R. Astron. Soc.* **237** 845
Hansen C J, Cox J P and Van Horn H M 1977 *Astrophys. J.* **217** 151
Hansen J P 1973 *Phys. Rev.* A **8** 3096
Hardorp J, Shore S N and Wittmann A 1976 *Physics of Ap Stars* IAU Coll. No. **32** ed W W Weiss,

H Jenker and H J Wood p 419
Harper R van and Rose W K 1970 *Astrophys.J* **162** 963
Henry R J W and O'Connell R F 1984 *Astrophys. J.* **282** L97
—— 1985 *Publ. Astron. Soc. Pacific* **97** 333
Hesser J E, Lasker B M and Neupert H E 1976 *Astrophys. J.* **209** 853
Hill J A 1987 *The Second Conference on Faint Blue Stars* IAU Coll. No. **95** ed A G D Philip, D S Hayes and J Liebert (Schenectady: L Davis Press) p 681
Hintzen P and Strittmatter P A 1974 *Astrophys. J.* **193** L111
Holberg J B, Wesemael F and Basile J 1986 *Astrophys. J.* **306** 629
Hubbard W B and Lampe M 1969 *Astrophys. J. Suppl.* **18** 297
Huebner W F, Merts A L, Magee N H Jr and Argo M F 1977 *Astrophysical Opacity Library, UC-34b*
Humason M L and Zwicky F 1947 *Astrophys. J.* **105** 85
Hutsemékers D and Surdej J 1989 *Astron. Astrophys.* **219** 237
Iben I Jr 1967 *Ann. Rev. Astron. Astrophys.* **5** 571
—— 1974 *Ann. Rev. Astron. Astrophys.* **12** 215
—— 1984 *Astrophys. J.* **277** 333
Iben I Jr and Laughlin G 1989 *Astrophys. J.* **341** 312
Iben I Jr and MacDonald J 1985 *Astrophys. J.* **295** 540
—— 1986 *Astrophys. J.* **301** 164
Iben I Jr and Renzini A 1983 *Ann. Rev. Astron. Astrophys.* **21** 271
—— 1984 *Phys. Rep.* **105** 330
Iben I Jr and Tutukov A V 1984 *Astrophys. J.* **282** 615
Illarionov A and Sunyaev R 1975 *Astron. Astrophys.* **39** 185
Isern J, Garcia-Berro E, Hernanz M and Mochkovitch R 1989 *White Dwarfs* IAU Coll. No. **114** ed G Wegner (Berlin: Springer) p 278
Itoh N 1989 *White Dwarfs* IAU Coll. No. **114** ed G Wegner (Berlin: Springer) p 66
Itoh N, Mitake S, Iyetomi H and Ichimaru S 1983 *Astrophys. J.* **273** 774
Itoh N, Kohyama Y, Matsumoto J and Seki M 1984 *Astrophys. J.* **285** 758
Jordan S 1989 *White Dwarfs* IAU Coll. No. **114** ed G Wegner (Berlin : Springer) p 333
Jordan S and Koester D 1986 *Astron. Astrophys. Suppl.* **65** 367
Jordan S, Koester D, Wulf-Mathis C and Brunner H 1987 *Astron. Astrophys.* **185** 253
Kahn S, Wesemael F, Liebert J, Raymond J, Steiner J and Shipman H L 1984 *Astrophys. J.* **278** 255
Kaplan S A 1949 *Naukovy Zapiski (Sci. Notes Univ. Lwow)* **15** 109
Kawaler S D 1987 *The Second Conference on Faint Blue Stars* IAU Coll.No. **95** ed A G D Philip, D S Hayes and J Liebert (Schenectady: L Davis Press) p 297
Kawaler S D and Hansen C J 1989 *White Dwarfs* IAU Coll. No. **114** ed G Wegner (Berlin: Springer) p 97
Kawaler S D, Winget D E and Hansen C J 1985 *Astrophys. J.* **298** 752
Kawaler S D, Winget D E, Hansen C J and Iben I Jr 1986 *Astrophys. J.* **306** L41
Kemic S B 1974 *Astrophys. J.* **193** 213
Kemp J C 1970 *Astrophys. J.* **162** 169
—— 1977 *Astrophys. J.* **213** 794
Kemp J C, Swedlund J B and Evans B D 1970a *Phys. Rev. Lett.* **24** 1211
Kemp J C, Swedlund J B, Landstreet J D and Angel J R P 1970b *Astrophys. J.* **161** L77
Kennicutt R C 1984 *Astrophys. J.* **277** 361
Kenyon S J, Shipman H L, Sion E M and Aannestad P A 1988 *Astrophys. J.* **328** L65
Kepler S O, Vauclair G, Nather R E, Winget D E and Robinson E L 1989 *White Dwarfs* IAU Coll. No. **114** ed G Wegner (Berlin: Springer) p 341
Kirzhnits D A 1960 *Sov. Phys.-JETP* **11** 365
Koester D 1972 *Astron. Astrophys.* **16** 459
—— 1976 *Astron. Astrophys.* **52** 415
—— 1978 *Astron. Astrophys.* **64** 289
—— 1982 *The Messenger* **28** 25
—— 1987a *The Second Conference on Faint Blue Stars* IAU Coll. No. **95** ed A G D Philip, D S Hayes and J Liebert (Schenectady: L Davis Press) p 329
—— 1987b *Astrophys. J.* **322** 852
—— 1989a *White Dwarfs* IAU Coll. No. **114** ed G Wegner (Berlin: Springer) p 206
—— 1989b *Astrophys. J.* **342** 999

Koester D and Herrero A 1988 *Astrophys. J.* **332** 910
Koester D and Reimers D 1981 *Astron. Astrophys.* **99** L8
—— 1985 *Astron. Astrophys.* **153** 260
Koester D and Schönberner D 1986 *Astron. Astrophys.* **154** 125
Koester D, Schulz H and Weidemann V 1979 *Astron. Astrophys.* **76** 262
Koester D, Vauclair G, Dolez N, Oke J B, Greenstein J L and Weidemann V 1985 *Astron. Astrophys.* **149** 423
Koester D, Wegner G and Kilkenny D 1989 *Astrophys. J.* in press
Koester D and Weidemann V 1980 *Astron. Astrophys.* **81** 145
—— 1989 *Astron. Astrophys.* **219** 276
Koester D, Weidemann V and Zeidler-K T E M 1982 *Astron. Astrophys.* **116** 147
Kothari D S 1931 *Phil. Mag.* **12** 665
—— 1936 *Mon. Not. R. Astron. Soc.* **96** 833
—— 1938 *Proc. R. Soc. London* A **165** 486
Kovetz A and Shaviv G 1970 *Astron. Astrophys.* **8** 398
Kugler A A 1969 *Ann. Phys., NY* **53** 133
Lamb D Q 1974 *Thesis* University of Rochester, Rochester
Lamb D Q and Van Horn H M 1975 *Astrophys. J.* **200** 306
Lamb F K and Sutherland P G 1974 *Physics of Dense Matter* ed C J Hansen (Dordrecht: Reidel) p 265
Lamontagne R, Wesemael F and Fontaine G 1987 *The Second Conference on Faint Blue Stars* IAU Coll. No. **95** ed A G D Philip, D S Hayes and J Liebert (Schenectady: L Davis Press) p 677
Lamontagne R, Wesemael F, Fontaine G, Wegner G and Nelan E P 1989 *White Dwarfs* IAU Coll. No. **114** ed G Wegner (Berlin: Springer) p 240
Landau L D 1932 *Phys. Z. Sowjet.* **1** 285
Landau L D and Lifshitz E M 1969 *Statistical Physics* (London: Addison-Wesley)
Landolt A U 1968 *Astrophys. J.* **153** 151
Landstreet J D 1986 *Mon. Not. R. Astron. Soc.* **225** 437
Landstreet J D and Angel J R P 1974 *Astrophys. J.* **190** L25
—— 1975 *Astrophys. J.* **196** 819
Lang K R and Gingerich O (eds) 1979 *A Source Book in Astronomy and Astrophysics, 1900–1975* (Cambridge: Harvard University Press) p 215
Lasker B M and Hesser J E 1969 *Astrophys. J.* **158** L171
—— 1971 *Astrophys. J.* **163** L89
Latter W B, Schmidt G D and Green R F 1987 *Astrophys. J.* **320** 308
Lawrence G M, Ostriker J P and Hesser J E 1967 *Astrophys. J.* **148** L161
Ledoux P 1958 *Handbuch der Physik* ed S Flügge (Berlin: Springer) **51** 605
Ledoux P and Sauvenier-Goffin E 1950 *Astrophys. J.* **111** 611
Ledoux P and Walraven T 1958 *Handb. der Physik* ed S.Flügge (Berlin: Springer) **51** 353
Lee T D 1950 *Astrophys. J.* **111** 625
Levy E M and Rose W K 1974 *Nature* **250** 40
Liebert J 1980 *Ann. Rev. Astron. Astrophys.* **18** 363
—— 1987 private communication
—— 1988 *Publ. Astron. Soc. Pacific* **100** 1302
Liebert J, Angel J R P and Landstreet J D 1975 *Astrophys. J.* **202** L139
Liebert J, Angel J R P, Stockman H S, Spinrad H and Beaver P A 1977 *Astrophys. J.* **214** 457
Liebert J, Dahn C C and Monet D G 1988 *Astrophys. J.* **332** 891
—— 1989 *White Dwarfs* IAU Coll. No. **114** ed G Wegner (Berlin: Springer) p 15
Liebert J, Fontaine G and Wesemael F 1987b *Mem. Soc. Astron. Italiana* **58** 17
Liebert J, Schmidt G D, Green R F, Stockman H S and McGraw J T 1983 *Astrophys. J.* **264** 262
Liebert J, Schmidt G D, Sion E M, Starrfield S G, Green R F and Boroson T A 1985 *Publ. Astron. Soc. Pacific* **97** 158
Liebert J and Stockman H S 1985 *Cataclysmic Variables and Low Mass X-ray Binaries* ed D Q Lamb and J Patterson (Dordrecht: Reidel) p 151
Liebert J and Strittmatter P A 1977 *Astrophys. J.* **217** L59
Liebert J, Wehrse R and Green R F 1987a *Astron. Astrophys.* **175** 173
Liebert J, Wesemael F, Hansen C J, Fontaine F, Shipman H L, Sion E M, Winget D E and Green R F 1986 *Astrophys. J.* **309** 241

Luyten W J 1970 *White Dwarfs* (Minneapolis: University of Minnesota Press)
—— 1977 *White Dwarfs - II* (Minneapolis: University of Minnesota Press)
MacDonald J 1989 *White Dwarfs* IAU Coll. No. **114** ed G Wegner (Berlin: Springer) p 172
Maeder A and Mermilliod J C 1981 *Astron. Astrophys.* **93** 136
Marshak R E 1940 *Astrophys. J.* **92** 321
Martin B and Wickramasinghe D T 1978 *Mon. Not. R. Atron. Soc.* **183** 533
—— 1984 *Mon. Not. R. Astron. Soc.* **206** 407
—— 1986 *Astrophys. J.* **301** 177
Mauche C W 1990 (ed) *Proc. 11th North American Workshop on CVs and LMXRBS* (Cambridge: Cambridge University Press) in press
Mazzitelli I and D'Antona F 1986 *Astrophys. J.* **308** 706
McCook G P and Sion E M 1987 *Astrophys. J. Suppl.* **65** 603
McGraw J T 1976 *Astrophys. J.* **210** L35
—— 1977 *Astrophys. J.* **214** L123
—— 1979 *Astrophys. J.* **229** 203
McGraw J T, Fontaine G, Dearborn D S P, Gustafson J, Lacombe P and Starrfield S G 1981 *Astrophys. J.* **250** 349
McGraw J T and Robinson E L 1975 *Astrophys. J.* **200** L89
—— 1976 *Astrophys. J.* **205** L155
McGraw J T, Starrfield S G, Liebert J and Green R F 1979 *White Dwarfs and Variable Degenerate Stars* IAU Coll. No. **53** ed H M Van Horn and V Weidemann (Rochester: University of Rochester Press) p 377
McMahan R K 1989 *Astrophys. J.* **336** 409
Meltzer D W and Thorne K S 1966 *Astrophys. J.* **218** 514
Mendez R H, Miguel C H, Heber U and Kudritzki R P 1986 *Hydrogen Deficient Stars and Related Objects* IAU Coll. No. **87** ed K Hunger, D Schönberner and N K Rao (Dordrecht: Reidel) p 323
Mendez R H, Kudritzki R P, Herrero A, Husfeld D and Groth H G 1988 *Astron. Astrophys.* **190** 113
Mengel J G 1976 *Astron. Astrophys.* **48** 83
Mengel J G, Sweigart A V, Demarque P and Gross P G 1979 *Astrophys. J. Suppl.* **40** 733
Mestel L 1950 *Proc. Cambridge Phil. Soc.* **46** 331
—— 1952 *Mon. Not. R. Astron. Soc.* **112** 583
—— 1965 *Stellar Structure* ed L H Aller and D B McLaughlin (Chicago: University of Chicago Press) p 297
Mestel L and Ruderman M A 1967 *Mon. Not. R. Astron. Soc.* **136** 27
Michaud G 1987 *The Second Conference on Faint Blue Stars* IAU Coll. No. **95** ed A G D Philip, D S Hayes and J Liebert (Schenectady: L Davis Press) p 249
Michaud G, Fontaine G and Charland Y 1984 *Astrophys. J.* **280** 247
Mihalas D 1978 *Stellar Atmospheres* (San Francisco: Freeman)
Minkowski R 1938 *Ann. Rep. Mt. Wilson Obs.* **55** 44
Mochkovitch R 1983 *Astron. Astrophys.* **122** 212
Morvan E, Vauclair G and Vauclair S 1986 *Astron. Astrophys.* **163** 145
Muchmore D 1984 *Astrophys. J.* **278** 769
Mullan D J 1971 *Ir. Astron. J.* **10** 25
Nather R E 1973 *Vistas in Astronomy* **15** 91
O'Donoghue D E 1980 *Astrophys. Space Sci.* **68** 273
Oke J B, Weidemann V and Koester D 1984 *Astrophys. J.* **281** 276
Osaki Y and Hansen C J 1973 *Astrophys. J.* **185** 277
Östreicher R, Seifert W, Ruder H and Wunner G 1987 *Astron. Astrophys.* **173** L15
Ostriker J P and Axel L 1969 *Low Luminosity Stars* ed S Kumar (New York: Gordon and Breach) p 357
Pacholczyk A G 1976 *Radio Galaxies* (Oxford: Pergamon) ch 3
Paerels F B S and Heise J 1989 *Astrophys. J.* **339** 1000
Paquette C, Pelletier C, Fontaine G and Michaud G 1986a *Astrophys. J. Suppl.* **61** 197
—— 1986b *Astrophys. J. Suppl.* **61** 177
Patterson J 1984 *Astrophys. J. Suppl.* **54** 443
Pelletier C, Fontaine G and Wesemael F 1989 *White Dwarfs* IAU Coll. No. **114** ed G Wegner (Berlin: Springer-Verlag) p 249
Pelletier C, Fontaine G, Wesemael F, Michaud G and Wegner G 1986 *Astrophys. J.* **307** 242

Perinotto M 1987 *Planetary and Proto-Planetary Nebulae: From IRAS to ISO* ed A Preite Martinez (Dordrecht: Reidel) p 13
Pesnell W D 1987 *Astrophys. J.* **314** 598
Petre R, Shipman H L and Canizares C R 1986 *Astrophys. J.* **304** 356
Pilachowski C A and Milkey R W 1984 *Publ. Astron. Soc. Pacific* **96** 821
—— 1987 *Publ. Astron. Soc. Pacific* **99** 836
Pollock E L and Hansen J P 1973 *Phys. Rev.* A **8** 3110
Praddaude H C 1972 *Phys. Rev.* A **6** 1321
Pravdo S H, Marshall F E, White N E and Giommi P 1986 *Astrophys. J.* **300** 819
Preston G W 1970 *Astrophys. J.* **160** L143
Reimers D 1975 *Mem. Soc. R. Sci. Liège* **8** 369
—— 1987 *Circumstellar Matter* IAU Symp. **122** ed I Appenzeller and C Jordan (Dordrecht: Reidel) p 307
Reimers D and Koester D 1982 *Astron. Astrophys.* **116** 341
—— 1988a *Astron. Astrophys.* **202** 77
—— 1988b *The Messenger* **54** 47
—— 1989 *Astron. Astrophys.* **218** 118
Richer H B and Ulrych T J 1974 *Astrophys. J.* **192** 719
Robinson E L 1984 *Astron. J.* **89** 1732
Robinson R L and McGraw J T 1976 *Astrophys. J.* **207** L37
Robinson E L, Stover R J, Nather R E and McGraw J T 1978 *Astrophys. J.* **220** 614
Rösner W, Wunner G, Herold H and Ruder H 1984 *J. Phys. B: At. Mol. Phys.* **17** 29
Romanishin W and Angel J R P 1980 *Astrophys. J.* **235** 992
Rosseland S 1949 *The Pulsation Theory of Variable Stars* (Oxford: Clarendon)
Ruderman M A and Sutherland R G 1973 *Nature Phys. Sci.* **246** 93
Rudkjøbing M 1952 *Publ. Köbenhavns Obs. No.* **160**
Ruiz M T and Maza J 1989 *White Dwarfs* IAU Coll. No. **114** ed G Wegner (Berlin: Springer-Verlag) p 126
Ruiz M T, Maza J, Wischnjewski M and Gonzáles L E 1986 *Astrophys. J.* **304** L25
Russell H N 1914 *Popular Astronomy* **22** 275
Saffer R A, Liebert J, Wagner R M, Sion E M and Starrfield S G 1989 preprint
Saio H, Winget D E and Robinson E L 1983 *Astrophys. J.* **265** 982
Salpeter E E 1961 *Astrophys. J.* **134** 669
Salpeter E E and Van Horn H M 1969 *Astrophys. J.* **155** 183
Sauvenier-Goffin E 1949 *Ann. Astrophys.* **12** 39
Schatzman E 1949 *Publ. Köbenhavns Obs.No* **149**
—— 1958 *White Dwarfs* (Amsterdam: North-Holland)
Schmidt G D 1987 *The Second Conference on Faint Blue Stars* IAU Coll. No. **95** ed A G D Philip, D S Hayes and J Liebert (Schenectady: L Davis Press) p 377
—— 1989 *White Dwarfs* IAU Coll. No. **114** ed G Wegner (Berlin: Springer-Verlag) p 305
Schmidt G D, West S C, Liebert J, Green R F and Stockman H S 1986 *Astrophys. J.* **309** 218
Schönberner D 1979 *Astron. Astrophys.* **79** 108
Shapiro S L and Teukolsky S A 1983 *Black Holes, White Dwarfs and Neutron Stars. The Physics of Compact Objects* (New York: Wiley)
Shaviv G and Kovetz A 1972 *Astron. Astrophys.* **16** 72
Shipman H L 1979 *Astrophys. J.* **228** 240
—— 1984 *The Future of Ultraviolet Astronomy Based on Six Years of IUE Research* ed J M Mead, R D Chapman and Y Kondo, NASA Conf. Publ. **2349** 281
—— 1987 *The Second Conference on Faint Blue Stars* IAU Coll. No. **95** ed A G D Philip, D S Hayes and J Liebert (Schenectady: L Davis Press) 273
—— 1989 *White Dwarfs* IAU Coll. No. **114** ed G Wegner (Berlin: Springer-Verlag) p 220
Shipman H L and Greenstein J L 1983 *Astrophys. J.* **266** 761
Shipman H L, Greenstein J L and Boksenberg A 1977 *Astron. J.* **82** 480
Shipman H L, Liebert J and Green R F 1987 *Astrophys. J.* **315** 239
Shipman H L and Sass C A 1980 *Astrophys. J.* **235** 177
Shulov O S and Kopalskaya E N 1971 *Astrofizika* **10** 117
Sion E M 1986 *Publ. Astron. Soc. Pacific* **98** 821
Sion E M, Aannestad P A and Kenyon S J 1988a *Astrophys. J.* **330** L55

Sion E M, Fritz M L, McMullin J P and Lallo M D 1988b *Astron. J.* **96** 251
Sion E M, Greenstein J L, Landstreet J D, Liebert J, Shipman H L and Wegner G A 1983 *Astrophys. J.* **269** 253
Sion E M, Liebert J, Schmidt G D and Starrfield S G 1984 *Bull. Am. Astron. Soc.* **16** 724
Sion E M, Shipman H L, Wagner R M, Liebert J and Starrfield S 1986 *Astrophys. J.* **308** L67
Skilling J 1968 *Nature* **218** 923
Slattery W L, Doolen G D and DeWitt H E 1980 *Phys. Rev.* A **21** 2087
Smeyers P 1967 *Bull. Soc. R. Sci. Liège* **36** 357
Smith E R 1972 *Phys. Rev.* D **6** 3700
Smith E R, Henry R J W, Surmelian G L, O'Connell R F and Rajagopal A K 1972 *Phys. Rev.* D **6** 3700
Smith F G 1977 *Pulsars* (Cambridge: Cambridge University Press)
Starrfield S G, Cox A N, Hodson S W and Clancy S P 1983 *Astrophys. J.* **269** 645
Starrfield S G, Cox A N, Hodson S W and Pesnell W D 1982 *Pulsations in Classical and Cataclysmic Variable Stars* ed J P Cox and C J Hansen (Boulder: University of Colorado Press) p 78
Stevenson D G 1980 *J. Physique. Suppl. 3* **41** C2/61
Stoner E C 1930 *Phil. Mag.* **9** 944
Stover R J, Hesser J E, Lasker B M, Nather R E and Robinson E L 1980 *Astrophys. J.* **240** 865
Strittmatter P A and Wickramasinghe D T 1971 *Mon. Not. R. Astron. Soc.* **152** 47
Sweeney M A 1976 *Astron. Astrophys.* **49** 375
Sweigart A V and Gross P G 1978 *Astrophys. J. Suppl.* **36** 405
Tammann G A 1974 *Supernovae and Supernova Remnants* ed C B Cosmovici (Dordrecht: Reidel)
Tassoul M and Tassoul J-L 1983 *Astrophys. J.* **267** 334
Thejll P and Shipman H L 1986 *Publ. Astron. Soc. Pacific* **98** 922
Tomaney A B 1987 *The Second Conference on Faint Blue Stars* IAU Coll. No. **95** ed A G D Philip, D S Hayes and J Liebert (Schenectady: L Davis Press) p 673
Unno W 1956 *Publ. Astron. Soc. Japan* **8** 1956
Urpin V A and Yakovlev D G 1980 *Soviet Astron.* **24** 425
van den Heuvel E P J 1975 *Astrophys. J.* **196** L121
Van Horn H M 1968 *Astrophys. J.* **151** 227
—— 1971 *White Dwarfs* IAU Sympos. No. **42** ed W Luyten (Dordrecht: Reidel) p 87
—— 1984 *Theoretical Problems in Stellar Stability and Oscillations* ed A Noels and M Gabriel (Cointe-Ougree: Université de Liège)
Van Horn H M and Liebert J 1989 preprint
Van Maanen A 1913 *Publ. Astron. Soc. Pacific* **29** 258
Vauclair G 1971a *Astrophys. Lett.* **9** 161
—— 1971b *White Dwarfs* IAU Sympos. No. **42** ed R J Luyten (Dordrecht: Reidel) p 145
—— 1989 *White Dwarfs* IAU Coll. No. **114** ed G Wegner (Berlin: Springer-Verlag) p 176
Vauclair G, Dolez N and Chevreton M 1981b *Astron. Astrophys.* **103** L17
—— 1987 *Astron. Astrophys.* **175** L13
Vauclair G and Liebert J 1987 *Exploring the Universe with the IUE Satellite* ed Y Kondo (Dordrecht: Reidel) p 355
Vauclair G and Reisse C 1977 *Astron. Astrophys.* **61** 415
Vauclair S and Vauclair G 1982 *Ann. Rev. Astron. Astrophys.* **20** 37
Vauclair G, Vauclair S and Greenstein J L 1979 *Astron. Astrophys.* **80** 79
Vauclair G, Weidemann V and Koester D 1981a *Astron. Astrophys.* 100 113
Vennes S, Fontaine G and Wesemael F 1989 *White Dwarfs* IAU Coll. No. **114** ed G Wegner (Berlin: Springer-Verlag) p 368
Vogt H 1925 *Astron. Nachrichten* **227** 325
Wagner R M, Sion E M, Liebert J and Starrfield S G 1988 *Astrophys. J.* **328** 213
Wapstra A H and Bos K 1976 *At. Data Nucl. Data Tables* **17** 474
Warner B and Robinson E L 1972 *Nature Phys. Sci.* **239** 2
Wegner G 1971 *Publ. Astron. Soc. Pacific* **83** 205
—— 1981 *Astrophys. J.* **245** L27
—— 1983 *Astrophys. J.* **268** 282
—— 1989a (ed) *White Dwarfs* IAU Coll.No. **114** (Berlin: Springer-Verlag)
—— 1989b *White Dwarfs* IAU Coll. No. **114** ed G Wegner (Berlin: Springer-Verlag) p 401
Wegner G and Koester D 1985 *Astrophys. J.* **288** 746

Wegner G, McMahan R K and Boley F I 1987 *Astron. J.* **94** 1271
Wegner G and Nelan E P 1987 *Astrophys. J.* **319** 9[illegible]6
Wegner G, Reid I N and McMahan R K 1989 *White Dwarfs* IAU Coll. No. **114** ed G Wegner (Berlin: Springer-Verlag) p 378
Wegner G and Yackovich F H 1983 *Astrophys. J.* **275** 240
—— 1984 *Astrophys. J.* **284** 257
Wehrse R and Liebert J 1980 *Astron. Astrophys.* **86** 139
Weidemann V 1967 *Z. Astrophys.* **67** 286
—— 1987 *Astron. Astrophys.* **188** 74
—— 1990 *Ann. Rev. Astron. Astrophys.* in press
Weidemann V, Koester D and Vauclair G 1981 *Astron. Astrophys.* **95** L9
Weidemann V and Koester D 1983 *Astron. Astrophys.* **121** 77
—— 1984 *Astron. Astrophys.* **132** 195
Weidemann V and Yuan J W 1989 *White Dwarfs* IAU Coll. No. **114** ed G Wegner (Berlin: Springer-Verlag) p 1
Wendell C E, Van Horn H M and Sargent D 1987 *Astrophys. J.* **313** 284
Werner K, Heber U and Hunger K 1989 *White Dwarfs* IAU Coll. No. **114** ed G Wegner (Berlin: Springer-Verlag) p 194
Wesemael F, Green R F and Liebert J 1985 *Astrophys. J. Suppl.* **58** 379
Wesemael F, Lamontagne R and Fontaine G 1986 *Astron. J.* **91** 1376
Wesemael F and Truran J W 1982 *Astrophys. J.* **260** 807
Wheeler J C, Hansen C J and Cox J P 1968 *Astrophys. Lett.* **2** 253
White N E and Stella L 1988 *Nature* **332** 416
Wickramasinghe D T 1972 *Mon. Not. R. Astron. Soc.* **76** 129
—— 1987 *The Second Conference on Faint Blue Stars* IAU Coll. No. **95** ed A G D Philip, D S Hayes and J Liebert (Schenectady: L Davis Press) p 389
Wickramasinghe D T and Bessell M S 1976 *Astrophys. J.* **203** L39
Wickramasinghe D T and Cropper M 1988 *Mon. Not. R. Astron. Soc.* **235** 1451
Wickramasinghe D T and Ferrario L 1988 *Astrophys. J.* **327** 222
Wickramasinghe D T and Martin B 1979 *Mon. Not. R. Astron. Soc.* **188** 165
Wickramasinghe D T and Reid N 1983 *Mon. Not. R. Astron. Soc.* **203** 887
Wigner E 1932 *Phys. Rev.* **40** 749
Wigner E and Seitz F 1934 *Phys. Rev.* **46** 523
Wildhack W A 1940 *Phys. Rev.* **57** 81
Winget D E 1981 *Thesis* University of Rochester
—— 1986 *Highlights of Astronomy* **7** 221
Winget D E and Claver C F 1989 *White Dwarfs* IAU Coll. No. **114** ed G Wegner (Berlin: Springer-Verlag) p 290
Winget D E, Kepler S O, Robinson E L, Nather R E and O'Donoghue D 1985 *Astrophys. J.* **292** 606
Winget D E, Nather R E and Hill J A 1987b *Astrophys. J.* **316** 305
Winget D E, Robinson E L and Nather R E 1984 *Astrophys. J.* **279** L15
Winget D E, Robinson E L, Nather R E and Fontaine G 1982b *Astrophys. J.* **262** L11
Winget D E and Van Horn H M 1987 *The Second Conference on Faint Blue Stars* IAU Coll. No. **95** ed A G D Philip, D S Hayes and J Liebert (Schenectady: L Davis Press) p 363
Winget D E, Van Horn H M and Hansen C J 1981 *Astrophys. J.* **245** L33
Winget D E, Van Horn H M, Tassoul M, Hansen C J and Fontaine G 1983 *Astrophys. J.* **268** L33
Winget D E, Van Horn H M, Tassoul M, Hansen C J, Fontaine G and Carroll B W 1982a *Astrophys. J.* **252** L65
Winget D E, Hansen C J, Liebert J, Van Horn H M, Fontaine G, Nather R E, Kepler S O and Lamb D Q 1987a *Astrophys. J.* **307** 659
Woltjer L 1964 *Astrophys. J.* **140** 1309
Wunner G, Rösner W, Herold H and Ruder H 1985 *Astron. Astrophys.* **149** 102
Wunner G, Geyer F and Ruder H 1987 *Astrophys. Space Sci.* **131** 595
Yafet Y, Keyes R W and Adams E N 1956 *J. Phys. Chem. Solid* **1** 137
Yakovlev D G and Urpin V A 1980 *Soviet Astron.* **24** 303
Zapolski H S 1960 *Newman Laboratory of Nuclear Studies, Cornell University* unpublished report
Zeidler-K.T. E M, Weidemann V and Koester D 1986 *Astron. Astrophys.* **155** 356